Enantioselective capillary electrophoresis: Fundamental aspects and application to the *in vitro* assessment of CYP3A4 mediated ketamine N-demethylation

Inauguraldissertation

zur

Erlangung der Würde eines Doktors der Philosophie

vorgelegt der

Philosophisch-Naturwissenschaftlichen Fakultät

der Universität Basel

von

Hiu Ying Kwan

aus Bern, BE

Basel, 2012

creative commons

Attribution-Noncommercial-No Derivative Works 2.5 Switzerland

---

You are free:

to Share — to copy, distribute and transmit the work

Under the following conditions:

Attribution. You must attribute the work in the manner specified by the author or licensor (but not in any way that suggests that they endorse you or your use of the work).

Noncommercial. You may not use this work for commercial purposes.

No Derivative Works. You may not alter, transform, or build upon this work.

- For any reuse or distribution, you must make clear to others the license terms of this work. The best way to do this is with a link to this web page.

- Any of the above conditions can be waived if you get permission from the copyright holder.

- Nothing in this license impairs or restricts the author's moral rights.

Quelle: http://creativecommons.org/licenses/by-nc-nd/2.5/ch/deed.en   Datum: 3.4.2009

Genehmigt von der Philosophisch-Naturwissenschaftlichen Fakultät

auf Antrag von

Prof. Dr. Stephan Krähenbühl

Prof. Dr. Wolfgang Thormann

Prof. Dr. Jörg Huwyler

Basel, den 24. April 2012

Prof. Dr. Martin Spiess

Dekan

For my parents,

my brother

and Ruedi

Acknowledgements

Finally I would love to thank **my parents** for supporting me by appeasing my hunger after long working days and for their comprehension of not visiting them so often due to higher work-load. My parents and also **my brother** were always there to cheer me up.

Last but not least, many thanks to **Ruedi** for his support during my thesis but also for the beautiful moments in our free time, for reading all my drafts of the dissertation, for practicing my presentation skill and especially for his love, patience and encouragement in good times as in bad.

Summary

A large number of pharmaceutical substances are administered as racemates, consisting of two enantiomers with typically different pharmacodynamic and pharmacokinetic profiles. Thus, stereoselective analysis is important in drug development, therapeutic drug monitoring and research. Chiral separation by chromatographic methods such as HPLC and GC require expensive stationary phases. In contrast, in capillary electrophoresis (CE), enantioselective separation can be obtained using one or several chiral selectors which are added to the background electrolyte. Separation of enantiomers is based on different binding affinities with the enantiomers and/or different migration velocities of the formed analyte-selector complexes. High resolution can be achieved by varying type and concentration of chiral selector as well as buffer properties (pH, ionic strength, other additives etc.). Typical chiral selectors are neutral or charged cyclodextrins, proteins and bile acids. The simplicity of the technique makes enantioselective CE an attractive, promising and economic methodology for drug and metabolite analysis in pharmaceutical preparations, body fluids, tissues and microsomal preparations.

In the first part of this thesis, fundamental aspects of enantioselective CE were investigated using computer simulation. Dynamic computer simulators provide insight into the buffer system and improve understanding of the electrophoretic separation process. Simulation allows to predict proper separation and detection conditions for analytes prior to experiments. Using an extended version of the dynamic computer simulator GENTRANS, the interaction of methadone and its main metabolite EDDP with neutral chiral selectors were simulated. Experimentally determined complexation constants and mobilites of the formed complexes were employed as additional input parameters. Simulated electropherograms were qualitatively in good agreement with the experimental results.

In the second and third parts of the thesis, enantioselective CE was applied to study ketamine metabolism in an off-line study. Ketamine is a chiral phencyclidine derivative used in anesthesia. *In vitro* and also *in vivo* studies showed a higher affinity for the NMDA-receptors, higher anesthetic potency and shorter recovery time for S-ketamine compared to R-ketamine. The aims in this project were to characterize the kinetics of CYP 3A4 mediated ketamine N-demethylation *in vitro* including K_M, V_{max} and to investigate the stereoselective metabolism of this pathway. Furthermore, the inhibition kinetics of this pathway by ketoconazole, a potent CYP3A4 inhibitor, was investigated. Results showed a higher formation rate for S-norketamine after incubation of racemic ketamine as well as incubation of the single

enantiomers. Data obtained in the absence of ketoconazole revealed that the N-demethylation occurred stereoselectively. Inhibition kinetics by ketoconazole fitted best to a one-site competitive model and no stereoselectivity could be demonstrated.

In the forth and final part of this thesis, an on-line method was developed to investigate the *in vitro* N-demethylation of ketamine via CYP3A4, with the incubation performed in-capillary with subsequent electrophoretic separation and detection of the ketamine enantiomers. Kinetic parameters obtained compared well with those of the off-line study mentioned above and the metabolic step was stereoselective, confirming the results of the off-line assay. After additional improvements, the in-capillary method should be widely applicable to assess enzymatic activity in a fast, low-cost and automated way.

Table of Contents

Abbreviations

CD	Cyclodextrin
CE	Capillary electrophoresis
CEC	Capillary electrochromatography
CITP	Capillary isotachophoresis
CL_{int}	Intrinsic clearance
CL_{max}	Maximal clearance
CYP	Cytochrome P450
CZE	Capillary zone electrophoresis
DIMEB	Heptakis(2,6-di-O-methyl)-β-cyclodextrin
EDDP	2-ethylidene-1,5-dimethyl-3,3-diphenylpyrrolidine
EKC	Electrokinetic capillary chromatography
EMMA	Electrophoretically mediated microanalysis
EOF	Electroosmotic flow
FMO	Flavin-containing monooxygenase
GC	Gas chromatography
H_3PO_4	Phosphoric acid
HCl	Hydrochloric acid
HLM	Human liver microsomes
HPLC	High-performance liquid chromatography
hz	Hertz
ID	Inner diameter
ITP	Isotachophoresis
KH_2PO_4	Potassium dihydrogen phosphate
K_i	Inhibition constant
K_m	Michaelis-Menten constant
LC-MS	Liquid chromatography–mass spectrometry
mAU	Milli absorbance unit
MECC	Micellar electrokinetic capillary electrophoresis
$MgCl_2$	Magnesium chloride
$NaCH_3COO$	Sodium acetate
NADPH	Nicotinamide adenine dinucleotide phosphate
NaH_2PO_4	Sodium dihydrogen phosphate
NaOH	Sodium hydroxide
NMDA	N-methyl-D-aspartate
OHP-β-CD	(2-hydroxypropyl)-β-cyclodextrin
psi	Pound per square inch
RSD	Relative standard deviation
UHPLC	Ultra high-performance liquid chromatography
UV	Ultraviolet
V_{max}	Maximum formation rate

A.   Introduction

A.1. Enantioselective capillary electrophoresis

Many pharmaceutical substances are administrated as racemates, consisting of two enantiomers with different affinities for binding receptors or metabolizing enzymes. Thus, stereoselective analysis and quantitation is important for investigating pharmacokinetics in the context of drug development and for routine therapeutic drug monitoring [1-4]. Chromatographic methods, such as HPLC and GC, with expensive chiral stationary phases, are widely applied for stereoselective analysis of drugs and metabolites [1]. Due to high resolution, short analysis time, low consumption of chemicals and solvents, and low cost of columns, enantioselective capillary electrophoresis (CE) is an established and attractive methodology for drug and metabolite analysis in pharmaceutical preparations, body fluids, tissues and microsomal preparations [5-12]. In this approach, the presence of one or several chiral selectors, such as charged or neutral cyclodextrins, proteins, bile acids or crown ethers, enable the separation of the enantiomers under the influence of an electric field [13]. Enantioselective separation is based upon different binding affinities of the enantiomers to the chiral selector and/or different migration velocities of the formed complexes. For a given pair of enantiomers, high-resolution depends on type and concentration of the chiral selector as well as buffer properties (pH, ionic strength, other additives etc.). In most CE modes, including capillary zone electrophoresis (CZE), capillary isotachophoresis (CITP) and micellar electrokinetic capillary chromatography (MECC), the chiral selector is a buffer additive. The selector can also be bound to a packing material (capillary electrochromatography (CEC)) [14] or attached to the inner wall of a capillary (open tubular CEC) [15].

A.2. Computer simulation of electrophoretic processes

Dynamic computer simulators for electrophoresis are useful tools to provide insight into buffer systems and to investigate the electrophoretic transport of analytes. The performance of simulations prior to laboratory experiments does not only improve the understanding of the underlying processes, including the dynamics of separation, but might also ease to find proper separation and detection conditions for analytes [16-22].

Dynamic computer models are based upon equations derived from the transport concepts in solution together with user-inputted conditions, such as concentrations, mobilities, diffusion coefficients, pKa values, electric field strength or current density, column length and its segmentation. Component distributions are calculated and profiles of the column properties as function of electrophoresis time are obtained. Many dynamic models of various degrees of complexity have been described in the literature [17,18]. Most of them, including GENTRANS [19], SIMUL5 [20] and SPRESSO [21] which differ in certain aspects but produce identical results when employed with equal input data [22], are one-dimensional with the transport of each component through the electrophoretic space being the result of protolysis, electromigration, diffusion and imposed and/or electrically driven bulk flow. Recently, GENTRANS and SIMUL5 were extended for handling chiral electrophoretic separations. This required the inclusion of complexation constants and specific mobilities of formed 1:1 analyte-selector complexes in solution [23,24].

A.3. Ketamine

Ketamine is not only known as a drug of abuse in rave parties [25]. The use of this phencyclidine derivative in human and veterinary clinical practices has been established since 1970 [26-29]. Ketamine is used for the induction of anesthesia and as an anesthetic drug for short term surgical interventions. Also, in subanesthetic doses, it is used as an analgesic for postoperative pain relief. Furthermore, when applied perioperatively, ketamine was also shown to reduce postoperative pain and opioid consumption, and reported to prevent induction of postoperative hyperalgesia [30,31]. Its use in the treatment of major depressive disorders is also being investigated and discussed [32]. The rapid onset of the antidepressant effect of ketamine is a relevant advantage compared to currently available antidepressant medications, which take several weeks to months to achieve the effects. Ketamine binds with high-affinity as a noncompetitive antagonist mainly on N-methyl-D-aspartate (NMDA) receptors. Interactions with opioid receptors, muscarinic acetylcholine receptors, voltage-gated channels and monoaminergic receptors also contribute to the neuropharmacological effects of ketamine [26-29,33].

Ketamine consists of a racemic mixture of two enantiomers, S- and R-ketamine. The S-enantiomer has a four times higher affinity for the NMDA receptor than the R-enantiomer and also binds to the μ- and κ- opioid receptors. S-Ketamine has a two to three-fold higher

anesthetic potency compared to the racemate. Lower doses of the S-enentiomer are therefore needed to maintain an equal state of anesthesia. Also, fewer side effects and shorter recovery times are seen with the single enantiomer preparation [33-35].

The metabolism of ketamine has been studied in humans and various animal species, both *in vivo* and *in vitro*. It was found that ketamine is metabolized by a superfamily of a hepatic enzyme system, the cytochrome P450 (CYP) enzymes, through the N-demethylation to norketamine followed by hydroxylation of norketamine at various locations of the cyclohexanone and chlorophenyl rings and the formation of 5,6-dehydronorketamine. To a marginal extent, direct hydroxylation of ketamine prior to N-demethylation is also shown to occur [36–44]. With various CYP enzymes involved in the metabolic pathway of ketamine, drug-drug interactions must be taken into account. The activity of the metabolizing enzymes can be influenced by genetic and extrinsic factors. Genetic variations of several CYP enzymes and co-administration of other drugs which are substrates, inhibitors or inducers of these enzymes result in inter- and intra-individual variations in the pharmacokinetic profiles. In particular, when a chiral drug undergoing stereoselective metabolism is applied as a racemic mixture, these factors will impact on the pharmacokinetics of the enantiomers, possibly also resulting in a different pharmacodynamic profile. Thus, to describe the pharmacokinetic profile of enantiomers with different pharmacodynamics by determining the relevant kinetic parameters and to predict the potential for drug-drug interactions is important and of major interest in established drugs as well as those under investigation [45,46].

A.4. Goals of this dissertation

The goals of this dissertation were to study fundamental aspects of enantioselective CE and to assess the CYP3A4 mediated N-demethylation of ketamine *in vitro* using enantioselective CE for analysis of the samples. The sulfated β-cyclodextrin used so far as chiral selector in the ketamine project consists of an ill-defined mixture of stereoisomers which varies from batch to batch resulting in separation variations and limitations [47]. Thus, during the course of this dissertation, highly sulfated γ-cyclodextrin was introduced for the CE separation and analysis of ketamine and norketamine enantiomers.

In the first study, the dynamics of the enantioselective CE separation was investigated by computer simulation using GENTRANS with the new extension for handling complexation equilibria in solution [23]. For that purpose, complexation constants as well as mobilities of cationic model drugs in absence and presence of neutral cyclodextrins had to be

determined using CZE at low pH. These data, together with the conditions of the buffer systems, were used as inputs for the simulations and simulated electropherograms were compared to those obtained experimentally.

The second project comprised the complete characterization of the CYP3A4 mediated ketamine metabolism *in vitro* using enantioselective capillary electrophoresis. This work was performed in the context of an ongoing multidisciplinary research cooperation involving clinicians, pharmacologists, scientists from Vetsuisse Bern and Zürich, US, Argentina and our laboratory. This longterm research cooperation includes *in vitro* and *in vivo* studies of stereoselective metabolism of ketamine in different species, using sulfated cylcodextrins as chiral selectors for the enantioselective CE separation [43,44,48-53]. The present study started with the identification of human CYP450 enzymes involved in the biotransformation of ketamine and norketamine. Ketamine N-demethylation activity was shown for several CYP enzymes, mainly CYP3A4 and CYP2B6, whereas norketamine metabolites were formed only by CYP2B6 and CYP2A6. The results from this qualitative study, which was the subject of the master thesis of S. Portmann (University of Basel, 2008), revealed that CYP3A4 shows no activity on the metabolism of norketamine. Thus, the goal of my work was to elucidate the kinetics of the stereoselective N-demethylation of ketamine to norketamine mediated by CYP3A4 [54,55]. Ketoconazole is a potent and specific CYP3A4 inhibitor and was therefore used to determine the inhibition kinetics including the inhibition constant, after incubation of ketamine as racemate and as single enantiomers, as a third project [55].

All *in vitro* experiments performed so far were carried out manually. Incubation samples were extracted at alkaline pH and analysed with capillary electrophoresis. In addition to the ecologic and economic advantages mentioned above, CE also offers to be a unique and efficient microreactor for chemical reactions with subsequent on-line separation and detection of the reaction products. Advantages compared to off-line assays such as automation, lower consumption of materials and lower cost, are obvious. This technique, known as electrophoretically mediated microanalysis (EMMA), is based on mixing of injected zones containing the analyte and the reagents, followed by the occurrence of the enzymatic reaction either in presence or absence of the applied electric field, and finally the electrokinetic transport of the detectable product through an on-column detector or into a detector placed at the capillary end. Latest advances of this technique and its applications are well summarized in recent reviews [56,57]. The aim of the fourth topic of the present dissertation was to develop a suitable EMMA method to characterize the *in vitro* kinetics of ketamine N-demethylation mediated by CYP3A4. The kinetic Michaelis-Menten parameters V_{max} and K_m

together with the stereoselectivity of this pathway determined by this EMMA method were compared with the data obtained by the off-line assay.

B.   Methods, results and discussions

The content of this dissertation is subject of three publications and one manuscript accepted for publication. Therefore, the present chapter contains these manuscripts describing the development of this thesis, starting with the study of the fundamental aspects of enantioselective capillary electrophoresis, followed by investigation of CYP3A4 mediated ketamine metabolism using enantioselective CE in an off-line modus and ending by the development of an EMMA method to investigate this pathway in an on-line assay.

B.1. Dynamic high-resolution computer simulation of electrophoretic enantiomer separations with neutral cyclodextrins as chiral selectors

(Electrophoresis 2012, 33, in press.)

Dynamic high-resolution computer simulation of electrophoretic enantiomer separations with neutral cyclodextrins as chiral selectors

Michael C. Breadmore[1], Hiu Ying Kwan[2], Jitka Caslavska[2] and Wolfgang Thormann[2]

1) Australian Centre for Research on Separation Science, School of Chemistry, University of Tasmania, Hobart, Tasmania, Australia.
2) Department of Clinical Pharmacology and Visceral Research, University of Bern, Bern, Switzerland.

Abstract

GENTRANS, a comprehensive one-dimensional dynamic simulator for electrophoretic separations and transport, was extended for handling electrokinetic chiral separations with a neutral ligand. The code can be employed to study the 1:1 interaction of monovalent weak and strong acids and bases with a single monovalent weak or strong acid or base additive, including a neutral cyclodextrin, under real experimental conditions. It is a tool to investigate the dynamics of chiral separations and to provide insight into the buffer systems used in chiral capillary zone electrophoresis (CZE) and chiral isotachophoresis. Analyte stacking across conductivity and buffer additive gradients, changes of additive concentration, buffer component concentration, pH and conductivity across migrating sample zones and peaks, and the formation and migration of system peaks can thereby be investigated in a hitherto inaccessible way. For model systems with charged weak bases and neutral modified β-cyclodextrins at acidic pH, for which complexation constants, ionic mobilities and mobilities of selector-analyte complexes have been determined by CZE, simulated and experimentally determined electropherograms and isotachopherograms are shown to be in good agreement. Simulation data reveal that CZE separations of cationic enantiomers performed in phosphate buffers at low pH occur behind a fast cationic migrating system peak which has a small impact on the buffer composition under which enantiomeric separation takes place.

1 Introduction

Enantiomeric resolution is of central importance in pharmaceutical, pharmacological, agrochemical, environmental, biomedical and forensic considerations. Not surprisingly, the demand for enantioselective separation and analysis techniques increased considerably over the years. Stereospecific analyte monitoring is widely accomplished via use of chromatographic methods which require rather expensive chiral stationary phases [1-2]. During the past two decades, enantioselective separations by capillary electromigration methods have undergone a spectacular development and have shown to provide high-resolution at low cost [3-9]. For enantiomeric separation under electrokinetic conditions, a chiral selector or a mixture of selectors, proper buffer conditions (pH, ionic strength, micelles, additives etc.) and temperature are required. Compared to HPLC, capillary electrophoresis (CE) provides higher efficiency, is simpler, faster and cheaper, and consumes no or a much smaller amount of organic solvents. CE not only represents a complementary tool to the widely applied chromatographic methods, it also offers the possibility of bringing enantioselective separations and analyses into the routine arena. Enantiomeric separation in CE is based upon differential interaction between analytes and the selector or selectors and/or differences in the migration of the formed complexes. Thus, complex formation and the migration behavior of complexed and free solutes are the phenomena to be assessed for proper description of chiral CE [5,10-16].

Dynamic computer simulation of electrophoretic processes has demonstrated considerable value as a tool to gain insight into particular combinations of experimental conditions, to determine separation conditions well before any laboratory experiments are undertaken, and for educational purposes. Dynamic computer models are based upon equations derived from the transport concepts in solution together with user-inputted conditions, such as concentrations, mobilities, diffusion coefficients, pK_a values, electric field strength or current density, column length and its segmentation. Component distributions are calculated and profiles of the column properties as function of electrophoresis time are obtained. Many dynamic models of various degrees of complexity have been described in the literature [17,18]. Most of them, including GENTRANS [19], SIMUL5 [20] and SPRESSO [21] which differ in certain aspects but produce identical results when employed with equal input data [22], are one-dimensional with the transport of each component through the electrophoretic space being the result of protolysis, electromigration, diffusion and imposed and/or electrically driven bulk flow. These models do not include any chemical equilibria

with buffer additives, conversion equilibria of solutes, or solute interactions with column walls or filling material, and can thus not be employed for electrokinetic capillary chromatography (EKC), including enantiomeric separations.

For free solution configurations, only few dynamic electrophoretic models dealing with non acid-base chemical equilibria were reported. Dubrovčáková et al. [23] presented a mathematical model and numerical solution for the addition of a neutral complexation agent to moving boundary systems of strong electrolytes. Tesařová et al. [24] described a version of SIMUL which accounts for the additional equilibria that occur in the EKC separation of analytes in the presence of a neutral cyclodextrin and a charged surfactant (SDS) which includes the monomer-micelle equilibrium of the surfactant. Horáková et al. [25] have used this code to examine the mechanism of the accumulation of a weak acid using a dynamic pH junction and then mobilization of the neutral analyte by a sweeping front. In another effort and using simplified continuity equations, Dubský et al. [26] reported the development of a dynamic model of CE of interconverting enantiomers. Recently, GENTRANS was extended with algorithms that describe chemical equilibria between solutes and a buffer additive, an approach that enables simulation of the impact of chemical interactions in EKC [27], including those of transient trapping and sweeping in micellar EKC [28].

The only existing software for prediction of chiral separations in capillary zone electrophoresis is based upon a steady-state simulation program and allows the study of the impact of complex formation constants and mobilities on enantiomer separation [29,30]. Thus far, no generalized code which permits the simulation of the dynamics of electrokinetic chiral separations has been reported in the literature. This prompted us to extent the GENTRANS EKC code for handling of chiral separations, i.e. consideration of complexation constants and specific mobilities of formed 1:1 analyte-selector complexes in solution. For evaluation, complexation constants and mobilities of protonated cationic model drugs in presence of neutral cyclodextrins were determined experimentally by capillary zone electrophoresis (CZE) at low pH and simulated electropherograms and isotachopherograms were compared to those obtained experimentally. Furthermore, simulation data could be compared to those predicted by a newly developed version of SIMUL5 into which 1:1 complexation equilibria were incorporated and which became available to us prior to its publication [31,32].

2 Simulation of enantiomer migration with GENTRANS

GENTRANS is based upon the one-dimensional isothermal electrophoretic computer simulation model of Bier et al. [33] which is described in detail in Mosher et al. [34] and later publications [18,19,22]. The computer program used for simulating enantiomer separations is essentially the same as that previously used for the high-resolution simulation of EKC separations of alkylphenyl ketones under real experimental conditions [27] and for the examination of the mechanisms of transient trapping and sweeping in normal migration micellar EKC [28]. The EKC version of GENTRANS allows the study of the impact of chemical equilibria other than protolysis on the dynamics of electrophoretic separations. For that purpose it comprises algorithms to account for the interaction with an electrolyte additive. It is restricted to the interaction of monovalent weak and strong acids and bases with a single monovalent weak or strong acid or base additive and considers the following four relationships.

(i) interaction of dissociated analyte (A) with dissociated additive (Add)

$$A + Add \rightleftharpoons A\text{-}Add \qquad K_1 = \frac{[A\text{-}Add]}{[A][Add]} \qquad (1)$$
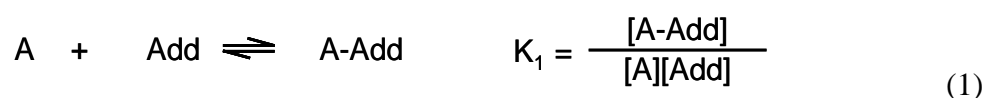
(ii) interaction of dissociated analyte (A) with undissociated additive (HAdd)

$$A + HAdd \rightleftharpoons A\text{-}HAdd \qquad K_2 = \frac{[A\text{-}HAdd]}{[A][HAdd]} \qquad (2)$$
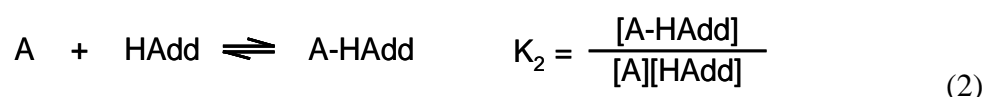
(iii) interaction of undissociated analyte (HA) with dissociated additive (Add)

$$HA + Add \rightleftharpoons HA\text{-}Add \qquad K_3 = \frac{[HA\text{-}Add]}{[HA][Add]} \qquad (3)$$

(iv) interaction of undissociated analyte (HA) with undissociated additive (HAdd)

$$HA + HAdd \rightleftharpoons HA\text{-}HAdd \qquad K_4 = \frac{[HA\text{-}HAdd]}{[HA][HAdd]} \qquad (4)$$

In all cases it is assumed that the equilibria are instantaneous which means that the kinetics of complex formation do not play a considerable role during migration. In contrast to the previous version, in which the analyte-additive complex was assumed to have the same electrophoretic mobility as the additive [27], the code was modified to allow the specification of distinct mobilities of all analyte-additive complexes. For the simulation of charged

enantiomer separation in presence of a neutral additive, this was an important change as the code would have otherwise not accounted for the migration of the charged complexes. Furthermore, GENTRANS calculates diffusion from entered mobilities. Thus, in an addition to the electrophoretic mobility and the pK_a values of each component in the system, it is also necessary to input the complexation constants and the mobilities of the analyte-additive complexes. A neutral additive, such as the neutral cyclodextrins used in this work at low pH, is implemented as a weak acid with a pK_a value of 14. To simplify matters, the model does not take into account the dependence of mobilities, pK_a values and complexation constants on ionic strength, viscosity and temperature.

3 Materials and Methods

3.1 Chemicals and samples

All chemicals used were of analytical or research grade. Racemic methadone (as hydrochloride) and codeine were obtained from the Inselspital Pharmacy (Bern, Switzerland). Racemic 2-ethylidene-1,5-dimethyl-3,3-diphenylpyrrolidine (EDDP, as hydroiodide) was from Alltech-Applied Science Labs (State College, PA, USA). NaH_2PO_4, KH_2PO_4 and $NaCH_3COO$ were from Merck (Darmstadt, Germany). Heptakis(2,6-di-O-methyl)-β-cyclodextrin (DIMEB) and methanol were from Sigma Aldrich (Buchs, Switzerland) and (2-hydroxypropyl)-β-cyclodextrin (OHP-β-CD) with a degree of substitution of ~0.6 was purchased from Fluka (Buchs, Switzerland). The pH of the separation buffers was adjusted with concentrated phosphoric acid (85%, Merck, Darmstadt, Germany) or acetic acid (Merck, Darmstadt, Germany). Samples for CZE were prepared in 10-fold diluted running buffer in absence of a chiral selector.

3.2 Electrophoretic instrumentation for CZE and running conditions

All CZE measurements were performed on a BioFocus 3000 capillary electrophoresis system (Bio-Rad Laboratories, Hercules, CA, USA), equipped with a 50 µm ID untreated fused-silica capillary (Polymicro Technologies, Phoenix, AZ, USA). The total length of the capillary was 50 cm (45.4 cm to the detector). The capillary was mounted in a user-assembled

cartridge. Sample injection was effected by applying a positive pressure of 5 psi*s (initial sample zone: about 1.2 % of column length). Carousel and cartridge temperatures were maintained at 25°C and detection was effected at 195 nm. Each day, the capillary was first rinsed for 5 min with 0.1 M NaOH, 5 min with water and 3 min with running buffer. Between runs the capillary was rinsed with running buffer containing the chiral selector for 3 min. Three buffer systems were investigated, configurations that were previously employed for the analysis of methadone and EDDP enantiomers [35-38]. System 1 comprised OHP-β-CD in a 75 mM KH_2PO_4 (which was adjusted to pH 2.5 with concentrated phosphoric acid). A constant voltage of 17 kV (current about 62 µA) was applied and the OHP-β-CD concentration was varied between 0 and 64 mM. System 2 contained DIMEB in 90 mM NaH_2PO_4 (adjusted to pH 2.3 with concentrated phosphoric acid) and 10 % methanol. The applied voltage was 20 kV (current about 59 µA) and the DIMEB concentration ranged between 0 and 57.6 mM. System 3 comprised OHP-β-CD in a 42.82 mM sodium acetate (adjusted to pH 4.07 with concentrated acetic acid, voltage: 20 kV, current about 7.5 µA, 0-64 mM chiral selector). For estimation of electroosmosis, caffeine (50 µg/mL) was used as sample.

3.3   Determination of complex constants and complex mobilities

The electrophoretic mobilities of the detected protonated bases were determined as function of cyclodextrin (additive) concentration under consideration of electroosmosis. For each concentration, the electroosmotic mobility was calculated from the detected caffeine peak and the obtained value was subtracted from the experimentally determined net mobility of the analyte, this providing the effective mobility (u_{eff}) of the analyte. Then, u_{eff} vs. additive concentration plots were constructed and the data were correlated with the relationship [10-16]

$$u_{eff} = (u_f + u_cKx)/(1 + Kx) \tag{5}$$

where u_f and u_c are the mobilities of the free analyte and the analyte-additive complex, respectively, K is the apparent complexation constant, and x is the cyclodextrin concentration. Non-linear regression analysis using SigmaPlot Scientific Graphing Software version 10 (SPSS, Chicago, IL, USA) provided values for u_c and K while values for u_f were determined experimentally (u_{eff} in absence of cyclodextrin).

3.4 ITP data

The capillary ITP data are those of Lanz et al. [38] and were obtained on a Tachophor 2127 analyzer (LKB AB, Bromma, Sweden) featuring conductivity detection at the column end. It was equipped with a 28 cm PTFE capillary of 0.5 mm ID and the cooling temperature was set to 13 °C. Separations were performed at a constant current of 200 μA (voltage: 4-8 kV) and, for detection, the current was reduced to 50 μA after 10 min of current flow. 1 μL of 10 mM racemic methadone hydrochloride was used as sample. The leader (catholyte) was composed of 10 mM sodium acetate that was adjusted with acetic acid to pH 4.3 and contained OHP-β-CD as chiral selector. 10 mM acetic acid was used as anolyte (terminator).

3.5 Execution of computer simulations and data evaluation

The programs were executed on Windows XP or Windows 7 based PC's featuring Intel Core i5 2.8 GHz processors. The component's input data for simulation are summarized in Tables 1 and 2. Simulation data were evaluated as profiles along the column at specified time intervals and, for comparison with experimental data, as time-based profiles which would be produced by a detector at a specified column location, i.e. segment number. For making plots, simulation data were imported into SigmaPlot Scientific Graphing Software version 10 (SPSS, Chicago, IL, USA).

Table 1. Physico-chemical input parameters of buffer components used for simulation

System	Compound	pK_a	Mobility (10^{-8} m^2/Vs)
1	Potassium	-	7.62
	Phosphoric acid	2.00 [b]	3.67
	Chloride	-	7.96
	OHP-β-CD	[a]	1.00
2	Sodium	-	5.19
	Phosphoric acid	2.00 [b]	3.67
	Chloride	-	7.96
	Iodide		7.96
	DIMEB	[a]	1.00
3	Sodium	-	5.19
	Acetic acid	4.76	4.24
	Chloride	-	7.12
	OHP-β-CD	[a]	1.00

a) Neutral cyclodextrins were entered as a weak acid with pKa = 14.
b) Phosphoric acid was treated as monovalent weak acid.

Table 2. Analyte parameters used for simulations

Sys-tem	Chiral selector	Compound	pK_a	Compound mobility [a] $(10^{-8}$ m^2/Vs)	Complex constant [b] (L/mol)	Complex mobility [b] $(10^{-8}$ m^2/Vs)
1	OHP-β-CD	S-methadone	8.9	1.80	187.6	0.536
		R-methadone	8.9	1.80	131.7	0.510
2	DIMEB	S-methadone	8.9	1.35	473.9	0.418
		R-methadone	8.9	1.35	379.0	0.402
		R-EDDP	9.6	1.55	366.6	0.406
		S-EDDP	9.6	1.55	344.5	0.402
		Codeine	8.2	1.35	0	0
		Marker [c]	8.2	1.00	100000	0.200
3	OHP-β-CD	S-methadone	8.9	2.14	197.0	0.817
		R-methadone	8.9	2.14	136.9	0.796

a) Free analyte mobility u_f determined by CZE under consideration of electroosmosis (cf. Section 3.3).
b) Complex constant and complex mobility values are those for complexation of the protonated bases with the neutral cyclodextrin obtained by non-linear regression analysis to Eq. 5.
c) Hypothetical marker with large complexation constant and assumed mobilities.

4   Results and discussions

4.1   Selection of separation systems and determination of input parameters for simulation

Methadone has become the most widely used drug for opiate dependency treatment and is also administered for the management of chronic pain. Both methadone and its primary metabolite EDDP are chiral weak bases. Their enantiomers were analyzed in our laboratory in urinary extracts and in *in vitro* samples using CE at acidic pH with neutral cyclodextrins as chiral selectors [35-37]. Furthermore, the enantiomers of methadone were separated by analytical and preparative enantioselective isotachophoresis [38]. Thus, methadone and EDDP enantiomers served as model compounds for simulations.

For the three CZE systems listed in Section 3.2, complexation constants and the mobilities of the selector-analyte complexes were determined as described in Section 3.3. In absence of the chiral selectors, electroosmotic mobilities for systems 1 to 3 were determined to be 0.327 x 10^{-8} m^2/Vs, 0.455 x 10^{-8} m^2/Vs and 2.46 x 10^{-8} m^2/Vs, respectively. Due to an increase of viscosity, somewhat smaller values (up to 20 % and in a selector concentration dependent fashion) were obtained in presence of the buffer additives. Complexation constants and mobilities of the selector-analyte complexes are presented in Table 2. As an example, regression graphs for the two methadone enantiomers in system 1 are presented in Figure 1

together with a graph showing the difference of the effective mobilities of the two methadone enantiomers as function of the OHP-β-CD concentration. Similar graphs were obtained with the other systems (data not shown). The calculated selectivities and conditions for maximum resolution are summarized in Table 3.
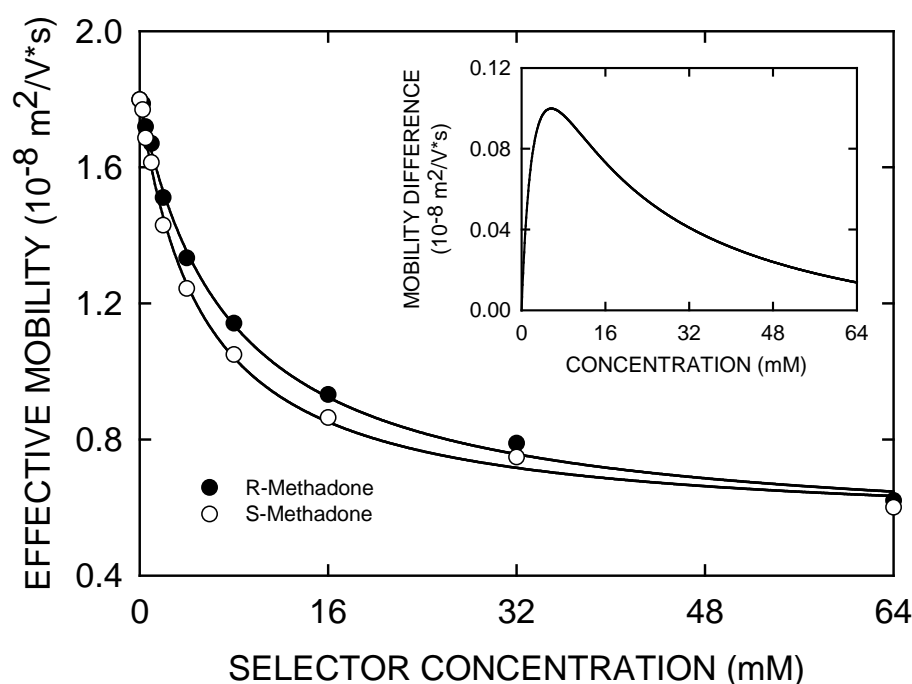
Figure 1. Effective methadone enantiomer mobility as function of OHP-β-CD concentration together with regression graphs for buffer system 1. The insert depicts the calculated difference of methadone enantiomer mobilities as function of OHP-β-CD concentration.

For the enantiomers of methadone and EDDP, complexation constants were determined to be between 130 and 480 L/mol (Table 2). These values are comparable to those of many other small molecular mass compounds (a comprehensive list of K values is given as Table 2 in the supporting information of Ref. [39]). In all three systems, R-methadone was found to have a lower binding affinity than S-methadone (Table 2) and the enantiomers of methadone could be separated easily (Table 3) which is in agreement with previous data from our laboratory [35-37]. For the separation of EDDP enantiomers, DIMEB [37] was known to be the superior selector compared to OHP-β-CD [35]. Thus, data for the latter buffer additive were not assessed. With DIMEB as selector, R-EDDP was found to bind more strongly than S-EDDP (Table 2). Separability of the two enantiomers is significantly lower compared to the enantiomers of methadone (Table 3). The selector concentrations at which highest mobility

differences are present are similar (1.9 and 2.3 mM for methadone and EDDP, respectively, Table 3).

The mobility values of the selector-analyte complexes for the enantiomers of methadone and EDDP were noted to be between 0.4×10^{-8} m^2/Vs and 0.8×10^{-8} m^2/Vs (Table 2). It was interesting to realize that, for all three systems, the mobilities of the S-methadone complexes were somewhat higher compared to those of the R-methadone complexes. In analogy to the work of Dubský et al. [16], it is assumed that this is due to the fact that the chiral selectors used are products comprising multiple isomers. For EDDP, the mobility difference is smaller. In all cases studied, the complex with a higher complexation constant has also a higher mobility of the complex.

Table 3. Enantioselectivity of binding and conditions of maximum mobility difference

System	Chiral selector	Compound	$alpha_{R/S}$ [a)]	du_{max} [b)] $(10^{-9}$ $m^2/Vs)$	Selector concentration at du_{max} (mM)
1	OHP-β-CD	Methadone	0.702	0.999	5.7
2	DIMEB	Methadone	0.800	0.457	1.9
2	DIMEB	EDDP	1.064	0.157	2.3
3	OHP-β-CD	Methadone	0.695	1.098	5.6

a)   Enantioselectivity of binding: AlphaR/S= KR/KS
b)   Maximum difference of effective mobilities of enantiomers

4.2   CZE separation of methadone enantiomers

The separation of methadone enantiomers in presence of OHP-β-CD was investigated using the potassium phosphate buffer at pH 2.5 (system 1 of Tables 1 to 3). The buffer used for simulation was composed of 75 mM KOH and 102.22 mM phosphoric acid (calculated pH: 2.51) and contained 8 mM OHP-β-CD. Having a sample comprising racemic methadone and chloride (28.90 µM each) in 10-fold diluted buffer without chiral selector and using the input data listed in Tables 1 and 2 provided the separation dynamics of the methadone enantiomers presented in Figure 2A. The two buffer components, as well as chloride, were assumed to have no interaction with OHP-β-CD. Under the employed conditions of constant current density (27328.7 A/m^2 which corresponds to 53.66 µA in a 50 µm ID capillary) and constant electroosmotic flow (EOF, 102.43 µm/s; mobility of 0.301×10^{-8} m^2/Vs), the two enantiomers are predicted to become separated within 1 min and require a separation distance of less than 4 cm. The current density applied corresponds to the initial voltage gradient of

340 V/cm which was used in the experiment. Similarly, the EOF value corresponds to that determined experimentally. For the simulation in absence of the chiral selector, the same current density was employed, but a somewhat larger EOF (111.18 µm/s; mobility of 0.327 x 10^{-8} m^2/Vs) which corresponds to that determined experimentally was used. As expected, the enantiomers of methadone comigrated in absence of the chiral selector (Figure 2B).
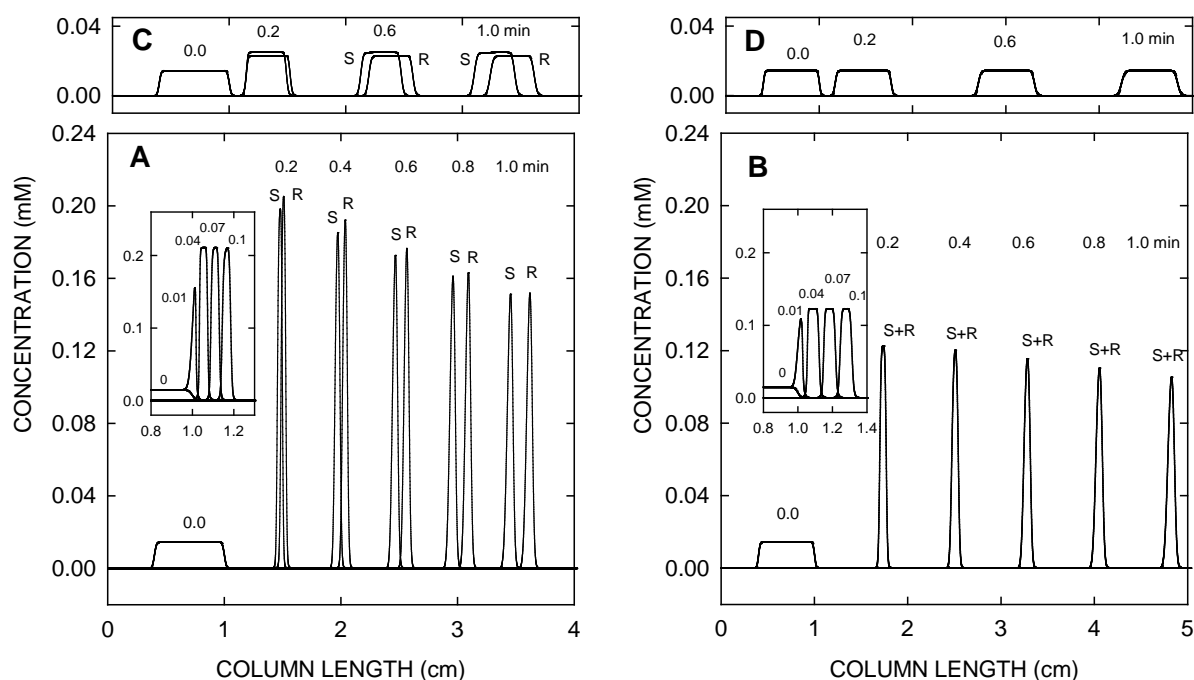
Figure 2. Separation of methadone enantiomers with 8 mM OHP-β-CD in buffer system 1 with a sample composed of racemic methadone and chloride (28.9 µM each) in 10-fold diluted buffer without additive. Computer predicted dynamics of methadone between 0 and 1 min (at 0.2 min interval) with the cathode on the right, (A) in presence and (B) in absence of the chiral selector. The sample initially occupied 3 % of column length. The simulation was performed with a 20 cm column divided into 50000 segments (4 µm mesh) at a constant current density of 27328.7 A/m^2 (initial voltage: 6800 V) and a constant EOF of (A) 102.43 µm/s and (B) 111.18 µm/s. The inserts in panels A and B depict the stacking of S-methadone between 0.01 and 1.0 min predicted by simulation in absence of EOF. Methadone simulation data obtained with undiluted buffer in the sample in presence and absence of complexation with OHP-β-CD are depicted in panels C and D, respectively. All other conditions are identical to those of panels A and B, respectively. S and R refer to S-methadone and R-methadone, respectively.

Simulation provides insight into sample stacking which occurs at the interface between sample and buffer. This is particularly the case when the conductivity of the sample solution is lower compared to the conductivity of the buffer [40] and is thus seen in the data presented in panels A and B of Figure 2. Stacking is predicted to occur rapidly after power application

(within the first 2 s; see data presented as inserts in Figure 2 which were obtained in simulations without EOF). In absence of the chiral selector, the enantiomers of methadone become concentrated about eight-fold (insert Figure 2B). Complexation with the neutral cyclodextrin is predicted to further enhance this effect almost two-fold (insert Figure 2A). A simulation performed in absence of the electric field gradient between sample and buffer (sample dissolved in buffer without chiral selector) revealed the concentration enhancement by complexation alone (Figure 2C). With less stacking, separation of the enantiomers proceeds at a lower pace and thus requires a larger separation distance (compare data of panels A and C of Figure 2). In absence of complexation and an electric field gradient, no change in the methadone plateau concentration and no enantiomer separation are predicted during analyte migration (Figure 2D).

The simulations of Figure 2 were conducted under conditions which are typically used in laboratory experiments. For 1 min of electrophoresis, simulation time intervals for the data of Figures 2A and 2B were 28.13 h and 24.15 h, respectively. Having a sample prepared in buffer without the chiral selector, i.e. without the buffer discontinuity due to the sample matrix, the time intervals were much shorter (1.88 h and 1.60 h for data of panels 2C and 2D, respectively), indicating that handling of the strong buffer gradient which provides the required stacking of the analytes is the bottleneck in simulation. With GENTRANS, a mesh of 4 µm and data smoothing [22] are required to solve this task in the mentioned time frame. In order to be able to simulate detector profiles comparable to those monitored experimentally in a capillary of 50 cm length, a total of 125000 segments together with an electrophoresis time of about 18 min (Figure 3B) would be required. This would take up to several months to complete. Thus, in order to cut the execution time, the 20 cm column used for the simulation of Figure 2 was periodically extended by a specified number of segments at the cathodic end and cut by the same amount of segments at the anodic end such that the actual simulation column always had a 20 cm length and a mesh of 4 µm. Care had to be taken that the methadone enantiomers were not removed by the shift. The simulation of the detector profile at 90 % of column length could thereby be accomplished in less than one week. Detector profiles for the configuration of Figures 2A and 2B with detection at 45 cm are depicted in Figure 3A. These data reveal that peak concentrations are significantly higher at the point of detection compared to the analyte concentration in the sample (compare peak concentrations with those of Figures 2A, 2B and 4), indicating that analyte stacking remains effective

throughout the separation column. Simulation data (Figure 3A) were found to qualitatively compare well with those obtained experimentally (Figure 3B).
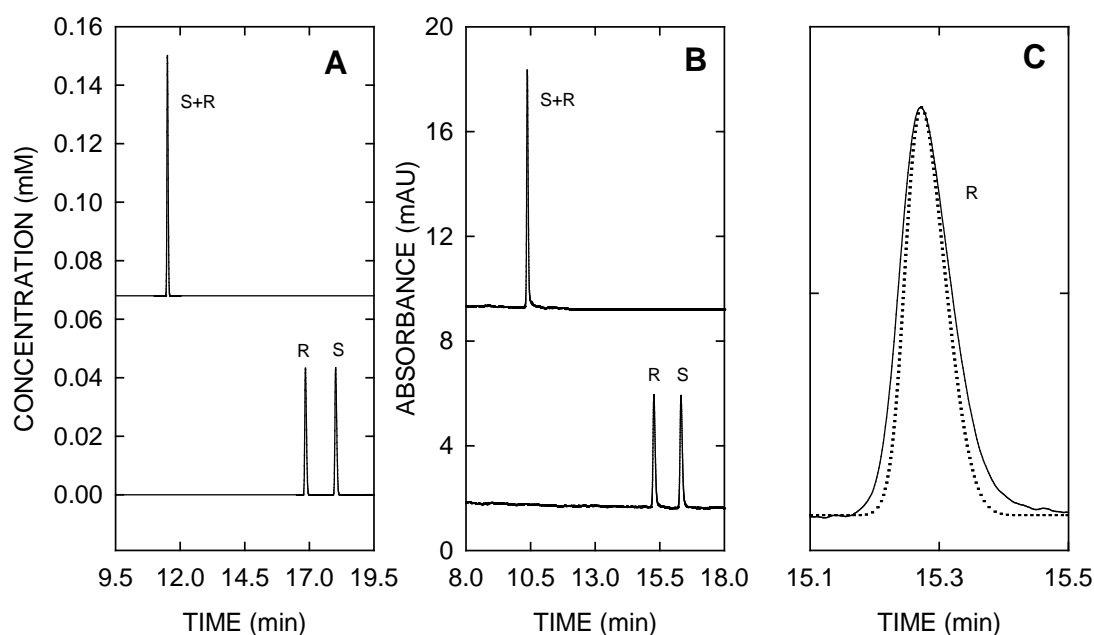
Figure 3. CZE detector data of the configuration of Figure 2 with a 50 cm capillary and having an absorption detector placed at 45 cm (90 % of column length). (A) Computer predicted detector profiles at 6 Hz (for simulation conditions see text), (B) experimental data and (C) comparison of detected (solid line) and simulated (dotted line) peak shape for R-methadone. The upper graphs in panels A and B are data obtained in absence of the chiral selector (data depicted with a y-axis offset). S and R refer to S-methadone and R-methadone, respectively.

Experimentally detected analyte peaks were found to be somewhat broader than those predicted by simulation and this despite the shorter detection time interval in the experiment compared to that of the simulation data. For visualisation, the predicted peak for R-methadone was shifted along the x-axis and adjusted in peak height to match the experimental data (Figure 3C). The narrower peak width obtained in the simulation suggests that not all dispersing factors are considered in the simulation. It is important to note that experiments and simulations used approximately the same initial sample plug length, namely 1.2 % of the total column length. Thus, a significant impact of a difference in the sampled amount can be ruled out. The experiments were performed at constant voltage which explains the differences in detection times of the peaks. Under constant voltage conditions and the buffer discontinuity due to the sample matrix, both the current and the electroosmotic flow are not constant [19,40]. During the course of the run, the current increases between 5 and 10 %. Furthermore,

input data for buffer components (Table 1) are temperature, ionic strength and medium dependent and are therefore not exactly reflecting those which are present under the experimental conditions.

The buffer additive responsible for complexation of the analytes, OHP-β-CD, is predicted to deviate from its initial value of 8 mM at the locations of the two interacting analytes (Figure 4). No such changes of the OHP-β-CD concentration are predicted with the use of zero mobility for the selector-analyte complexes which indicates that the migration of the charged complexes produces the OHP-β-CD peaks (data not shown). OHP-β-CD itself is neutral and does not migrate under the influence of the electric field. The predicted concentration peaks created by the analytes are small (less than 1 % deviation from the preset 8 mM of OHP-β-CD). They migrate in the same way as the concentration bulges of the neutral complexing additive previously described by Dubrovčáková et al. [23] for isotachophoretic configurations of monovalent strong components. During the course of electrophoretic transport, the peaks become smaller and diffuse as they are associated with the peaks of the analytes (Figure 4). Predicted OHP-β-CD peak profiles reflect the separation of the methadone enantiomers (insert in Figure 4).
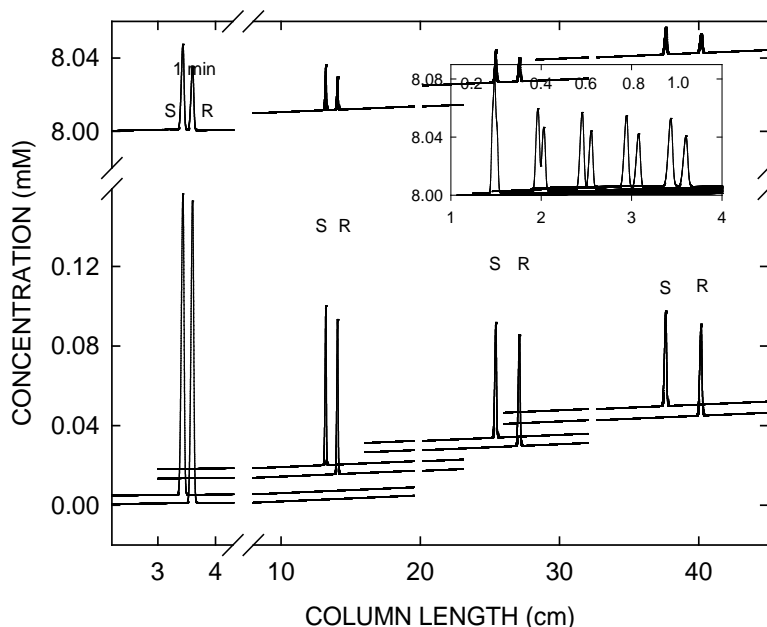
Figure 4. Computer predicted concentration distributions of the two methadone enantiomers (lower graphs) and associated profiles of OHP-β-CD (top graphs) after 1, 5, 10 and 15 min of power application for the configurations of Figures 2A and 3. The insert depicts the OHP-β-CD deviations across the migrating sample components during enantiomer separation (0.2, 0.4, 0.6, 0.8 and 1.0 min time points of Figure 2A). S and R refer to S-methadone and R-methadone, respectively.

4.3 Visualization of buffer system insights by computer simulation

Simulation can be employed to provide insight into the buffer system used. Chiral separations of cationic compounds are most often conducted at low pH, e.g. via use of phosphate buffers. Thus, the second system studied here was a pH 2.4 buffer composed of 90 mM NaOH, 132 mM phosphoric acid (calculated pH: 2.39), 1.8 mM DIMEB and 10 % methanol, a buffer which was previously used to analyze the enantiomers of methadone and EDDP in alkaline extracts of urine and *in vitro* samples after incubation of methadone with single CYP450 enzymes [37]. Simulation was employed to visualize the separation of the enantiomers of methadone and EDDP (K values between 344 and 474 L/mol, Table 2) together with two achiral marker compounds in an electroosmosis free environment (Figure 5). To characterize the configuration, codeine with no experimental evidence of an interaction with DIMEB (K = 0 L/mol) and a hypothetical marker substance M with a very large interaction constant (100000 L/mol) were added to the sample. In that example, codeine is migrating without retardation due to complexation whereas M is migrating with the mobility of its complex with DIMEB (Figure 5). The two buffer components, as well as chloride and iodide from the sample, were assumed to have no interaction with DIMEB. All input data used for simulation are listed in Tables 1 and 2. The simulation was performed in a 5 cm column divided into 10000 segments at a constant 1000 V for 2 min of electrophoresis (current density change from 17663.4 to 18321.9 A/m^2) and in absence of electroosmosis.

The data presented in Figure 5 were obtained with the sample being applied in 10-fold diluted buffer and without chiral selector. Initial distributions of analytes, buffer components, pH and conductivity are depicted as dotted line graphs whereas solid line profiles represent those obtained after 12 s of power application (200 V/cm). For the presented time point, analytes are shown to become stacked as was discussed for Figure 2A and the distributions of the enantiomers of methadone and EDDP indicate that enantiomeric separation is in progress. Codeine, which has an ionic mobility equal to methadone but lower compared to EDDP, is migrating the fastest. Both EDDP and methadone are retarded due to complexation with DIMEB. The same is true for the hypothetical marker M. Diffusion is calculated from the mobility values. Thus, codeine which is not complexed appears as the broadest peak and M with its highest affinity to DIMEB is predicted as sharpest peak. Using SIMUL5 in the newly

extended complex version [31] with the same input data provided identical results (data not shown).

In addition to the analyte dynamics, simulation provides insight into the distributions of all buffer components, ionic strength, pH and conductivity. The buffer additive responsible for complexation of the analytes, DIMEB, is predicted to deviate from its initial value of 1.8 mM at the locations of the analytes in a K value dependent fashion. The higher the complexation constant, the stronger becomes the increase of DIMEB. For codeine, there is no change (see insert in Figure 5), for marker M almost 0.1 mM. No changes of the DIMEB concentration are predicted with the use of zero mobility for the selector-analyte complexes which indicates that the migration of the charged complexes produces the DIMEB peaks as was discussed for the OHP-β-CD case presented in Figure 4. DIMEB itself is neutral and does not migrate under the influence of the electric field. Computer simulation also reveals small deviations of phosphoric acid and sodium, conductivity and pH across the analyte peaks (Figure 5). Furthermore, simulation visualizes the formation of a cationic migrating system peak which has a much higher mobility than the analytes (Figure 5). Using Peakmaster [41], the system eigenmobility was calculated to be 4.38 x 10^{-8} m^2/Vs, a value which corresponds with the migration predicted by simulation. A comparative migrating system peak with a mobility of 5.24 x 10^{-8} m^2/Vs is predicted for the buffer configuration of Figure 2 (data not shown). The migrating system peak depicted in Figure 5 encompasses deviations in the two buffer components, conductivity and pH. As there is no interaction between phosphoric acid and sodium with DIMEB assumed, there is no change in DIMEB across the migrating system peak. Simulation further reveals a rather broad shape of the rear boundary of the migrating system peak. This boundary essentially extends all the way to the stationary boundary at the location of the initial interface between sample and buffer. Thus, the actual buffer composition around the locations of the analytes is slightly different compared to the initial buffer (Figure 5).
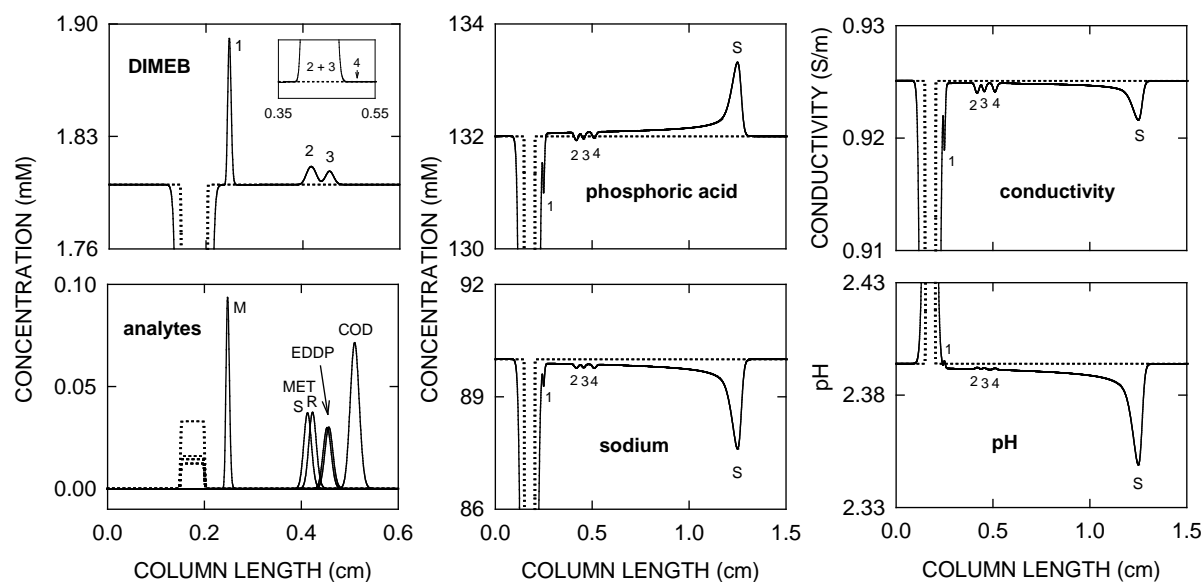
Figure 5. Simulation data for buffer system 2 with 1.8 mM DIMEB and having a sample composed of racemic methadone (28.90 µM), racemic EDDP (24.68 µM), codeine (33.4 µM), a marker base M (16 µM), chloride (28.90 µM), iodide (24.68 µM) and 10-fold diluted buffer without additive. The sample initially occupied 1 % of column length and was placed between 3 and 4 % of column length. The simulation was performed with a 5 cm column divided into 10000 segments (5 µm mesh) at a constant voltage of 1000 V and in absence of EOF. Solid line graphs are profiles obtained after 0.2 min of power application whereas initial profiles are drawn as dotted lines. S represents a cationically migrating system peak, M refers to a cationic marker with K=100000 L/mol, MET refers to methadone and COD stands for codeine. Peaks 1, 2, 3 and 4 refer to changes associated with M, methadone, EDDP and codeine, respectively. The cathode is on the right.

Simulation and experimental detector plots for the configuration of Figure 5 are presented in Figure 6. Enantioselective simulations were performed with a 20 cm long capillary as described for Figure 3 having a 4 µm mesh, a constant current density of 32365.34 A/m^2 (initial voltage: 8000 V) and a constant EOF of 160 µm/s towards the cathode. Simulations in absence of DIMEB were made at the same current density and with an EOF of 180 µm/s. Computer predicted electropherograms depicting the analytes as concentration peaks are presented in Figure 6A. For the simulation data presented in panel B of Figure 6, concentration values were adjusted to absorption at 195 nm in relation to methadone. Using 20 µM solutions, EDDP and codeine were determined to absorb 1.173-fold and 0.334-fold compared to methadone at this wavelength. Comparison of these data with those monitored experimentally (compare data of panel B and C of Figure 6) suggest that there is qualitative agreement between simulation and experimental data and this despite the fact that the buffer

contained 10 % methanol and the input parameters of the buffer components used (Table 1) are those for an aqueous system.
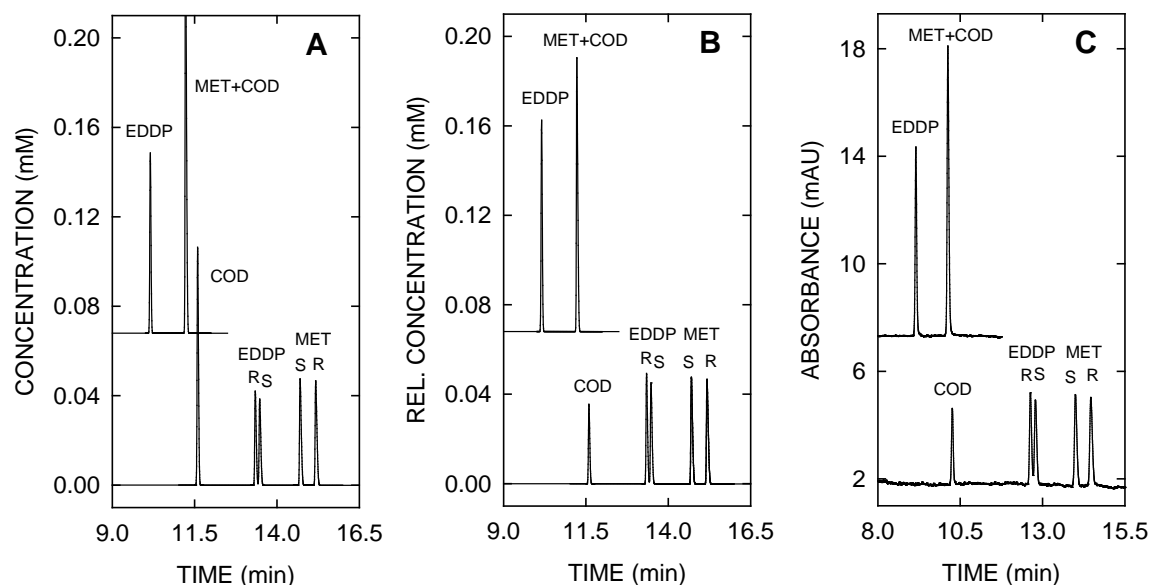
Figure 6. CZE detector plots of the configuration of Figure 5 in a 50 cm capillary having an absorption detector placed at 45 cm (90 % of column length). Computer predicted detector responses at 6 Hz showing the peaks (A) in concentration units and (B) in concentration units adjusted to differences in absorption. Panel C depicts the experimental data. Simulations were performed with a 4 µm mesh at a constant current density of 32365.34 A/m^2 and a constant EOF of 160 µm/s. The upper graphs, depicted with a y-axis offset, are corresponding data

4.4 Simulation of isotachophoretic separation of methadone enantiomers

The simulation code is not restricted to the use of CZE configurations with analytes that interact with an additive. Other electrophoretic modes, including isotachophoresis, and the interaction between buffer components and the additive can also be considered as was previously shown by Dubrovčáková et al. [23] for moving boundary configurations comprising strong electrolytes. Our code was employed to simulate the isotachophoretic separation of methadone enantiomers in presence of OHP-β-CD, a configuration which was previously characterized by capillary isotachophoresis and employed for the isolation of methadone enantiomers by recycling free fluid isotachophoresis [38]. The leader was composed of 10 mM NaOH and 40 mM acetic acid (calculated pH 4.29). The sample comprised racemic methadone and chloride (20 mM each) and 10 mM acetic acid (pH 3.39) served as terminator. For simulation, a 10 cm column divided into 20000 segments (5 µm

mesh) with the sample being placed between 5 and 6 % of column length was assumed and a constant current density of 250 A/m^2 was applied. Input values used for the simulation are those of system 3 given in Tables 1 and 2. It is important to realize that the CZE buffer used to determine the analyte parameters had a similar but not equal composition as the ITP leader. Computer predicted isotachophoretic zone patterns in presence and absence of an interaction between the methadone enantiomers and 5 mM of OHP-β-CD are depicted in panels A and B, respectively, of Figure 7. All other components were assumed not to be complexed with OHP-β-CD. In absence of the interaction (Figure 7B), there is no enantiomer separation. Methadone is shown to produce a cationic isotachophoretic zone with a 2.81 mM plateau concentration for each methadone enantiomer which migrates between sodium (leading ion) and H$^+$ (terminating ion). The zone is characterized with sharp front and rear boundaries. The rear boundary features a conductivity dip which is comparable to previously described isotachophoretic configurations [42]. Having the interaction between the methadone enantiomers and 5 mM OHP-β-CD (Figure 7A), simulation predicts an ITP separation of the methadone enantiomers. R-methadone with the lower complexation constant is forming an isotachophoretic zone between leader and S-methadone because its net mobility (1.65 x 10^{-8} m^2/Vs in the ITP zone) is larger compared to that of S-methadone (1.54 x 10^{-8} m^2/Vs). The formed zones not only differ in the enantiomer plateau concentration (4.34 vs. 4.00 mM), pH (3.90 vs. 3.86), conductivity (29.6 vs. 27.7 mS/m) and acetic acid concentration (36.74 vs. 36.87 mM), but also in the concentration of OHP-β-CD (5.76 vs. 5.95 mM). OHP-β-CD itself is neutral and does not migrate under the influence of the electric field. The deviation from the supplied 5 mM OHP-β-CD across the ITP zones is due to the migration of the charged complexes and comparable to the predictions of Dubrovčáková et al. [23] for strong electrolytes. No changes of the OHP-β-CD concentration are predicted with the use of zero mobility for the selector-analyte complexes (data not shown). Furthermore, the S-methadone zone is predicted to slowly decompose at its rear end with an increasing part of S-methadone extending into the adjusted acetic acid terminator where its mobility (effective mobility of S-methadone of 1.49 x 10^{-8} m^2/Vs behind moving boundary at position 8.6 cm of Figure 7A) is insufficient to catch up with the plateau zone in which the effective mobility of S-methadone is 1.54 x 10^{-8} m^2/Vs. The S-methadone plateau migrates in an enforced isotachophoretic configuration with the conductivity of the zone being lower compared to that of the terminator (Figure 7A, upper graph). Using SIMUL5 in the newly extended complex version [31] with

the same input data provided comparable results (data not shown). A careful study of the instability of the S-methadone zone is outside the scope of this investigation.
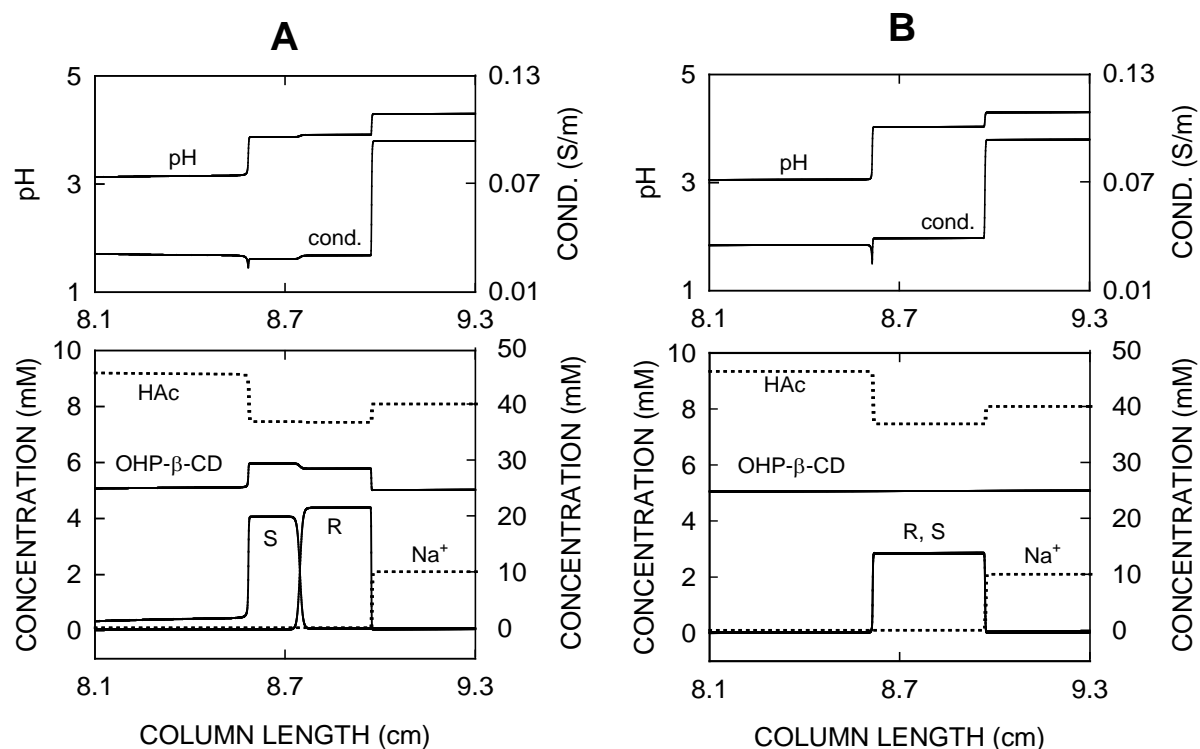
Figure 7. Isotachophoresis of methadone enantiomers (A) in presence and (B) in absence of the interaction with 5 mM OHP-β-CD between a leader composed of 10 mM NaOH and 40 mM acetic acid (calculated pH 4.29) and 10 mM acetic acid (pH 3.39) as terminator. The sample comprised racemic methadone and chloride (20 mM each) and initially occupied 1 % of column length at the anodic column end. Simulations were performed with a 10 cm column divided into 20000 segments (5 µm mesh) at a constant current density of 250 A/m^2 and without any EOF. Profiles presented are for 10 min of electrophoresis time. The cathode is to the right. In the lower panels, the y-axis scale for the buffer components (dotted lines) is on the right. Key: HAc, acetic acid; S, S-methadone; R, R-methadone.

ITP data of methadone predicted by computer simulation were compared with experimental results from the literature [38]. Figure 8A depicts simulated detector profiles obtained for the configurations of Figure 7 and having a conductivity detector placed at 85 % of column length (column position 8.5 cm). The data are presented as 1/conductivity vs. time profiles and are compared to experimental data from the literature (Figure 8B). Without a chiral selector (top graphs of Figure 8), methadone is producing a cationic isotachophoretic zone between leader (L) and adjusted terminator (T) which is characterized with a sharp front boundary and a rear boundary featuring a conductivity dip. The conductivity of the methadone zone is predicted and experimentally determined to be between the conductivities

of the leader and the adjusted terminator. By adding 5 mM of OHP-β-CD to the leader, enantiomeric separation was predicted by simulation and observed experimentally (lower graphs in Figure 8). R-methadone with the lower complexation constant is forming an isotachophoretic zone between leader and S-methadone. The obtained conductivity patterns were found to compare well to those monitored experimentally. This suggests that simulation with input data which were determined by CZE in a buffer similar to the leading electrolyte predicts realistic isotachophoretic patterns.
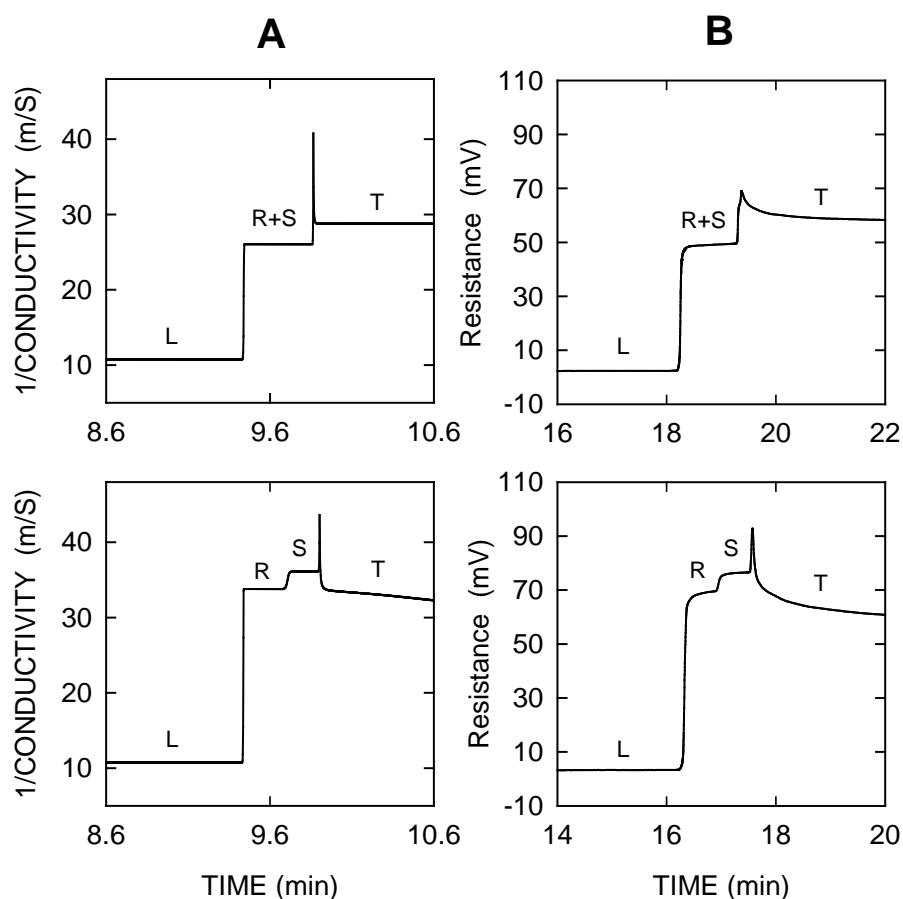
Figure 8. Cationic isotachopherograms (A) predicted by computer simulation and (B) monitored experimentally for analysis of racemic methadone with no chiral selector (top graphs), and 5.0 mM OHP-β-CD (bottom graphs) in the leader. The simulated responses represent 10 Hz data of 1/conductivity for a detector positioned at 85 % of column length of the configurations depicted in Figure 7. For other conditions see text. The experimental data are from Ref. [38]. Key: L, leader; T, adjusted terminator; S, S-methadone; R, R-methadone.

5   Concluding remarks

GENTRANS extended for handling the interaction of monovalent compounds with neutral cyclodextrins is demonstrated to be a valuable tool to investigate the dynamics of

chiral separations and provide insight into the buffer systems used in chiral CE and chiral isotachophoresis at power levels that are typically used in experiments. Analyte stacking across conductivity and cyclodextrin gradients, changes of cyclodextrin concentration, buffer concentration, pH and conductivity across migrating sample zones and peaks, and the formation and migration of system peaks can thereby be investigated in a straightforward way which was hitherto inaccessible by dynamic computer simulation. For model systems with chiral charged weak bases and neutral modified β-CDs at acidic pH, for which complexation constants, ionic mobilities and mobilities of selector-analyte complexes have been determined by CZE, simulated and experimentally determined electropherograms and isotachopherograms are shown to be in good agreement. CZE data obtained with protonated weak bases and a neutral modified β-CD as chiral selector in acidic phosphate buffers illustrate that (i) such chiral separations are best performed with the sample being applied in diluted separation buffer without complexing agent, and (ii) chiral separation takes place behind a cationic migrating system peaks with a broad rear boundary that slightly changes the buffer composition at the site of enantiomer migration and separation. In addition to the increase in analytical sensitivity, sample stacking provides faster enantiomer separation along a shorter distance. The one-dimensional and isothermal code is not restricted to the investigated cases which feature interactions between weak bases as samples and neutral cyclodextrins as buffer additives. It is general and can be employed to study the interaction of monovalent weak and strong acids and bases in any electrophoretic configuration with a single weak or strong acid or base additive.

Acknowledgments

References

[1] Caldwell, J., J. Chromatogr. A 1995, 694, 39-48.

[2] Francotte, E., Lindner, W., Eds., Chirality in Drug Research, Wiley-VCH, Weinheim, Germany, 2006.

[3] Snopek, J., Jelínek, I., Smolková-Keulemansová, E., J. Chromatogr. 1992, 609, 1-17.

[4] Fanali, S., J. Chromatogr. A 1996, 735, 77-121.

[5] Chankvetadze, B., Capillary Electrophoresis in Chiral Analysis, John Wiley & Sons, Chichester, 1997.

[6] Gübitz, G., Schmid, M.G., J. Chromatogr. A 2008, 1204, 140-156.

[7] Van Eeckhaut, A., Michotte, Y., Chiral separations by capillary electrophoresis, CRC Press, Boca Raton, USA, 2010.

[8] Zaugg, S., Thormann, W., J. Chromatogr. A 2000, 875, 27-41.

[9] Caslavska, J., Thormann, W., J. Chromatogr. A 2011, 1218, 588-601.

[10] Wren, S.A.C., Rowe, R.C., J. Chromatogr. 1992, 603, 235-241.

[11] Wren, S.A.C., J. Chromatogr. 1993, 636, 57-62.

[12] Rawjee, Y.Y., Williams, R.L., Vigh, G., J. Chromatogr. A 1993, 652, 233-245.

[13] Penn, S.G., Bergström, T., Knights, I., Liu, G., Ruddick, A., Goodall, D.M., J. Phys. Chem. 1995, 99, 3875-3880.

[14] Reijenga, J.C., Ingelse, B.A., Everaerts, F.M., J. Chromatogr. A 1997, 792, 371-378.

[15] Lomsadze, K., Martinez-Giron, A.B., Castro-Puyana, M., Chankvetadze, L., Crego, A.L., Salgado, A., Marina, M.L., Chankvetadze, B., Electrophoresis 2009, 30, 2803-2811.

[16] Dubský, P., Svobodová, J., Tesařová, E., Gaš, B., Electrophoresis 2010, 31, 1435-1441.

[17] Thormann, W., Caslavska, J., Breadmore, M.C., Mosher, R.A., Electrophoresis 2009, 30, S16-S26.

[18] Thormann, W., Breadmore, M.C., Caslavska, J., Mosher, R.A., Electrophoresis 2010, 31, 726-754.

[19] Thormann, W., Zhang, C.-X., Caslavska, J., Gebauer, P., Mosher, R.A., Anal. Chem. 1998, 70, 549-562.

[20] Hruška, V., Jaroš, M., Gaš, B., Electrophoresis 2006, 27, 984-991.

[21] Bercovici, M., Lele, S.K., Santiago, J.G., J. Chromatogr. A 2009, 1216, 1008-1018.

[22] Mosher, R.A., Breadmore, M.C., Thormann, W., Electrophoresis 2011, 32, 532-541.

[23]   Dubrovčáková, E., Gaš, B., Vacík, J., Smolková-Keulemansová, E., J. Chromatogr. 1992, 623, 337-344.

[24]   Tesařová, E., Ševčík, J., Gaš, B., Armstrong, D.W., Electrophoresis 2004, 25, 2693-2700.

[25]   Horáková, J., Petr, J., Maier, V., Tesařová, E., Veis, L., Armstrong, D. W., Gaš, B., Ševčík, J., Electrophoresis 2007, 28, 1540-1547.

[26]   Dubský, P., Tesařová, E., Gaš, B., Electrophoresis 2004, 25, 733-742.

[27]   Breadmore, M.C., Quirino, J.P., Thormann, W., Electrophoresis 2009, 30, 570-578.

[28]   Breadmore, M.C., Quirino, J.P., Thormann, W., Electrophoresis 2011, 32, 542-549.

[29]   Reijenga, J.C., Ingelse, B.A., Everaerts, F.M., J. Chromatogr. A 1997, 772, 195-202.

[30]   Ingelse, B.A., Sarmini, K., Reijenga, J.C., Kenndler, E., Everaerts, F.M., Electrophoresis 1997, 18, 938-942.

[31]   Hruška, V., Beneš, M., Svobodová, J., Zusková, I., Gaš, B., Electrophoresis, submitted for publication.

[32]   Svobodová, J., Beneš, M., Hruška, V., Ušelová-Včeláková, K., Gaš, B., Electrophoresis, submitted for publication.

[33]   Bier, M., Palusinski, O.A., Mosher, R.A., Saville, D.A., Science 1983, 219, 1281-1287.

[34]   Mosher, R.A., Saville, D.A., Thormann, W., The Dynamics of Electrophoresis, VCH Publishers, Weinheim, 1992.

[35]   Lanz, M., Thormann, W., Electrophoresis 1996, 17, 1945-1949.

[36]   Ramseier, A., Caslavska, J., Thormann, W., Electrophoresis 1999, 20, 2726-2738.

[37]   Prost, F., Thormann, W., Electrophoresis 2003, 24, 2577-2587.

[38]   Lanz, M., Caslavska, J., Thormann, W., Electrophoresis 1998, 19, 1081-1090.

[39]   Ušelová-Včeláková, K., Zusková, I., Gaš, B, Electrophoresis 2007, 28, 2145-2152.

[40]   Mosher, R.A., Zhang, C.-X., Caslavska, J., Thormann, W., J. Chromatogr. A 1995, 716, 17-26.

[41]   Gaš, B., Jaroš, M., Hruška, V., Zusková, I., Štědrý, M., LC-GC Eur. 2005, 18, 282-288.

[42]   Mosher, R.A., Thormann, W., Bier, M., J. Chromatogr. 1985, 320, 23-32.

B.2. Enantioselective capillary electrophoresis for identification and characterization of human cytochrome P450 enzymes which metabolize ketamine and norketamine *in vitro*

(J. Chromatogr. A 2010, 1217, 7942–7948.)

Enantioselective capillary electrophoresis for identification and characterization of human cytochrome P450 enzymes which metabolize ketamine and norketamine *in vitro*

Simone Portmann[1], Hiu Ying Kwan[1], Regula Theurillat[1],
Andrea Schmitz[2], Meike Mevissen[2] and Wolfgang Thormann[1]

[1]Department of Clinical Pharmacology and Visceral Research,
University of Bern, 3010 Bern, Switzerland
[2]Division of Veterinary Pharmacology and Toxicology, Vetsuisse Faculty,
University of Bern, 3012 Bern, Switzerland

Abstract

Ketamine, a phencyclidine derivative, is used for induction of anesthesia, as an anesthetic drug for short term surgical interventions and in subanesthetic doses for postoperative pain relief. Ketamine undergoes extensive hepatic first-pass metabolism. Enantioselective capillary electrophoresis with multiple isomer sulfated β-cyclodextrin as chiral selector was used to identify cytochrome P450 enzymes involved in hepatic ketamine and norketamine biotransformation *in vitro*. The N-demethylation of ketamine to norketamine and subsequently the biotransformation of norketamine to other metabolites were studied via analysis of alkaline extracts of *in vitro* incubations of racemic ketamine and racemic norketamine with nine recombinantly expressed human cytochrome P450 enzymes and human liver microsomes. Norketamine was formed by CYP3A4, CYP2C19, CYP2B6, CYP2A6, CYP2D6 and CYP2C9, whereas CYP2B6 and CYP2A6 were identified to be the only enzymes which enable the hydroxylation of norketamine. The latter two enzymes produced metabolic patterns similar to those found in incubations with human liver microsomes. The kinetic data of ketamine N-demethylation with CYP3A4 and CYP2B6 were best described with the Michaelis-Menten model and the Hill equation, respectively. This is the first study elucidating the individual enzymes responsible for hydroxylation of norketamine. The obtained data suggest that *in vitro* biotransformation of ketamine and norketamine is stereoselective.

1   Introduction

Ketamine ((R,S-2-(2-chlorophenyl)-2-methylamino)cyclohexanon, for chemical structure see Fig. 1), is a phencyclidine derivative that is used in human and veterinary clinical practice since 1970. Ketamine's mechanism of action has not been fully elucidated yet, but it is considered that the most important neuropharmacological effects of ketamine are mediated through its non-competitive antagonism at the N-methyl-D-aspartate (NMDA) receptor. Interactions of ketamine with opioid receptors, muscarinic acetylcholine receptors and different voltage-gated channels have been described. Because of rapid onset and short duration of action, ketamine is frequently used for induction of anesthesia and for short term surgical procedures. Due to its hallucinogenic effects even at subanesthetic doses it is abused by medical personnel and ketamine (also known as special K) became popular among the European party scenes as a drug of abuse where it is taken intranasally, injected, smoked, or ingested as part of a drink. Ketamine consists of a racemic mixture of two enantiomers, S-ketamine and R-ketamine. The S-enantiomer has a four times higher affinity for the NMDA receptor than the R-enantiomer and also binds to the μ and κ opioid receptors. The anesthetic potency of S-ketamine is two to three times higher than that of the racemic mixture. The incidence of unwanted side-effects at equal plasma concentrations is identical for both enantiomers, but since lower doses of the S-enantiomer are needed to maintain an equal state of anesthesia, fewer side-effects and shorter recovery times are seen with the single enantiomer preparation. The pK_a value of ketamine is 7.5 and it is therefore positively charged at physiological pH. The partition coefficient, also named the log P (octanol/water) value, accounts for 3.1. Due to its high lipid solubility and low protein binding (20-50% is bound to plasma proteins), ketamine is extensively distributed throughout the body. The half-life of the parent compound has been reported to be about 3h and it can be administered intravenously, intramuscularly, orally, rectally, subcutaneously, epidurally and on the transnasal route [1-8].

The metabolism of ketamine has been studied in humans and various animal species. It was found that ketamine, incubated with human liver microsomes (HLM), is metabolized by the hepatic cytochrome P450 (CYP) enzyme system through N-demethylation to norketamine followed by hydroxylation of norketamine at various locations at the cyclohexanone and chlorophenyl rings and the formation of 5,6-dehydronorketamine [8-14]. The major metabolic phase I pathway for S-ketamine is depicted in Fig. 1. Direct hydroxylation of ketamine prior to N-demethylation is also possible but occurs to a marginal extent. The same metabolites are

observed for other species *in vitro* [14-17], as well as *in vivo* in humans and animals [15,18-23].
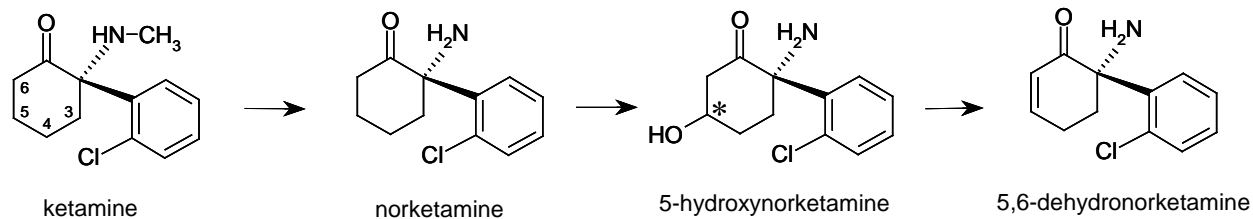
Figure 1. Chemical structures for S-ketamine, S-norketamine, 5-hydroxynorketamine and S-5,6-dehydronorketamine. The asterisk marks the formation of a carbon stereogenic center which is formed upon hydroxylation of norketamine at the cyclohexanone ring.

The pharmacological activities of the metabolites have not been well studied in humans. In view of the growing interest concerning ketamine as a therapeutic agent and a drug of abuse, knowledge of the metabolism of ketamine in humans and the involved cytochrome P450 enzymes is of importance. Previous studies with lymphoblast-expressed CYP enzymes evidenced that CYP3A4, CYP2B6 and CYP2C9 are mainly responsible for the biotransformation of ketamine to its active metabolite norketamine [11,12]. Furthermore, incubation of the two ketamine enantiomers with 12 single CYP enzymes revealed also N-demethylation activities for CYP2A6, CYP2C8, CYP2C19 and CYP2D6 [11]. *In vitro* studies with individual enzymes concerning metabolites other than norketamine could not be found in the literature. Thus, efforts in elucidating the CYP enzymes involved in the metabolism of ketamine and norketamine were undertaken. In addition the stereoselectivity of each metabolic pathway was investigated. This work was executed in the context of a multidisciplinary research cooperation elucidating the metabolism and the pharmacokinetics of ketamine in different species. The project includes studies *in vitro* [14,15,17,24] and *in vivo* [15,22,23,25-29] for which enantioselective capillary electrophoresis (CE) with multiple isomer sulfated β-cyclodextrin (β-CD) as chiral selector [15,22,23] was employed to analyze the stereoisomers of ketamine and its metabolites in equine, canine and human biosamples.

The main goal of this project was to identify human CYP enzymes which are involved in the biotransformation of ketamine to norketamine *in vitro* and to elucidate which of these enzymes catalyze the formation of further metabolites. Individual recombinant human CYP enzymes from a baculovirus expression system (referred to as SUPERSOMES) were used for that task. Special emphasis was put on the stereoselective aspect of ketamine

biotransformation by using enantioselective CE for detection of analytes. Racemic ketamine and norketamine were incubated with CYP1A1, CYP1A2, CYP2A6, CYP2B6, CYP2C9, CYP2C19, CYP2D6, CYP3A4 and CYP2E1 SUPERSOMES, and data were compared to those obtained with incubation of the same compounds with HLM and human liver cytosol. Furthermore, the kinetics of ketamine to norketamine N-demethylation were examined for CYP3A4 and CYP2B6 and compared to those obtained with HLM. Two kinetic models (Michaelis-Menten and Hill) were fitted to the experimental data.

2   Materials and Methods

2.1   Chemicals, reagents and solutions

Racemic ketamine hydrochloride was obtained from the pharmacy of the Inselspital (Bern, Switzerland). Norketamine as hydrochloride solution in methanol (1 mg/mL of the free base) was purchased from Cerilliant (Round Rock, USA) and (+)-pseudoephedrine hydrochloride was from Fluka (Buchs, Switzerland). Sulfated β-CD (7-11 mol sulfate/mol β-CD) was obtained from Sigma-Aldrich Chemie (Schnelldorf, Germany). Tris and HCl (37 %) were from Merck (Darmstadt, Germany), H_3PO_4 (85 %), ethyl acetate and diammonium hydrogenphosphate from Fluka (Buchs, Switzerland), and dichloromethane from Biosolve (Valkenswaard, The Netherlands). Calibrator and control samples used for quantification of ketamine and norketamine enantiomers were prepared in 100 mM phosphate buffer (pH 7.4).

Baculovirus-insect-cell-expressed human CYP3A4 + P450 Reductase + cytochrome b5 SUPERSOMES™, human CYP2C19 + P450 Reductase + cytochrome b5 SUPERSOMES™, human CYP2D6*1 + P450 Reductase SUPERSOMES™, human CYP1A1 + P450 Reductase SUPERSOMES™, human CYP1A2 + P450 Reductase SUPERSOMES™, human CYP2C9*1 (Arg_{144}) + P450 Reductase + cytochrome b5 SUPERSOMES™, human CYP2B6 + P450 Reductase + cytochrome b5 SUPERSOMES™, human CYP2A6 + P450 Reductase + cytochrome b5 SUPERSOMES™, and human CYP2E1 + P450 Reductase + cytochrome b5 SUPERSOMES™ were purchased from Gentest (Woburn, MA, USA, distributed through Anawa Trading, Wangen, Switzerland). The mixed gender pool of HLM, containing CYP1A2, CYP2A6, CYP2B6, CYP2C8, CYP2C9, CYP2C19, CYP2D6, CYP2E1, CYP3A4, CYP4A and flavin monooxygenase (FMO), with a protein concentration of 20 mg/mL in 250 mM sucrose, pooled human liver cytosol and the nicotinamide adenine

dinucleotide phosphate (NADPH) regenerating system were also from Gentest. The regenerating system comprises two solutions, solution A composed of 31.0 mM $NADP^+$, 66 mM glucose-6-phosphate (G-6-P) and 66 mM $MgCl_2$ and solution B containing 40 U/mL glucose-6-phophate dehydrogenase in 5 mM sodium citrate. The microsomes were stored in aliquots at –80 °C and the NADPH regenerating system was kept at –18 °C until use.

2.2 *In vitro* reactions and sample preparation for metabolic studies

A mixture containing substrate (either 50 µM racemic ketamine or 50 µM racemic norketamine) and NADPH regenerating system (1.55 mM $NADP^+$, 3.3 mM G-6-P, 0.4 U/mL G-6-P dehydrogenase, 3.3 mM $MgCl_2$) in 100 mM potassium phosphate buffer (pH 7.4) was preincubated at 37°C for 3 min. In case of CYP2C9, a 100 mM Tris buffer (pH 7.5) was used instead of the phosphate buffer. For most CYP enzymes (1A1, 1A2, 3A4, 2C19, 2D6 and 2C9 with CYP content of 1000 pmol/mL), the enzymatic reaction was started at 37°C after addition of a 16.3 µL aliquot of SUPERSOMES to a 760 µL reaction solution, which provided microsomal incubation mixtures comprising 21 pmol CYP/mL. For CYP2E1, which has twice the CYP content compared to the other SUPERSOMES used, the microsomal solution was diluted two-fold prior to addition of 16.3 µL of the diluted solution. Aliquots of 200 µL were withdrawn from the reaction mixture after 0, 60 and 120 min of incubation and immediately mixed with 500 µL sodium hydroxide (0.2 M) and 30 µL of the internal standard solution (30 µg/mL (+)-pseudoephedrine hydrochloride). For CYP2B6, CYP2A6, HLM and cytosol, the reaction was commenced with 32.5 µL of SUPERSOMES, HLM or cytosol added to 1510 µL reaction solution and aliquots of 200 µL were withdrawn from the reaction mixture after 0, 60, 120 and 180 min of incubation. All experiments were performed in duplicates. For extraction, 5 mL of a dichloromethane/ethylacetate (75:25 %, v/v) solvent mixture was added to the sample. The tubes were closed, shaken for 10 min and centrifuged at about 3500 x *g* for 5 min. The upper aqueous phase and the protein aggregates were removed with a glass pipette under vacuum and the organic phase was decanted into a rounded bottom tube. After acidification with a drop of hydrochloric acid (37 %), the organic solvent was evaporated under a stream of air at about 40°C. Residues from the evaporation were dissolved in 200 µL methanol and vortexed. After evaporation, the residues were redissolved in 30 µL of 5 mM Tris-phosphate buffer (pH 2.5).

2.3 *In vitro* reactions and sample preparation for kinetic studies

For the characterization of the ketamine N-demethylation with individual CYPs, kinetic studies were performed with 10 substrate concentrations of racemic ketamine ranging from 5 to 1000 µM. The CYP content was 24 pmol/mL, the incubation time was 8 min and the final volume was 200 µL. Linearity of the norketamine formation rate was established previously with respect to microsomal protein and incubation time [14,17]. After incubation, enzymatic reactions were stopped by adding 500 µL sodium hydroxide (0.2 M) to the sample. 50 µL of the internal standard solution was added prior to extraction. All experiments were performed in duplicates. For the extraction, 3 mL of dichloromethane/ethylacetate (75:25 %, v/v) was added to the sample. The closed tubes were shaken for 10 min and centrifuged at about 3500 x *g* for 5 min. The upper aqueous phase and the protein aggregates were removed and the organic phase was decanted into a rounded bottom tube. After acidification with a drop of 50 mM phosphoric acid (phosphoric acid was used instead of HCL to prevent corrosion of the water bath), the organic solvent was evaporated under a stream of air at about 45 °C. Residues were dissolved in 200 µL methanol and vortexed, evaporated to dryness and redissolved in 50 µL of 5 mM Tris-phosphate buffer (pH 2.5).

2.4 CE instrumentation and analytical conditions

A Proteome Lab PA 800 instrument or a P/ACE MDQ capillary electrophoretic system (both Beckman Coulter, Fullerton, CA, USA) equipped with a 50 µm ID fused-silica capillary (Polymicro Technologies) of 45 cm total length (effective length of 34 cm) was used. Samples were introduced from 0.5 mL polypropylene vials by applying a vacuum of 1.0 psi (1 psi = 6894.8 Pa) for 7 s (metabolic pattern) or for 6 s (kinetic study). The applied voltages were -17.0 kV (reversed polarity, current about –35 µA) and –20 kV (about -45 µA), respectively. The temperature of the circulating cooling fluid in the capillary cartridge and around sample trays was set to 20 ^{0}C. A positive pressure of 0.1 psi to induce a buffer flow towards the anode was applied during the entire run. An on-column UV variable wavelength detector set to 195 nm was employed for analyte detection. The running buffer was composed of 35 mM (metabolic pattern) and 50 mM (kinetic study) Tris, phosphoric acid (pH 2.5) and 10 mg/mL of sulfated β-CD (70%/30% blend of batches 13112JD and 13307MA). Fresh buffer was prepared every day. Before each experiment, the capillary was sequentially rinsed

with 0.1 M NaOH (2 min, 20 psi), bidistilled water (1 min, 20 psi) and running buffer (1 min, 20 psi). Quantitation of ketamine and norketamine enantiomers was based upon internal calibration using corrected peak areas (areas divided by detection time). Aqueous calibrators containing 0.5, 2.5, 7.5, 15.0 and 30.0 µM of each enantiomer were employed as described previously [14]. A typical electropherogram obtained with a calibrator sample is shown as top graph in Fig. 2. Assay specifications were the same as reported by Schmitz et al. [14,17]. Small differences of the chiral selector concentration in the running buffer resulted in appreciable differences in detection times from day to day (Fig. 2). Based on the internal calibration used and frequent renewal of the calibration data, however, these variations did not have an impact on quantitation.
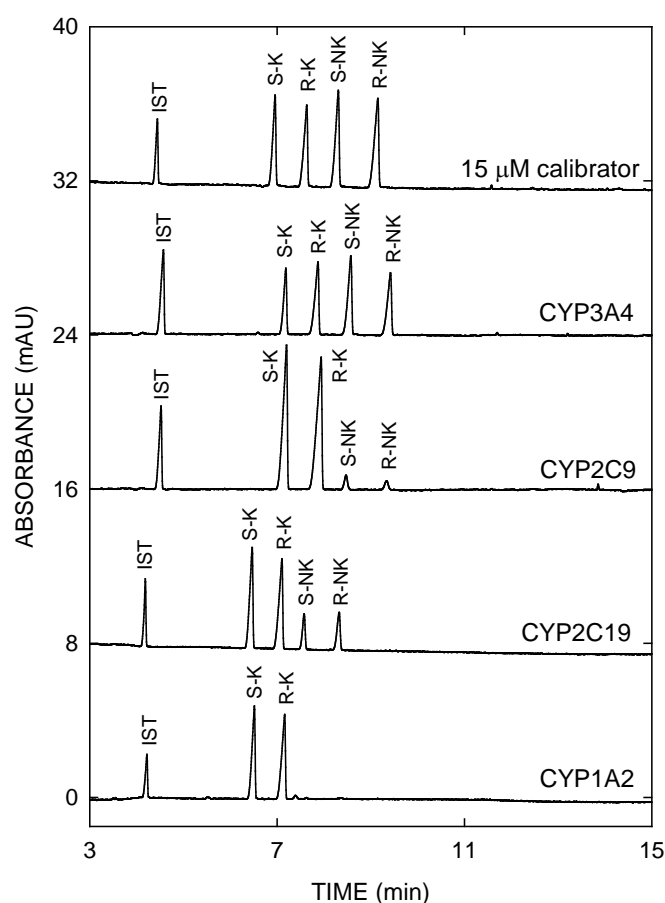
Figure 2. Electropherograms obtained after a 2 h incubation of selected single CYP enzymes with 50 µM racemic ketamine and a calibrator sample containing 15 µM of each ketamine and norketamine enantiomer. For presentation purposes, data are plotted with a y-scale offset of 8 mAU. Key: S-K, S-ketamine, R-K, R-ketamine, S-NK, S-norketamine, R-NK, R-norketamine, IST, internal standard.

2.5 Data analysis

Initial enantiomer substrate concentration against the norketamine formation rate (pmol norketamine/min/pmol CYP) was plotted and analyzed by two mathematical models (Michaelis-Menten and Hill) using nonlinear least square regression analysis on the Graph Pad Prism 4 software (Graph Pad Software, San Diego, USA) and SigmaPlot version 10.0 (SPSS, Chicago, IL, USA). Curves were compared between enantiomers with a paired student´s T-test using Microsoft Excel software (Microsoft, Seattle, USA). A p value < 0.05 was considered significant.

3   Results and Discussion

3.1 Identification of enzymes catalyzing N-demethylation of ketamine

Screening of nine human CYP enzymes for ketamine N-demethylation was performed in 2-h incubations using 50 μM racemic ketamine. Samples withdrawn at 0, 60 and 120 min were analyzed be enantioselective CE using a 35 mM Tris-phosphate buffer (pH 2.5) containing 10 mg/mL of sulfated β-CD as a mixture from two different lots. Selected electropherograms are presented in Fig. 2 and N-demethylation results are summarized in Fig. 3. The data reveal that CYP3A4, CYP2C9, CYP2A6, CYP2D6, CYP2B6 and CYP2C19 are responsible for norketamine formation. Norketamine was not detected in the samples comprising CYP1A2, CYP1A1, CYP2E1 and human liver cytosol instead of a CYP (bottom graph in Fig. 2, other data not shown). Quantitation of the enantiomers of ketamine and norketamine was accomplished as described previously for HLM and liver microsomes of other species [14].

The data presented in Fig. 3 suggest that highest demethylation activity is obtained with CYP2B6, followed by CYP3A4, CYP2C19, CYP2A6, CYP2C9 and CYP2D6. Similarly, Yanagihara et al. [11] reported ketamine N-demethylation activities in microsomes from human B-lymphoblastoid cell lines expressing the same six enzymes and CYP2C8, CYP2E1 and CYP1A1, whereas no responses were observed for CYP1A2, CYP1B1 and CYP4A11. Among the CYP enzymes tested, only CYP2B6, CYP3A4 and CYP2C9 showed high activities, whereas the responses with the other enzymes were small with those of

CYP2E1 and CYP1A1 being the smallest. Furthermore, Hijazi and Boulieu [12] reported that lymphoblast expressed CYP2B6 showed higher demethylation activity than CYP3A4 and CYP2C9 which is in agreement with the Yanagihara et al. [11] data for the same three enzymes. Our data were generated with individual baculovirus cDNA-expressed human CYP enzymes. Compared to the behavior of the lymphoblast expressed enzymes reported in the literature, a higher activity of CYP2C19 compared to that of CYP2C9 was observed. Otherwise, qualitative agreement was noted between the two systems. The fact that CYP1A1 and CYP2E1 did not reveal any activity does not make a significant difference as the activities reported by Yanagihara et al. [11] were very small. Lack of analytical sensitivity of the CE assay used in our work could be responsible for this difference.
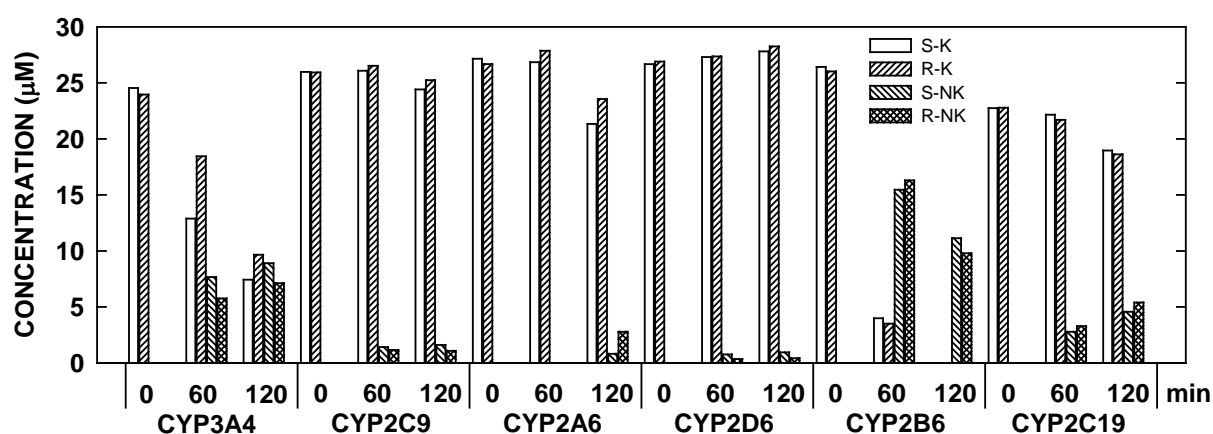
Figure 3. Ketamine demethylation data of single CYP enzymes for incubations with 50 µM racemic ketamine after 0, 60 and 120 min of incubation time. Key: S-K, S-ketamine, R-K, R-ketamine, S-NK, S-norketamine, R-NK, R-norketamine.

The data presented in Figs. 2 and 3 suggest that ketamine is demethylated in a stereoselective manner. Electropherograms obtained after metabolism of ketamine in the presence of single CYP enzymes reveal apparent stereoselectivities. This is particularly obvious for CYP3A4 when its electropherogram (second graph from top in Fig. 2) is compared to that of a calibrator sample in which equal amounts of the enantiomers are present (top graph in Fig. 2). For CE analysis of racemic mixtures, the first detected enantiomer peak is higher compared to the second (top graph in Fig. 2). For the CYP3A4 data, the peak for S-ketamine is smaller than that of R-ketamine which indicates that S-ketamine is faster metabolized compared to R-ketamine. The same is true for the quantitative data presented in Fig. 3. Furthermore, data obtained with CYP2B6 revealed the formation of other peaks that

could be related to metabolites of norketamine (cf. Section 3.2). Norketamine peaks at 120 min are smaller compared to those at 60 min suggesting that further metabolites are formed from norketamine (Fig. 3). Similarly, incubation of ketamine with HLM revealed the presence of norketamine and four of its metabolites, as previously described [14].

3.2 Identification of enzymes catalyzing the formation of norketamine metabolites

Incubation of 50 µM racemic norketamine with the nine SUPERSOMES revealed the CYP enzymes involved in the formation of norketamine metabolites. Analysis of the samples was done in the same way as for the incubations of ketamine. Selected electropherograms are presented in Fig. 4. The data revealed that norketamine metabolites are formed by CYP2A6 and CYP2B6. No norketamine metabolites were detected by enantioselective CE for CYP3A4, CYP2C9, CYP2C19, CYP2D6, CYP1A1, CYP1A2 and CYP2E1 (Fig. 4, depicting data for CYP3A4 only).

The obtained electropherograms monitored for the incubations with CYP2B6 and CYP2A6 revealed peaks for the stereoisomers of norketamine, 5,6-dehydronorketamine and three hydroxylated norketamine metabolites with hydroxylation at the cyclohexanone ring as shown in Fig. 4. The enantiomers of 5,6-dehydronorketamine were identified as described in [23], whereas hydroxylated norketamine metabolite peaks (peaks I, III and IV in Fig. 4) were identified as described in [15]. Identification of the metabolites occurred via spiking with standards which were extracted from pony urine and characterized by LC-MS and LC-MS[n] [15,23]. All peaks labeled with the prefixes S and R stem from S-norketamine and R-norketamine, respectively. In previous work from our laboratory working with *in vivo* and *in vitro* samples of equines [15], it could be concluded that compounds I and III are precursors of 5,6-dehydronorketamine. Furthermore, because Woolf and Adams [9] did not observe the formation of 5,6-dehydronorketamine in incubations of 6-hydroxynorketamine with HLM, it could be assumed that hydroxynorketamine compounds I and III represent stereoisomers of 5-hydroxynorketamine. The data presented here are in agreement with this assumption. 5,6-dehydronorketamine is detected in the experiments with CYP2B6 in which hydoxynorketamine compounds III and I were found (center graph of Fig. 4). The data obtained with CYP2A6 did reveal a significant amount of compound I but almost no compound III (tiny peak for R-III only) and a small amount of R-DHNK (top graph of Fig. 4).

This suggests that compound III is more likely to be converted into 5,6-dehydronorketamine. Without having standards of these compounds, however, absolute proof cannot be obtained. As discussed previously, compound IV is most likely (Z)-6-hydroxynorketamine [15]. The formation of compound II (tentatively assigned to 4-hydroxynorketamine), which was found in *in vivo* samples of equines [15] and possibly also *in vitro* with HLM [14], was not observed in the experiments with the two individual CYP enzymes. Compounds I, III and IV are identical to those found in incubations of ketamine with liver microsomes of humans, cats and horses [14] and in incubations of norketamine with HLM (data not shown).
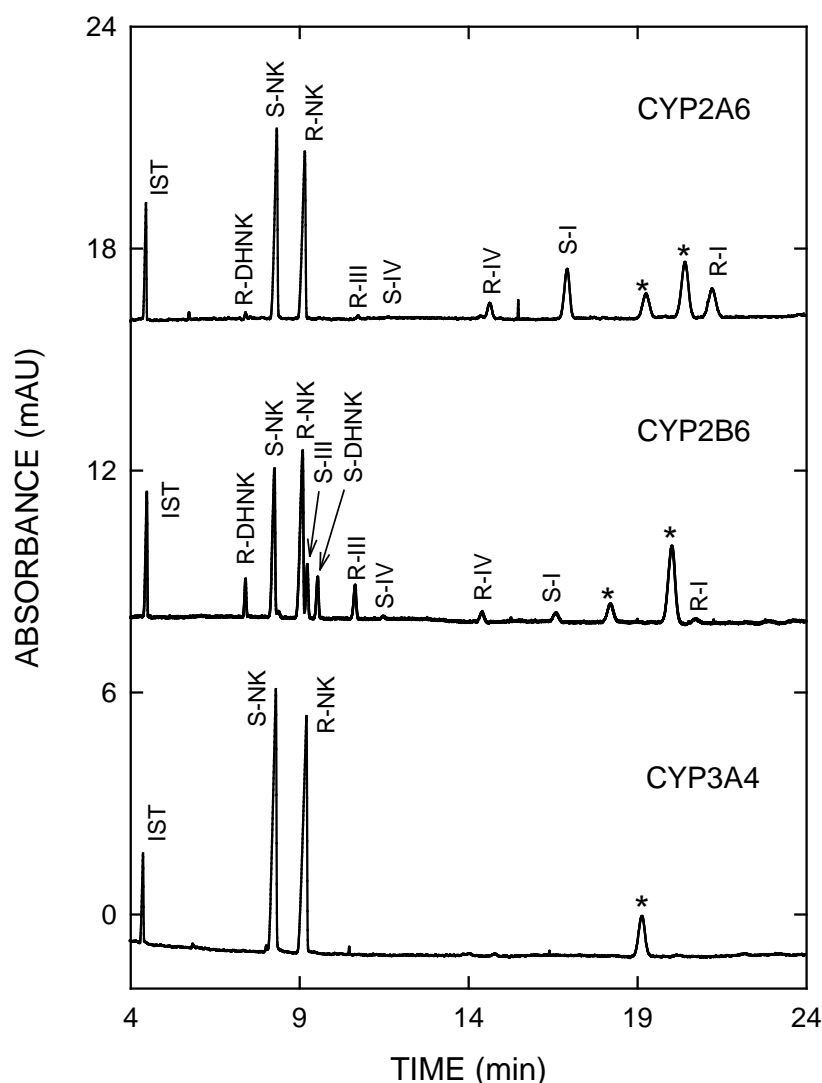
Figure 4. Electropherograms obtained after a 2 h incubation of selected single CYP enzymes with 50 µM racemic norketamine. For presentation purposes, data are plotted with a y-scale offset of 8 mAU. Asterisks mark peaks that are unrelated to norketamine metabolites. Key: S-NK, S-norketamine, R-NK, R-norketamine, S-DHNK, S-5,6-dehydronorketamine, R-DHNK, R-5,6-dehydronorketamine, I, II and IV, hydoxylated norketamine metabolites, IST, internal standard.

Incubation of CYP2B6 with racemic norketamine revealed that S-norketamine was metabolized faster than R-norketamine (center graph of Fig. 4). This difference was not observed with CYP2A6 (top graph of Fig. 4). However, it is apparent that hydroxylated norketamine metabolites and 5,6-dehydronorketamine is formed in a stereoselective manner. The specific content of individual CYP450 isoforms in HLM vary strongly. Relative amounts of the CYP2A6, CYP2B6 and CYP3A4 enzymes are reported to be 4.0, 0.2 and 28.8 %, respectively [30]. Thus, it was interesting to find that norketamine is only metabolized by two CYP enzymes which have a low abundance (total of 4.2 % of CYP content in liver mirosomes). To the contrary, ketamine is demethylated by CYP enzymes whose total CYP content in liver microsomes approximates 53 %.

3.3 Characterization of N-demethylation kinetics of ketamine

For CYP2B6 and CYP3A4, the two enzymes with highest demethylation activity (Fig. 3), the demethylation kinetics were assessed via determination of the norketamine formation rate as function of substrate concentration using an incubation time interval of 8 min. Preliminary experiments revealed that an 8 min incubation was within the linear range of norketamine formation and did not produce any detectable metabolites of norketamine. Racemic ketamine was applied and the ketamine enantiomer concentration was varied between 2.5 and 500 μM. The concentrations of the norketamine enantiomers were determined by enantioselective CE and their formation rates were calculated in relation to the incubation time and the amount of CYP enzyme involved. Data are presented in Fig. 5 and were evaluated according to the Michaelis-Menten and Hill kinetic models. The single site Michaelis-Menten model is based on

$$v = V_{max} [S] / (K_m + [S]) \tag{1}$$

whereas the Hill equation is expressed by

$$v = V_{max} [S]^n / (K'^n + [S]^n) \tag{2}$$

where v is the product formation rate (velocity) of the metabolic reaction, $[S]$ is the substrate concentration, K_m is the Michaelis-Menten constant which is the concentration at which the formation rate is 50 % of V_{max}, V_{max} is the maximum formation rate, K' is a constant of the autoactivation model which is equivalent to K_m when $n = 1$, and n is the Hill coefficient [17,31,32]. Standard parameters such as regression coefficient (R^2) and F-test were used to

determine the quality of a fit to a specific model. For model comparison with the F-test, $p < 0.05$ means that the alternative model (Hill model) fits the data significantly better. The determined parameters are summarized in Table 1. For the experiment with CYP3A4, the Hill equation (Eq. (2)) did not provide a better fit to the experimental data ($p > 0.05$, Table 1), indicating that autoactivation does not take place. No difference was found for the correlation coefficients (R^2) and n values were determined to be close to unity (Table 1). Thus, the experimental data can best be described with the Michaelis-Menten model (Eq. (1)). For the kinetics of S- and R-ketamine N-demethylation, significant differences between K_m and V_{max} values were observed with both values being higher for the formation of S-norketamine compared to R-norketamine (Table 1). The two curves were found to differ significantly ($p = 0.004$). Thus, the conclusion can be drawn that the demethylation of ketamine via CYP3A4 occurs stereoselectively. For the experiment with CYP2B6 the Hill equation (Eq. (2)) was found to provide a better fit to the experimental data ($p < 0.05$, Table 1), indicating that autoactivation does take place. The correlation coefficients (R^2) obtained for the Hill model were closer to unity compared to those with the Michaelis-Menten model (Table 1). The Hill coefficients for S-norketamine and R-norketamine formation were 0.47 and 0.59, respectively. In contrast to the case with CYP3A4, these values are not close to unity. The regression curves for S-norketamine and R-norketamine formation appear to be almost superimposed with that for R-norketamine being lower compared to that for S-norketamine (Fig. 5B) and calculated V_{max} values differ less than 10 % (Table 1). It was surprising to realize, that the two curves were found to differ significantly ($p = 0.018$) from a statistical point of view, indicating that N-demethylation of ketamine by CYP2B6 is stereoselective as well. There would be no significant difference if the regression curves would intersect.
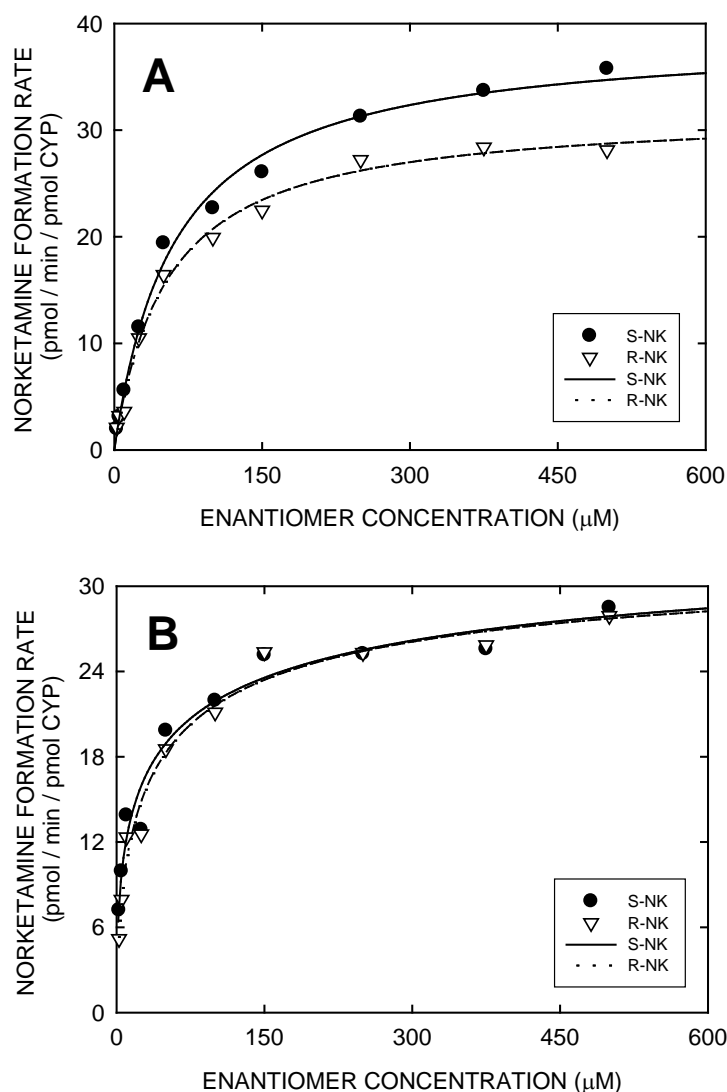
Figure 5. Enantioselective kinetics of norketamine formation by (A) CYP3A4 and (B) CYP2B6. Racemic ketamine was incubated for 8 min with 24 pmol CYP/mL reaction mixture and norketamine formed was quantitated by enantioselective capillary electrophoresis. Symbols denote the mean of duplicates. Solid and dotted lines are predicted values based on nonlinear regression analysis using (A) the Michaelis-Menten equation and (B) the Hill equation. Key: ● = S-norketamine (S-NK), ▽ = R-norketamine (R-NK).

Intrinsic clearance (CL_{int}), which defines the rate of metabolism for a given drug concentration, and maximal clearance due to autoactivation (CL_{max}), which provides an estimate of the highest clearance attained as substrate concentration increases before any saturation of the enzyme sites, were calculated according to $CL_{int} = V_{max} / K_m$ and $CL_{max} = (V_{max} / K') [(n-1) / n(n-1)^{1/n}]$, respectively [31]. Clearance values are listed in Table 1. The data reveal that the clearance for CYP2B6 is larger compared to CYP3A4. Furthermore, calculated clearance values for the formation of S-norketamine are significantly larger compared to those of R-norketamine in all cases.

Table 1. Kinetic parameters for N-demethylation of ketamine and model comparison [a]

Enzyme system	Product	Michaelis-Menten model				Hill model					F-test [f]
		R^2	K_m [μM]	V_{max} [pmol/min/ pmol CYP]	CL_{int} [b] [μL/min/ Pmol CYP]	R^2	K' [c] [μM]	V_{max} [pmol/min/ pmol CYP]	CL_{max} [d] [μL/min/ pmol CYP]	n [e]	p-value
CYP3A4	S-NK	0.9934	61.18	38.95	0.64	0.9951	76.27	42.21	0.87	0.8676	0.1644
CYP3A4	R-NK	0.9929	53.36	31.79	0.60	0.9929	53.79	31.89	0.62	0.9930	0.9501
CYP2B6	S-NK	0.8957	11.89	26.25	2.21	0.9639	43.08	36.60	3.65	0.4743	0.0083
CYP2B6	R-NK	0.9423	17.61	27.01	1.53	0.9773	37.38	33.66	2.81	0.5937	0.0135
HLM	S-NK	0.9705	62.80	13.41	0.21	0.9742	80.76	14.52	0.32	0.8194	0.3536
HLM	R-NK	0.9703	69.58	12.64	0.18	0.9723	83.60	13.42	0.26	0.8619	0.5132

a) Data for incubation of racemic ketamine derived from mean values of duplicate determinations.

b) $CL_{int} = V_{max} / K_m$.

c) K' is equivalent to K_m when n=1.

d) $CL_{max} = (V_{max} / K')\ [(n-1) / n(n-1)^{1/n}]$.

e) n = Hill coefficient.

f) Model comparison.

3.4 Comparison with *in vitro* data obtained with HLM

In order to approximate the *in vivo* situation metabolite formation from ketamine incubated with single CYP enzymes was compared to incubations with HLM containing a mixture of enzymes composed of CYP1A2, CYP2A6, CYP2B6, CYP2C8, CYP2C9, CYP2C19, CYP2D6, CYP2E1, CYP3A4, CYP4A and FMO. In incubations of HLM with ketamine and norketamine all metabolites produced by CYP2B6 and CYP2A6 were detected. These data suggest that the detected metabolites are mainly formed from norketamine and not via hydroxylation of ketamine followed by N-demethylation of hydroxyketamine metabolites. Thus, N-demethylation of ketamine is the major metabolic step in man as was previously reported for equines [15].

The kinetic data for the N-demethylation in presence of HLM, which were assessed with racemic ketamine at 10 different concentrations (6 - 2000 µM) and having a final protein concentration of 0.5 mg/mL (total CYP content: about 6 pmol/mL) [14], are included in Table 1. Data analysis with both models, Michaelis-Menten and Hill, resulted in reasonable fits. For both enantiomers, the p-values of the F-test were determined to be higher than 0.05 and the Hill coefficients (n) to be close to unity. This suggests that the Michaelis-Menten fit is better, which is in agreement with the results discussed by Kharasch et al. [10] and Schmitz et al. [14]. A difference in the N-demethylation rates of the ketamine enantiomers was observed with HLM. Compared to S-norketamine, a smaller amount of R-norketamine was formed which is consistent with our previous findings [14,24]. The formation curves for S- and R-norketamine were found to differ significantly (p = 0.0003). Furthermore, clearance for the S-enantiomer was significantly larger compared to the R-enantiomer, which is in agreement with data published by Yanagihara et al. [11]. The clearance values were smaller than those observed for the two single CYPs (Table 1).

4 Conclusions

The enantioselective CE assay for analysis of ketamine and its metabolites in microsomal preparations has been successfully used to identify individual CYP enzymes that are involved in the metabolism of ketamine and norketamine. The findings indicate that a large proportion of the CYP enzymes in the liver are involved in the demethylation of ketamine whereas only two low abundant enzymes metabolize norketamine. To our

knowledge, the presented data are the first which identify enzymes that are involved in biotransformation of norketamine to further metabolites in man. Results from our study reveal norketamine to be the major metabolite resulting from ketamine metabolism. Among the enzymes tested, CYP3A4 and CYP2B6 could be shown to be the major enzymes responsible for the N-demethylation of ketamine. Hijazi and Boulieu [12] observed that a correlation between ketamine N-demethylation activity and CYP3A4- and CYP2B6-specific activities exists in human microsomes. This conclusion is in agreement with our results. For these two enzymes, analysis by enantioselective CE provided the *in vitro* pharmacokinetics of the formation of the norketamine enantiomers in incubations with racemic ketamine. CE is thereby shown to be an attractive approach to elucidate differences in the stereoselectivity in the investigated metabolic steps *in vitro*. Furthermore, CYP2B6 and CYP2A6 were found to be the only CYP enzymes to produce all metabolites found in incubations with ketamine or norketamine and HLM. CYP2B6 was long considered not to be of importance in drug metabolism. New investigations indicate the high relevance of this enzyme in the metabolism of a number of drugs. It particularly catalyzes various oxidative reactions of non-planar, weakly basic and fairly lipophilic compounds with one or two hydrogen bond acceptors [33], such as ketamine [11,12] and methadone [34,35].

Acknowledgements

References

[1]   R.C. Baselt, R.H. Cravey, Disposition of Toxic Drugs and Chemicals in Man, 4th Edition, Chemical Toxicology Institute, Foster City, California, 1995, pp. 412-414.

[2]   A.C. Moffat, M.D. Osselton, B. Widdop, L.Y. Galichet, Eds., Clarke's Analysis of Drugs and Poisons in pharmaceuticals, body fluids and postmortem material, 3rd Edition, Pharmaceutical Press, London, UK, 2004, pp.1152-1153.

[3]   B. Sinner, B.M. Graf, Handb. Exp. Pharmacol. 182 (2008) 313-333.

[4]   R. Craven, Anaesthesia 62 (2007) 48-53.

[5]   L.C. Mathisen, P. Skjelbred, L.A. Skoglund, I. Oye, Pain 61 (1995) 215-220.

[6]   H.A. Adams, C. Werner, Anaesthesist 46 (1997) 1026-1042.

[7]   A. Cromhout, Emerg. Med. 15 (2003) 155-159.

[8]   M.K. Huang, C. Liu, J.H. Li, S.D. Huang, J. Chromatogr. B 820 (2005) 165-173.

[9]   T.F. Woolf, J.D. Adams, Xenobiotica 17 (1987) 839-847.

[10]   E.D. Kharasch, R. Labroo, Anesthesiology 77 (1992) 1201-1207.

[11]   Y. Yanagihara, S. Kariya, M. Ohtani, K. Uchino, T. Aoyama, Y. Yamamura, T. Iga, Drug Metab. Dispos. 29 (2001) 887-890.

[12]   Y. Hijazi, R. Boulieu, Drug Metab. Dispos. 30 (2002) 853-858.

[13]   S.C. Turfus, M.C. Parkin, D.A. Cowan, J.M. Halket, N.W. Smith, R.A. Braithwaite, S.P. Elliot, G.B. Steventon, A.T. Kicman, Drug Metab. Dispos. 37 (2009) 1769-1778.

[14]   A. Schmitz, W. Thormann, L. Moessner, R. Theurillat, K. Helmja, M. Mevissen, Electrophoresis 31 (2010) 1506-1516.

[15]   A. Schmitz, R. Theurillat, P.-G. Lassahn, M. Mevissen, W. Thormann, Electrophoresis 30 (2009) 2912-2921.

[16]   J.D. Adams, T.A. Baillie, A.J. Trevor, N. Castagnoli, Biomed. Mass Spectrom. 8 (1981) 527-538.

[17]   A. Schmitz, C.J. Portier, W. Thormann, R. Theurillat, M. Mevissen, J. Vet. Pharmacol. Ther. 31 (2008) 446-455.

[18]   S.A. Savchuk, E.S. Brodskii, B.A. Rudenko, A.A. Formanovskii, I.V. Mikhura, N.A. Davydova, J. Anal. Chem. 52 (1997) 1175-1186.

[19]   S. Bolze, R. Boulieu, Clin.Chem. 44 (1998) 560-564.

[20]   Y. Hijazi, C. Bodonian, M. Bolon, F. Salord, R. Boulieu, Br. J. Anaesth. 90 (2003) 155-160.

[21]   D.P.K. Lankveld, B. Driessen, L.R. Soma, P.J. Moate, J. Rudy, C.E. Uboh, P. van Dijk, L.J. Hellebrekers, J. Vet. Pharmacol. Ther. 29 (2006) 477-488.

[22]   R. Theurillat, M. Knobloch, O. Levionnois, P. Larenza, M. Mevissen, W. Thormann, Electrophoresis 26 (2005) 3942-3951.

[23]   R. Theurillat, M. Knobloch, A. Schmitz, P.G. Lassahn, M. Mevissen, W. Thormann, Electrophoresis 28 (2007) 2748-2757.

[24]   L. Capponi, A. Schmitz, W. Thormann, R. Theurillat, M. Mevissen, Am. J. Vet. Res. 70 (2009) 777-786.

[25]   M.P. Larenza, M.F. Landoni, O.L. Levionnois, M. Knobloch, P.W. Kronen, P. W., R. Theurillat, U. Schatzmann, W. Thormann, Br. J. Anaesth. 98 (2007) 204-212.

[26]   M.P. Larenza, M. Knobloch, M.F. Landoni, O.L. Levionnois, P.W. Kronen, R. Theurillat, U. Schatzmann, W. Thormann, Vet. J. 177 (2008) 432-435.

[27]   M. Knobloch, C.J. Portier, O.L. Levionnois, R. Theurillat, W. Thormann, C. Spadavecchia, M. Mevissen, Toxicol. Appl. Pharmacol. 216 (2006) 373-386.

[28]   C. Peterbauer, M.P. Larenza, M. Knobloch, R. Theurillat, W. Thormann, M. Mevissen, C. Spadavecchia, Vet. Anaesth. Analg. 35 (2008) 414-423.

[29]   M.P. Larenza. C. Peterbauer, M.F. Landoni, O.L. Levionnois, U. Schatzmann, C. Spadavecchia, W. Thormann, Am. J. Vet. Res. 70 (2009) 831-839.

[30]   J. Wojcikowski, L. Pichard-Garcia, P. Maurel, W.A. Daniel, Eur. Neuropsychopharmacol. 14 (2004) 199-208.

[31]   J.B. Houston, K.E. Kenworthy, Drug Metab. Dispos. 28 (2000) 246-254.

[32]   T.S. Tracy, M.A. Hummel, Drug Metab. Rev. 36 (2004) 231-242.

[33]   M. Turpeinen, H. Raunio, O. Pelkonen, Curr. Drug Metab. 7 (2006) 705-714.

[34]   J.G. Gerber, R.J. Rhodes, J. Gal, Chirality 16 (2004) 36-44.

[35] R.A. Totah, P. Sheffels, T. Roberts, D. Whittington, K. Thummel, E.D. Kharasch, Anesthesiology 108 (2008) 363-374.

B.3. Enantioselective capillary electrophoresis for the assessment of CYP3A4 mediated ketamine demethylation and inhibition *in vitro*

(Electrophoresis 2011, 32, 2738-2745.)

Enantioselective capillary electrophoresis for the assessment of CYP3A4 mediated ketamine demethylation and inhibition *in vitro*

Hiu Ying Kwan and Wolfgang Thormann

Department of Clinical Pharmacology and Visceral Research,
University of Bern, 3010 Bern, Switzerland.

Abstract

Enantioselective capillary electrophoresis with sulfated cyclodextrins as chiral selectors was used to determine the CYP3A4 catalyzed N-demethylation kinetics of ketamine to norketamine and its inhibition in the presence of ketoconazole *in vitro*. Ketamine, a chiral phencyclidine derivative, was incubated with recombinant human CYP3A4 from a baculovirus expression system as racemic mixture and as single enantiomers. Alkaline liquid/liquid extracts of the samples were analyzed with a pH 2.5 buffer comprising 50 mM Tris and phosphoric acid together with either multiple isomer sulfated β-cyclodextrin (10 mg/mL) or highly sulfated γ-cyclodextrin (2 %, w/v). Data obtained in absence of ketoconazole revealed that the N-demethylation occurred stereoselectively with Michaelis-Menten (incubation of racemic ketamine) and Hill (separate incubation of single enantiomers) kinetics. Data generated in the presence of ketoconazole as inhibitor could best be fitted to a one-site competitive model and inhibition constants were calculated using the equation of Cheng and Prusoff. No stereoselective difference was observed, but inhibition constants for the incubation of racemic ketamine were found to be larger compared with those obtained with the incubation of single ketamine enantiomers.

1   Introduction

Ketamine is a phencyclidine derivative that is used in human and veterinary clinical practice. Due to the rapid onset and short duration of action, ketamine is commonly used for the induction of anesthesia and for short-term surgical operations. Ketamine is also known as a popular drug of abuse. Among the interactions on opioid receptors, muscarinic acetylcholine receptors and different voltage-gated channels, its neurophysiological effect is mainly based on the noncompetitive antagonism on the N-methyl-D-aspartate (NMDA) receptor. Although the pharmacodynamic mechanism is not fully understood yet, there are discussions and investigations about the use of ketamine in the treatment of major depressive disorders. Due to the rapid onset of the antidepressant effect within days, ketamine shows relevant benefits compared with common antidepressants, which take weeks to months to achieve their effects. Ketamine consists of a racemic mixture of two enantiomers, S-ketamine and R-ketamine. The S-enantiomer has a four times higher affinity for the NMDA receptor than the R-enantiomer and also binds to the µ and κ opioid receptors. The anesthetic potency of S-ketamine is two to three times higher than that of the racemic mixture. The incidence of undesirable effects at equal plasma concentrations is identical for both enantiomers, but since lower doses of the S-enantiomer are needed to maintain an equal state of anesthesia, fewer side effects and shorter recovery times are seen with the single enantiomer preparation [1-7].

The metabolism of ketamine has been studied in humans and various animal species, both *in vivo* and *in vitro*. It was found that ketamine is metabolized by the cytochrome P450 (CYP) enzyme system through N-demethylation to norketamine followed by hydroxylation of norketamine at various locations of the cyclohexanone and chlorophenyl rings and the formation of 5,6-dehydronorketamine. Direct hydroxylation of ketamine prior to N-demethylation is also possible but occurs to a marginal extent [8-16]. Recently, the metabolism of ketamine via CYP enzymes was characterized *in vitro* [17]. Among several CYP enzymes investigated, CYP3A4 and CYP2B6 were identified as the most active enzymes involved in the N-demethylation of ketamine. Furthermore, CYP2B6 and CYP2A6 were noted to be the only enzymes responsible for the formation of norketamine metabolites [17]. The pharmacological activities of the metabolites have not been well studied. With so many involved CYP enzymes, drug-drug interactions must be taken into account, when ketamine is given with other substrates, inhibitors or inducers of the involved enzymes. Particularly when chiral drugs such as ketamine are given as a racemic mixture, the enantiomers might be metabolized differently, resulting in another pharmacokinetic profile.

Finding kinetic parameters for prediction of potential drug-drug interactions has been of major interest in drug discovery and development.

During the past two decades, enantioselective capillary electrophoresis (CE) was shown to represent an appealing methodology for the assessment of the stereoselectivity of drug metabolism [18-20], including the determination of kinetic parameters of enzymatic reactions *in vitro* [16,17,21-24]. A multidisciplinary research cooperation elucidating the metabolism and the pharmacokinetics of ketamine in different species is currently undertaken. The complete project includes studies *in vitro* and *in vivo* for which enantioselective CE with sulfated cyclodextrins (CD) as chiral selectors are being employed to determine the stereoisomers of ketamine and its metabolites in equine, canine and human biosamples [15-17,24,25-29]. Thus far, the metabolism of ketamine was characterized using enantioselective CE with multiple isomer sulfated β-CD, an ill-defined mixture of stereoisomers which varies from batch to batch resulting in undesired separation variations and limitations [29]. This prompted us to search for other suitable sulfated CDs, including highly sulfated γ-CD [30]. Data obtained with highly sulfated γ-CD for the analysis of ketamine and norketamine enantiomers in alkaline extracts of *in vitro* samples are reported in this paper for the first time. Enantioselective CE was used for the first time (i) to characterize the complete kinetics of N-demethylation of ketamine to norketamine via CYP3A4 and (ii) to determine the inhibitory effect of ketoconazole, a potent inhibitor on CYP3A4 [31], on the ketamine demethylation *in vitro*. For these tasks, ketamine in absence and presence of ketoconazole was incubated with recombinant human CYP3A4 from a baculovirus expression system as racemic mixture and as single enantiomer, and the stereoselectivity of the N-demethylation biotransformation pathway was investigated. For the elucidation of the kinetic parameters and the inhibition constants, obtained data were fitted to various models using nonlinear regression analysis.

2 Materials and methods

2.1 Chemicals and reagents

Racemic ketamine hydrochloride was obtained from the pharmacy of the Inselspital (Bern, Switzerland) and single enantiomers R- and S-ketamine were kindly provided from CU Chemie Uetikon (Lahr, Germany). Norketamine as hydrochloride solution in methanol (1 mg/mL of the free base) was from Cerilliant (Round Rock, USA) and (+)-pseudoephedrine

hydrochloride was from Fluka (Buchs, Switzerland). Sulfated β-CD (7-11 mol sulfate/mol β-CD) was obtained from Sigma-Aldrich Chemie (Schnelldorf, Germany) and highly sulfated γ-CD (20 % w/v solution) was kindly provided by Beckman Coulter (Fullerton, CA, USA). Ketoconazole was from Sigma-Aldrich (Buchs, Switzerland), Tris from Merck (Darmstadt, Germany), H_3PO_4 (85 %), potassium dihydrogen phosphate and di-potassium hydrogen phosphate from Fluka, and ethyl acetate and dichloromethane from VWR International (Leuven, Belgium). Calibrators and controls used for quantification were prepared in 100 mM phosphate buffer (pH 7.4). Baculovirus-insect-cell-expressed human CYP3A4 + P450 reductase + cytochrome b5 SUPERSOMES™ as well as the nicotinamide adenine dinucleotide phosphate (NADPH) regenerating system were from Gentest (Woburn, MA, USA, distributed through Anawa Trading, Wangen, Switzerland). The enzyme was stored as aliquots at -80°C.

2.2 *In vitro* reactions for kinetic studies

Racemic ketamine, S- and R- ketamine were incubated with CYP3A4 at ten substrate concentrations ranging from 2.5 to 500 μM per enantiomer. The incubation mixture had a final volume of 200 μL and also included NADPH regenerating system consisting of 1.55 mM $NADP^+$, 3.3 mM glucose-6-phosphate, 0.4 U/mL glucose-6-phosphate dehydrogenase, 3.3 mM $MgCl_2$ and 50 μM sodium citrate in 100 mM potassium phosphate buffer (pH 7.4). The mixture was preincubated at 37°C for 4 min. The enzymatic reaction was initiated by adding CYP3A4 (CYP content: 24 pmol/mL), lasted 8 min and was stopped with 500 μL sodium hydroxide (0.2 M) [17]. After addition of 50 μL internal standard solution (30 μg/mL), the samples were extracted as described in Section 2.4. All experiments were performed in duplicates.

2.3 *In vitro* reactions for inhibition studies

Substrate, NADPH regenerating system and ketoconazole in 100 mM potassium phosphate buffer (pH 7.4) were mixed and preincubated at 37°C for 4 min. The enzymatic reaction was started by addition of CYP3A4 (24 pmol/mL), lasted 8 min and was stopped by adding 500 μL sodium hydroxide (0.2 M) to the sample. After adding 50 μL of internal

standard solution, the samples were extracted as described in Section 2.4. All experiments were performed in duplicates.

2.4   Sample preparation

For the extraction, 3 mL of dichloromethane/ethylacetate (75:25 %, v/v) were added to the sample. The closed tubes were shaken for 10 min and centrifuged at about 3500 x *g* for 5 min. The upper aqueous phase and the protein aggregates were removed and the organic phase was decanted into a rounded bottom tube. After acidification with 100 μL of 50 mM phosphoric acid, the organic solvent was evaporated under a stream of air at about 50 ^{0}C. Residues were dissolved in 200 µL methanol and vortexed, evaporated to dryness and redissolved in 50 µL of 5 mM Tris-phosphate buffer (pH 2.5).

2.5   CE instrumentation and analytical conditions

A Proteome Lab PA 800 instrument (Beckman Coulter, Fullerton, CA, USA) equipped with a 50 μm ID fused-silica capillary (Polymicro Technologies, AZ, USA) of 45 cm total length (effective length of 34 cm) was used. Samples were introduced from 0.5 mL polypropylene vials by applying a vacuum of 1.0 psi (1 psi = 6894.8 Pa) for 6 s. The temperature of the circulating cooling fluid in the capillary cartridge and around sample trays was set to 20 ^{0}C. A positive pressure of 0.1 psi to induce a buffer flow towards the anode was applied during the entire run. An on-column UV variable wavelength detector set to 195 nm was employed for analyte detection. The buffers used comprised 50 mM Tris, phosphoric acid (pH 2.5) and chiral selector. Ten milligram per milliliter of sulfated β-CD (50 %/50 % blend of batches 03711JA and 83297MJ) served as chiral selector for the determination of the kinetic constants and 2 % w/v of highly sulfated γ-CD was used for the inhibition studies. Fresh buffer was prepared every day. The applied voltage was –20 kV (currents of about -45 μA and -60 μA, respectively). Before each experiment, the capillary was sequentially rinsed with 0.1 M NaOH (2 min, 20 psi), bidistilled water (1 min, 20 psi) and running buffer (1 min, 20 psi). Quantitation of ketamine and norketamine enantiomers was based on internal calibration using corrected peak areas (areas divided by detection time). Aqueous calibrators containing 0.5, 2.5, 7.5, 15.0 and 30.0 μM of each enantiomer were employed as described previously [16,17,24]. Assay specifications were comparable to those reported by Schmitz et al. [16,24].

2.6 Data analysis

Initial enantiomer substrate concentration was plotted against the norketamine formation rate (pmol norketamine/min/pmol CYP) and analyzed by two mathematical models (Michaelis-Menten and Hill) using nonlinear least square regression analysis on the GraphPad Prism 4 software (GraphPad Software, San Diego, USA) and SigmaPlot version 10.0 (SPSS, Chicago, IL, USA). Various inhibition models and model comparisons with F-test ($p = 0.05$) were investigated with GraphPad Prism 5 (GraphPad Software). Kinetic curves were compared with paired Student´s t-test using Microsoft Excel (Microsoft, Seattle, WA, USA) and data sets were evaluated with the t-test using SigmaStat for Windows version 1.0 (Jandel, Corte Madera, CA, USA). A p-value < 0.05 was considered significant.

3 Results and discussion

3.1 Enantioselective CE of ketamine and norketamine with sulfated CDs

In this study, the enantioselective separation of ketamine and norketamine was performed with two different sulfated CDs. Multiple isomer sulfated β-CD (Aldrich) was employed for the characterization of the kinetic parameters of the N-demethylation and highly sulfated γ-CD (Beckman Coulter) for the inhibition study. As discussed previously, separation of the enantiomers of ketamine and norketamine can be obtained by using a 50 mM Tris-phosphate buffer (pH 2.5) containing 10 mg/mL of sulfated β-CD in an untreated fused-silica capillary and having reversed polarity, indicating that the migrating drug complexes have a negative charge (strong complexation) [15-17,28,29]. Sulfated β-CD from Aldrich comprises a mixture of β-CD molecules with 7-11 mol sulfate/mol β-CD [30] and the distribution of these molecules varies strongly from batch to batch which was found to have a significant impact on the separation of ketamine enantiomers but not for norketamine [29]. With selected batches, the ketamine enantiomers could not be completely resolved whereas others provided a nice separation of the ketamine enantiomers but R-ketamine almost comigrated with S-norketamine. Thus, best results for the resolution of the stereoisomers of ketamine and its metabolites were obtained with mixtures of two batches [17,29]. Typical electropherograms obtained with a 50:50 mixture of two batches (Section 2.5) are presented in Fig. 1. The samples analyzed are those from *in vitro* incubations containing ketamine and norketamine,

which were used to determine the CYP3A4 catalyzed kinetics of the N-demethylation of ketamine. In agreement with previous investigations [17], no additional ketamine and norketamine metabolites were detected.

It is worth noting that the used 50:50 mixture of two batches of sulfated β-CD is different to that used previously [16]. For every new batch, optimized conditions have to be elucidated. In order to avoid such efforts for our future activities with ketamine, highly sulfated CDs were tested for the analysis of the enantiomers of ketamine and norketamine. Compared with the sulfated β-CD product described above, highly sulfated CDs encompass a higher degree of sulfation (12 and 13 mol sulfate/mol CD for highly sulfated β-CD and γ-CD, respectively) and a much narrower heterogeneity [30]. Highly sulfated β-CD could not be used because ketamine enantiomers were not resolved [29]. Highly sulfated γ-CD, however, provided complete separation of ketamine and norketamine enantiomers (Fig. 2). This configuration was used to analyze the *in vitro* samples containing ketoconazole as inhibitor of CYP3A4. Compared with the data obtained with sulfated β-CD of Aldrich, the relative order of the enantiomers of ketamine and norketamine was the same. The appearance of the internal standard, however, was completely different (compare data of Figs. 1 and 2).

Figure 1. Electropherograms obtained with 10 mg/mL sulfated β-CD (A) for a calibrator sample containing 15 µM of each ketamine and norketamine enantiomer and (B-D) after 8 min incubation with CYP3A4 of (B) 50 µM racemic ketamine, (C) 25 µM S-ketamine and (D) 25 µM R-ketamine. Key: S-K, S-ketamine; R-K, R-ketamine; S-NK, S-norketamine; R-NK, R-norketamine; IST, internal standard ((+)-pseudoephedrine). Sample preparation and CE analysis were performed as described in Sections 2.4 and 2.5, respectively.
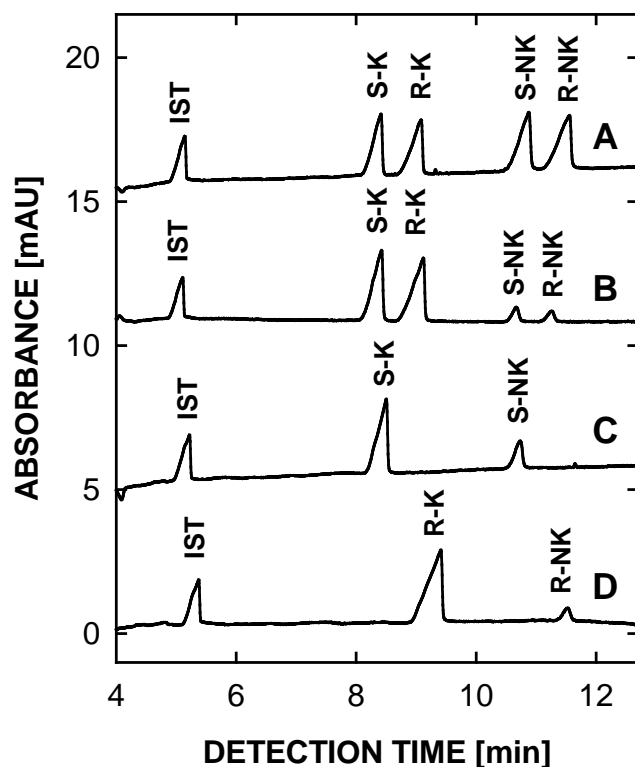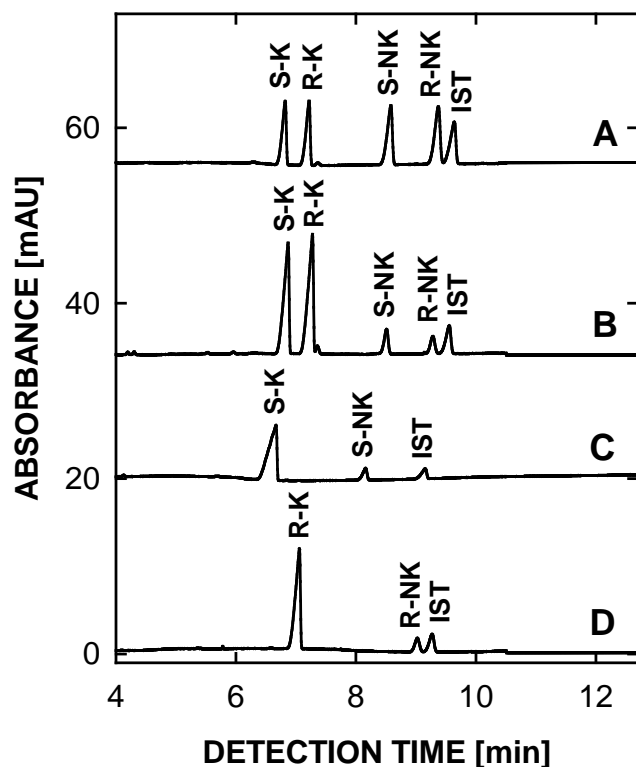
Figure 2. Electropherograms obtained with 2 % w/v of highly sulfated γ-CD (A) for a calibrator sample containing 15 µM of each ketamine and norketamine enantiomer and (B-D) after 8 min incubation with CYP3A4 of (B) 114.6 µM racemic ketamine, (C) 72.7 µM S-ketamine and (D) 57.2 µM R-ketamine. Other conditions and key as in Fig. 1.

3.2 CYP3A4 mediated N-demethylation kinetics of ketamine

CYP3A4 was recently shown to be one of the most active CYP enzymes which catalyze the demethylation of ketamine to norketamine and was found not to produce any further metabolites [17]. Racemic ketamine and single enantiomers were incubated at enantiomer concentrations between 2.5 and 500 µM. The demethylation pathway was investigated by enantioselective CE and the formation rate was calculated in relation to the incubation time and the amount of CYP enzyme involved. Typical electropherograms are presented in Fig. 1 and the calculated norketamine formation rates as function of substrate concentration are depicted in Fig. 3. Data were evaluated according to the Michaelis-Menten and Hill models. The single site Michaelis-Menten model is based on

$$v = V_{max} [S] / (K_m + [S]) \qquad (1)$$

whereas the Hill equation is expressed by

$$v = V_{max} [S]^n / (K'^n + [S]^n) \qquad (2)$$

where v is the product formation rate (velocity) of the metabolic reaction, [S] is the substrate concentration, K_m is the Michaelis-Menten constant which is the concentration at which the

formation rate is 50 % of V_{max}, V_{max} is the maximum formation rate, K' is a constant of the autoactivation model which is equivalent to K_m when $n = 1$, and n is the Hill coefficient [32,33]. Standard parameters such as coefficient of determination (R^2) and F-test were used to determine the quality of a fit to a specific model. For model comparison with the F-test, $p < 0.05$ means that the alternative model (Hill model) fits the data significantly better. The determined parameters are summarized in Table 1.

For the incubation of racemic ketamine with CYP3A4, the Hill equation (Eq. 2) did not provide a better fit to the experimental data ($p > 0.05$, Table 1), indicating that autoactivation does not take place. No difference was found for the correlation coefficients (R^2) and n values were determined to be close to unity (Table 1). Thus, for racemic ketamine, the experimental data can best be described with the Michaelis-Menten model (Eq. 1). For the kinetics of S- and R-ketamine N-demethylation, significant differences between K_m and V_{max} values were observed with both values being higher for the formation of S-norketamine compared to R-norketamine (Table 1). The experimental data from incubations with single enantiomers resulted in a better fit with the Hill equation ($p < 0.05$, Table 1). The corresponding n values were shown to be smaller than unity, indicating a model of negative cooperativity binding. As found in the incubations of racemic ketamine, incubation of single enantiomers also resulted in higher K_m and V_{max} values for the formation of S-norketamine compared to R-norketamine (Table 1). The kinetic parameters K_m and V_{max} were higher when single enantiomers were incubated separately. Similar observations were made for the incubation of ketamine with human liver microsomes [16]. After incubation of both, racemic ketamine and single enantiomers, the formation rates of S- and R-norketamine were found to differ significantly using a paired Student's t-test ($p = 0.004$ and $p = 0.002$, respectively). The stereoselective metabolism was particularly obvious when both enantiomers were incubated separately (Fig. 3). Intrinsic clearance (CL_{int}), which defines the rate of metabolism for a given drug concentration, and maximal clearance due to autoactivation (CL_{max}), which provides an estimate of the highest clearance attained as substrate concentration increases before any saturation of the enzyme sites, were calculated according to $CL_{int} = V_{max} / K_m$ and $CL_{max} = (V_{max} / K') [|(n-1)| / n(|n-1|)^{1/n}]$, respectively [32]. Clearance values are listed in Table 1. The calculated clearance values for incubations with single enantiomers were higher than in the experiments with racemic ketamine, and this for both enantiomers. After incubation with racemic ketamine as well as with single enantiomers, clearances for S-

norketamine are larger compared to those of R-norketamine. Thus, the conclusion can be drawn that the demethylation of ketamine via CYP3A4 occurs stereoselectively.
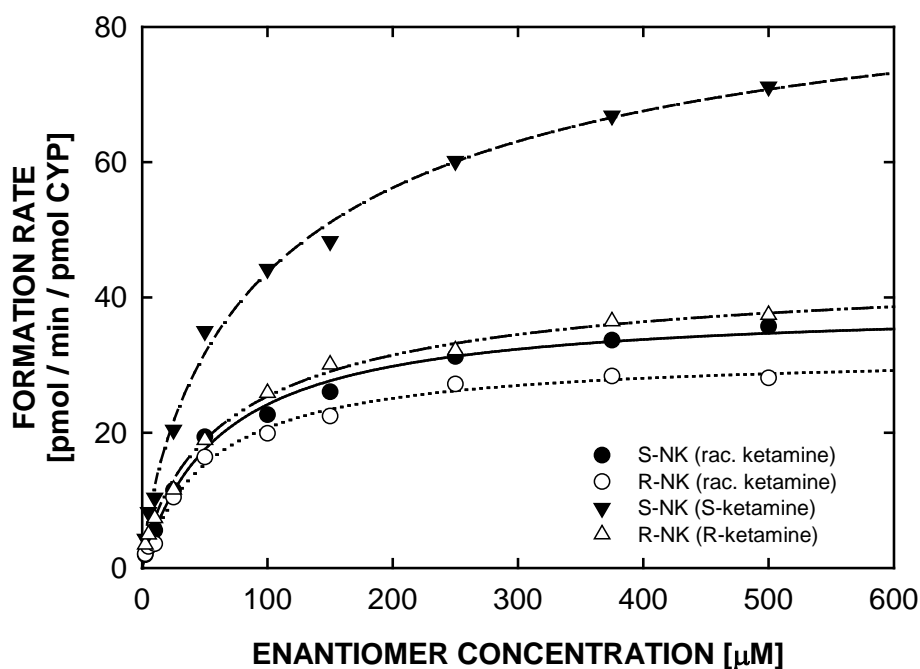
Figure 3. Norketamine formation by CYP3A4 for racemic ketamine and single ketamine enantiomers. Symbols denote the mean of duplicates. Lines are predicted values based on nonlinear regression analysis using the Michaelis-Menten model (for incubation of racemic ketamine) and the Hill equation (for single ketamine enantiomers).

Using data produced by enantioselective CE, the stereoselective kinetics of ketamine N-demethylation by CYP3A4 *in vitro* could be determined. Incubation of single enantiomers resulted in higher values for the kinetic parameters compared to incubation of racemic ketamine. This is plausible as the ketamine enantiomers have different enzyme affinities and might interfere in each other's metabolism. For incubation of racemic ketamine V_{max} of both enantiomers is up to 40 % smaller compared with the incubation of single enantiomers. The influence on the binding constant K_m is less impressive. The demethylation of ketamine via CYP3A4 occurs stereoselectively. Although this is an *in vitro* result, possible interactions should be considered when this racemic drug is administered *in vivo*.

Table 1. Kinetic parameters for N-demethylation of ketamine and model comparison [a]

Substrate	Product	Michaelis-Menten model				Hill model					F-test [b]
		R^2	K_m [μM]	V_{max} [pmol/min/ pmol CYP]	CL_{int} [c] [μL/min/ pmol CYP]	R^2	K' [d] [μM]	V_{max} [pmol/min/ pmol CYP]	CL_{max} [e] [μL/min/ pmol CYP]	n [f]	p-value
Rac. ketamine	S-NK	0.9934	61.18	38.95	0.64	0.9951	76.27	42.21	0.87	0.8676	0.1644
Rac. ketamine	R-NK	0.9929	53.36	31.79	0.60	0.9929	53.79	31.89	0.62	0.9930	0.9501
S-ketamine	S-NK	0.9904	72.65	78.71	1.08	0.9958	122.4	94.77	1.57	0.7686	0.0207
R-ketamine	R-NK	0.9931	57.21	41.17	0.72	0.9963	76.39	45.75	1.06	0.8223	0.0435

a) Data for all incubations derived from mean values of duplicate determinations.

b) Model comparison.

c) $CL_{int} = V_{max} / K_m$.

d) K' is equivalent to K_m when n=1.

e) $CL_{max} = (V_{max} / K') [| (n-1 |) / n(| n-1 |)^{1/n}]$.

f) n = Hill coefficient.

3.3 Ketoconazole inhibition of CYP3A4 catalyzed N-demethylation of ketamine

The inhibition of N-demethylation via CYP3A4 was investigated using ketoconazole as a potent and specific inhibitor of CYP3A4. The experiments were performed at inhibitor concentrations ranging from 0.1 to 2 μM. Based on recommendations of the Food and Drug Administration guidance [31], both substrate and inhibitor concentrations should be varied to cover ranges above and below the substrate's values for K_m and inhibition constant K_i. As the K_i values for ketoconazole reported in the literature cover a rather broad range (0.0037 – 0.18 μM in [31], 0.015 – 8 μM according to Thummel and Wilkinson [34]), inhibitor concentrations higher than those recommended in [31] were applied in this study. The adopted range of inhibitor concentration was determined experimentally. No metabolites could be detected when more than 2 μM of ketoconazole was applied, whereas almost no inhibition activity was observed at an inhibitor concentration < 0.1 μM. The substrate concentrations investigated were 0.25 K_m, 0.50 K_m, 1.0 K_m and 2.0 K_m (K_m values were determined in the kinetic studies described above, Table 1).

For each of all four substrate concentrations studied, the norketamine formation rate was plotted against the logarithm of inhibitor concentration and evaluated by nonlinear regression analysis according to the one-site competition model [35] based on

$$Y = Bottom + (Top-Bottom)/(1+10^{(X-LogIC_{50})}) \tag{3}$$

where X is the substrate concentration, Y is the logarithm of inhibitor concentration, IC_{50} is the concentration of inhibitor that reduces enzymatic activity to 50 %, whereas Top and Bottom are the upper and lower limits of the curve. In this context, the norketamine formation rate without inhibitor was set as the top of the curve, while zero was set as the lower limit as no metabolite would be expected with complete inhibition. With the calculated IC_{50}, the inhibition constant K_i can be determined according to the equation of Cheng and Prusoff [36]

$$K_i = IC_{50} / (1 + [S]/K_m) \tag{4}$$

where [S] is the substrate concentration and K_m is the Michaelis-Menten constant determined in the previous part of this study. Experimental data together with the fitted curves are presented in Fig. 4, and the determined values of IC_{50} and K_i (expressed as mean ± SD of the values obtained with the four substrate concentrations) are summarized in Table 2. For both enantiomers, the IC_{50} values and the inhibition constants were significantly higher for

incubation of racemic ketamine compared to the data obtained with incubation of the single enantiomers. The presence of one enantiomer seems to influence the inhibition of N-demethylation of the other, as the two substrates and the inhibitor compete for the same enzyme. Comparing the two enantiomers applied as racemate, the obtained IC_{50} and the K_i values do not differ ($p > 0.05$). The same is true for the corresponding values of the incubations with single enantiomers.

Table 2. IC_{50} values and inhibition constants with ketoconazole for CYP3A4 mediated N-demethylation of ketamine

Substrate	Product	IC_{50} [μM]	K_i [μM]
Racemic ketamine	**S-NK**	**0.66 ± 0.16**	**0.38 ± 0.15**
Racemic ketamine	**R-NK**	**0.70 ± 0.19**	**0.39 ± 0.20**
S-ketamine	**S-NK**	**0.25 ± 0.04**	**0.14 ± 0.03**
R-ketamine	**R-NK**	**0.27 ± 0.08**	**0.16 ± 0.09**

Data represent mean ± SD of the four data sets and values of each data set were derived from mean values of duplicate enantioselective CE determinations which were fitted to a one site competition model.

The used one-site competition model is based on a competitive model. The data sets were fitted by nonlinear regression analysis to various other inhibition models, including competitive inhibition, uncompetitive inhibition, noncompetitive inhibition and mixed mode inhibition, using the experimentally determined kinetic parameters V_{max} and K_m. For model comparison with the F-test, $p < 0.05$ means that the alternative inhibition model fits the data significantly better. For all data sets, the competitive model was found to be significantly better compared to the other models (data not shown), which validated the assumption that ketoconazole inhibits CYP3A4 mediated N-demethylation of ketamine in a competitive manner such that Eq. 3 can be used for data analysis.

With enantioselective CE, ketoconazole inhibition of the CYP3A4 mediated N-demethylation of ketamine could be characterized and the inhibition constants K_i were determined. In principle, an inhibition constant describes the affinity between inhibitor and enzyme, independent of the substrates. Specific experimental factors, such as the amount and type of enzyme and the substrates, were found to have an impact on the inhibition constant

[37]. Literature values for ketoconazole as the inhibitor of CYP3A4 using different substrates range from 0.0037 to 8 µM [31,34]. In the present study, K_i values between 0.14 and 0.40 µM were obtained. Incubation of racemic ketamine with ketoconazole resulted in higher K_i values for both enantiomers compared with incubations of single enantiomers. In the presence of two substrates with different affinities to the metabolizing enzyme and a specific competitive inhibitor on CYP3A4, it requires more inhibitor to reduce the enzyme activity, measured as norketamine formation rate, compared with incubations of single enantiomers where the inhibitor only has to compete with one substrate.
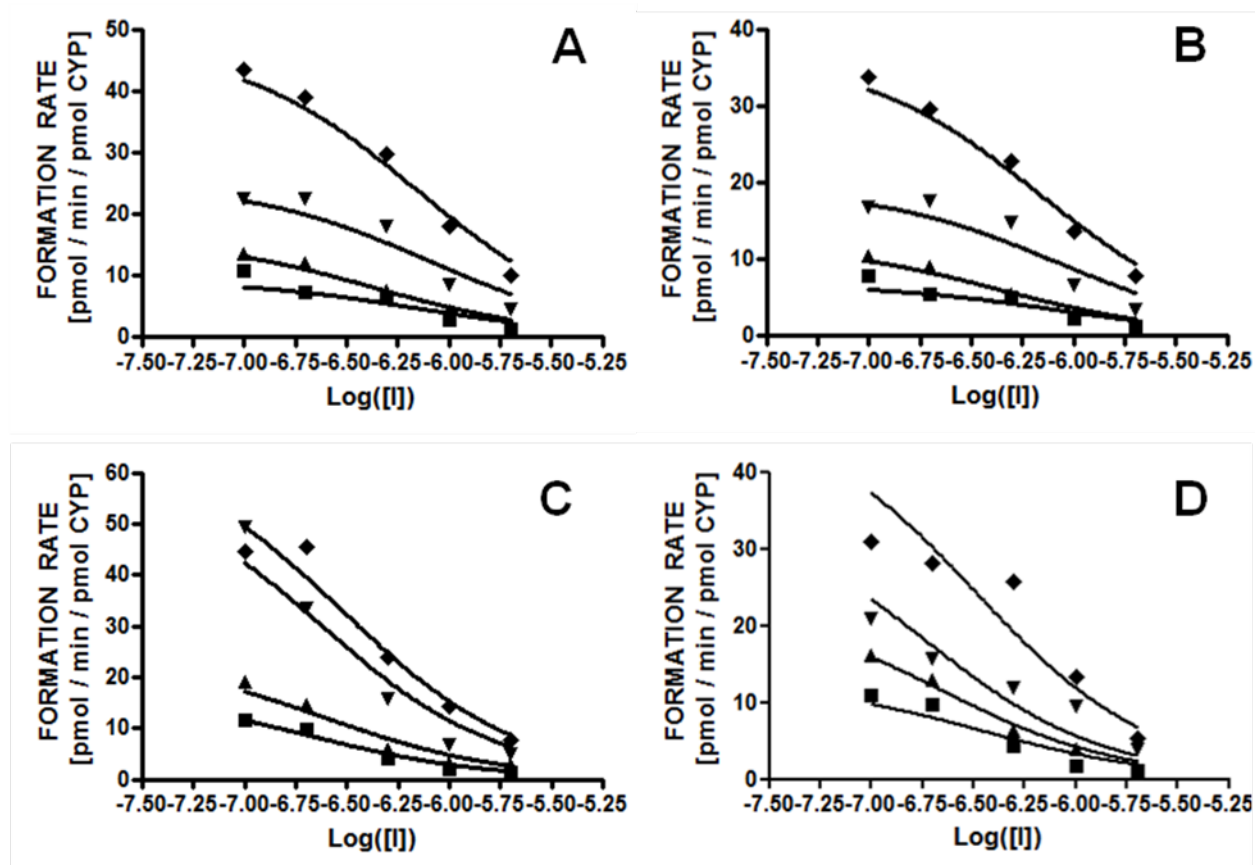
Figure 4. Enantioselective kinetics of CYP3A4 mediated N-demethylation of ketamine inhibited by ketoconazole to (A and C) S-norketamine and (B and D) R-norketamine after incubation of (A and B) racemic ketamine, (C) S-ketamine and (D) R-ketamine at four substrate concentrations. Inhibitor concentrations were varied from 0.1 to 2 µM. Symbols denote the mean of duplicates. Solid lines are predicted values based on nonlinear regression analysis using a one site competition model. Key: [I] = inhibitor concentration; substrate concentrations: ■ = 0.25 K_m, ▲ = 0.5 K_m, ▼ = 1 K_m, ♦ = 2 K_m (for K_m values, see Table 1).

4 Concluding remarks

Highly sulfated γ-CD was found to nicely separate the enantiomers of ketamine and norketamine and to be suitable for their determination in extracts of *in vitro* samples. With highly sulfated γ-CD, the disturbing batch-to-batch variations in ketamine enantiomer separation observed with sulfated β-CD are not expected. Using enantioselective CE for measuring the metabolite formation rate and evaluation of the data with different models, *in vitro* kinetics of N-demethylation of ketamine via CYP3A4 and inhibition by ketoconazole were characterized and relevant kinetic parameters V_{max}, K_m and inhibition constant K_i were determined. Significant differences in the metabolism pathway and also inhibition kinetics with ketoconazole were demonstrated. Data obtained in the absence of ketoconazole revealed that the N-demethylation occurred stereoselectively. No stereoselective difference was observed in the inhibition study with ketoconazole, but inhibition constants for the incubation of racemic ketamine were found to be larger compared with those obtained with incubation of single ketamine enantiomers. The calculated values must be interpreted with caution. Further studies and also *in vivo* results would be needed to emphasize the clinical relevance. Although this is an *in vitro* experiment, possible drug-drug interactions should be considered when racemic drugs are administered *in vivo*. To date, a number of papers appeared in the scientific literature in which the use of enantioselective CE for the determination of kinetic parameters of enzymatic reactions *in vitro* is discussed [16,17,21-24]. Although inhibitory effects on CYP enzymes have been studied before [25,38], to the best of our knowledge, this is the first publication in which enantioselective CE is being used to determine inhibition constants of a single CYP enzyme. Similarly, micellar electrokinetic capillary chromatography in an achiral medium was recently employed to determine K_i values for sulfaphenazole and ketoconazole to inhibit the CYP2C9 catalyzed hydroxylation of diclofenac [39]. The presented work demonstrates that enantioselective CE is an attractive methodology to assess the stereoselectivity of drug metabolic reactions *in vitro*.

Acknowledgments

References

[1]   Baselt, R.C., Cravey, R.H., Disposition of Toxic Drugs and Chemicals in Man, 4th Edition, Chemical Toxicology Institute, Foster City, California, 1995, pp. 412-414.

[2]   Moffat, A.C., Osselton, M.D., Widdop, B., Galichet, L.Y., Eds., Clarke's Analysis of Drugs and Poisons in Pharmaceuticals, Body Fluids and Postmortem Material, 3rd Edition, Pharmaceutical Press, London, UK, 2004, pp.1152-1153.

[3]   Adams, H.A., Werner, C., Anaesthesist 1997, 46, 1026-1042.

[4]   Craven, R., Anaesthesia 2007, 62, 48-53.

[5]   Sinner, B., Graf, B.M., Handb. Exp. Pharmacol. 2008, 182, 313-333.

[6]   Aroni, F., Iacovidou, N., Dontas, I., Pourzitaki, C., Xanthos, T., J. Clin. Phramacol. 2009, 49, 957-964.

[7]   Machado-Vieira, R., Salvadore, G., DiazGranados, N., Zarate, C.A., Pharmacol. Ther. 2009, 123, 143-150.

[8]   Adams, J.D., Baillie, T.A., Trevor, A.J., Castagnoli, N., Biomed. Mass Spectrom. 1981, 8, 527-538.

[9]   Woolf, T.F., Adams, J.D., Xenobiotica 1987, 17, 839-847.

[10] Kharasch, E.D., Labroo, R., Anesthesiology 1992, 77, 1201-1207.

[11] Savchuk, S.A., Brodskii, E.S., Rudenko, B.A., Formanovskii, A.A., Mikhura, I.V., Davydova, N.A., J. Anal. Chem. 1997, 52, 1175-1186.

[12] Yanagihara, Y., Kariya, S., Ohtani, M., Uchino, K., Aoyama, T., Yamamura, Y., Iga, T., Drug Metab. Dispos. 2001, 29, 887-890.

[13] Hijazi, Y., Boulieu, R., Drug Metab. Dispos. 2002, 30, 853-858.

[14] Turfus, S.C., Parkin, M.C., Cowan, D.A., Halket, J.M., Smith, N.W., Braithwaite, R.A., Elliot, S.P., Steventon, G.B., Kicman, A.T., Drug Metab. Dispos. 2009, 37, 1769-1778.

[15] Schmitz, A., Theurillat, R., Lassahn, P.-G. Mevissen, M., Thormann, W., Electrophoresis 2009, 30, 2912-2921.

[16] Schmitz, A., Thormann, W., Moessner, L., Theurillat, R., Helmja, K., Mevissen, M., Electrophoresis 2010, 31, 1506-1516.

[17]   Portmann, S. Kwan, H.Y., Theurillat, R., Schmitz, A., Mevissen, M., Thormann, W., J Chromatogr. A. 2010, 1217, 7942-7948.

[18]   Zaugg, S., Thormann, W., J. Chromatogr. A 2000, 875, 27-41.

[19]   Bonato, P.S., Electrophoresis 2003, 24, 4078-4094.

[20]   Caslavska, J., Thormann, W., J. Chromatogr. A 2011, 1218, 588-601.

[21]   Afshar, M., Thormann, W., Electrophoresis 2006, 27, 1526–1536.

[22]   Ha, P.T.T., Sluyts, I., Van Dyck, S., Zhang, J., Gilissen, R.A.H.J., Hoogmartens, J., Van Schepdael, A., J. Chromatogr. A 2006, 1120, 94-101.

[23]   Hai, X., Adams, E., Hoogmartens, J., Van Schepdael, A., Electrophoresis 2009, 30, 1248-1257.

[24]   Schmitz, A., Portier, C. J., Thormann, W., Theurillat, R., Mevissen, M., J. Vet. Pharmacol. Ther. 2008, 31, 446-455.

[25]   Capponi, L., Schmitz, A., Thormann, W., Theurillat, R., Mevissen, M., Am. J. Vet. Res. 2009, 70, 777-786.

[26]   Knobloch, M., Portier, C.J., Levionnois, O.L., Theurillat, R., Thormann, W., Spadavecchia, C., Mevissen, M., Toxicol. Appl. Pharmacol. 2006, 216, 373-386.

[27]   Larenza, M.P., Landoni, M.F., Levionnois, O.L., Knobloch, M., Kronen, P. W., Theurillat, R., Schatzmann, U., Thormann, W., Br. J. Anaesth. 2007, 98, 204-212.

[28]   Theurillat, R., Knobloch, M., Levionnois, O., Larenza, P., Mevissen, M., Thormann, W., Electrophoresis 2005, 26, 3942-3951.

[29]   Theurillat, R., Knobloch, M., Schmitz, A., Lassahn, P.G., Mevissen, M., Thormann, W., Electrophoresis 2007, 28, 2748-2757.

[30]   Chen, F.-T. A., Shen, G., Evangelista, R.A., J. Chromatogr. A 2001, 924, 523-532.

[31]   Guidance for industry: Drug Interactions Studies – Study Design, Data Analysis and Implications for Dosing and Labeling, Clinical Pharmacology, U.S. Department of Health and Human Services, Food and Drug Administration, Center for Drug Evaluation and Research and Center for Biologics Evaluation and Research, Rockville, MD, USA, 2006, 1-52.

[32]   Houston, J.B., Kenworthy, K.E., Drug Metab. Dispos. 2000, 28, 246-254.

[33] Tracy, T.S., Hummel, M.A., Drug Metab. Rev. 2004, 36, 231-242.

[34] Thummel, K.E., Wilkinson, G.R., Annu. Rev. Pharmacol. Toxicol. 1998, 38, 389–430.

[35] Motulsky, H., Christopoulos, A., Fitting Models to Biological Data Using Linear and Nonlinear Regression: A Practical Guide to Curve Fitting, Oxford University Press, New York, USA, 2004, p. 213.

[36] Cheng, Y., Prusoff , W.H., Biochem. Pharmacol. 1973, 22, 3099-3108.

[37] Lu, C., Hatsis, P., Berg, C., Lee, F.W., Balani, S.K., Drug Metab. Dispos. 2008, 36, 1255-1260.

[38] Moessner, L., Schmitz, A., Theurillat, R., Thormann, W., Mevissen, M., Am. J. Vet. Res. 2011, in press.

[39] Konečný, J., Mičíková, I., Řemínek, R., Glatz, Z., J. Chromatogr. A 2008, 1189, 274-277.

B.4. Electrophoretically mediated microanalysis for characterization of the enantioselective CYP3A4 catalyzed N-demethylation of ketamine

(Submitted for publication in Electrophoresis)

Electrophoretically mediated microanalysis for characterization of the enantioselective CYP3A4 catalyzed N-demethylation of ketamine

Hiu Ying Kwan and Wolfgang Thormann

Clinical Pharmacology Laboratory, Institute for Infectious Diseases, University of Bern, 3010 Bern, Switzerland.

Enantioselective capillary electrophoresis: Fundamental aspects and application to the *in vitro* assessment of CYP3A4 mediated ketamine N-demethlyation

Abstract

Execution of an enzymatic reaction performed in a capillary with subsequent electrophoretic analysis of the formed products is referred to as electrophoretically mediated microanalysis (EMMA). An EMMA method was developed to investigate the stereoselectivity of the CYP3A4 mediated N-demethylation of ketamine. Ketamine was incubated in a 50 µm ID bare fused-silica capillary together with human CYP3A4 Supersomes using a 100 mM phosphate buffer (pH 7.4) at 37°C. A plug containing racemic ketamine and the NADPH regenerating system including all required co-factors for the enzymatic reaction was injected, followed by a plug of the metabolizing enzyme CYP3A4 (500 nM). These two plugs were bracketed by plugs of incubation buffer to ensure proper conditions for the enzymatic reaction. The rest of the capillary was filled with a pH 2.5 running buffer comprising 50 mM Tris, phosphoric acid and 2 % w/v of highly sulfated γ-cyclodextrin. Mixing of reaction plugs was enhanced via application of -10 kV for 10 s. After an incubation time of 8 min at 37 °C without power application, the capillary was cooled to 25 °C within 3 min followed by application of - 10 kV for the separation and detection of the formed enantiomers of norketamine. Norketamine formation rates were fitted to the Michaelis-Menten model and the elucidated values for V_{max} and K_m were found to be comparable to those obtained from the off-line assay of a previous study. The data obtained revealed that CYP3A4 N-demethylation of ketamine occurs in a stereoselective manner.

1   Introduction

Investigation of drug metabolism has gained increasing interest and importance in drug discovery and development. Metabolism of drugs often involves the hepatic cytochrome P450 enzyme system. The pharmacokinetics of drugs, particularly chiral drugs undergoing stereoselective metabolism, can differ enormously, depending on the activities of the metabolizing enzymes, which are influenced by extrinsic and genetic factors. Metabolizing enzymes can be induced, inhibited or occupied by other drugs such that drug-drug interactions must be taken into account. Also, genetic variations of the enzymes can be very important. Thus, *in vitro* characterization of metabolism is essential during the research phase of drugs for elucidation of pharmacological data before going to preclinical and clinical stages.

Capillary electrophoresis (CE) is an established and attractive methodology for elucidation of the metabolism of drugs *in vitro* due to high resolution, short analysis time and low consumption of chemicals and solvents [1-5]. Such determinations are typically performed in an off-line modus. After incubation of the substrate with the enzymes and extraction of the products formed, samples are analyzed by CE. Furthermore, CE has been shown to lend itself as unique and efficient microreactor for chemical reactions followed by the on-line assay of a reaction product. This technique is referred to as electrophoretically mediated microanalysis (EMMA) and is based on merging zones containing the analyte and the reagents, the occurrence of the enzymatic reaction either in presence or absence of the applied electric field, and finally the electrokinetic transport of the detectable product through an on-column detector or into a detector placed at the capillary end. The first CE study with an in-capillary enzymatic reaction was published by Bao and Regnier [6]. Latest advances in this technology and its advantages over the classical off-line methods, including automation, reduced consumption of chemicals and lower cost, are summarized in recent reviews [7,8]. EMMA can be employed to investigate the activity of single isoenzyme molecules, measurement of enzyme activity and kinetics, screening of enzyme inhibitors, the determination of inhibition constants and IC_{50} [7-10]. EMMA was also used to investigate drug metabolism via CYP450 enzymes. Activity of CYP3A4 for the metabolism of testosterone and nifedipine was determined by quantification of the reactant and product co-factors NADPH and NADP [11]. Co-factor, CYP3A4, reaction buffer and substrate were each injected as separate plugs and mixed by application of voltage. K_m and V_{max} determined by EMMA were reported to be consistent with the values found in the off-line assay. In another

work, the metabolism of dextromethorphan to 3-methoxymorphinan by CYP3A4 in which the injected plugs were mixed by diffusion was studied [12]. Conditions for an EMMA-based stereoselective assay were reported for the S-oxygenation of cimetidine mediated by various isoforms of flavin-containing monooxygenase (FMO) [13]. Enantioselective separation was performed using sulfobuthylether-β-cyclodextrin as chiral selector. The kinetics of the stereoselective metabolism was evaluated and kinetic parameters were found to compare well to those obtained with an off-line incubation assay. In all these studies considerable efforts were necessary to optimize the in-capillary metabolic reaction and to separate, detect and quantify the metabolites produced. Alternatively to EMMA, a capillary microreactor was used to induce the metabolism of four different substrates mediated by CYP450 enzymes followed by collection of the whole content of the capillary and analysis of the samples by UHPLC – MS/MS [14].

In previous studies from our laboratory, the stereoselective metabolism of ketamine in different species was evaluated [15-20]. Ketamine, a chiral phencyclidine derivative, is known as an anesthetic drug and, in subanesthetic doses, as a postoperative analgesic. Due to the rapid onset of the antidepressant effect, its usage in major depressive disorders is being investigated. Ketamine interacts with opioid receptors, muscarinic acetylcholine receptors and different voltage gated channels. Its neurophysiological effect is mainly based on the noncompetitive antagonism on the N-methyl-D-aspartate (NMDA) receptor. For S-ketamine, affinity for the NMDA receptor was found to be four times higher than for the R-enantiomer and its anesthetic potency two to three times higher than that of the racemic mixture [21-27]. Based on *in vitro* and *in vivo* studies in humans and various animal species, it was shown that ketamine is metabolized mainly by the hepatic cytochrome P450 (CYP) enzyme system through N-demethylation to norketamine, which is then hydroxylated and further transformed to dehydronorketamine. To a marginal extent, direct hydroxylation of ketamine prior to N-demethylation is also possible [15,16,28,29].

Various CYP450 enzymes were screened for their metabolizing activity on ketamine and norketamine, including CYP1A1, CYP1A2, CYP2A6, CYP2B6, CYP2C9, CYP2C19, CYP2D6, CYP2E1 and CYP3A4, and a stereoselective metabolism via several enzymes was suspected [17]. Furthermore, CYP2C8 was found to catalyze the N-demethylation of ketamine but no metabolites of norketamine were detected (unpublished results). One of the main metabolic pathways goes via CYP3A4 whereas norketamine is not metabolized by this enzyme [17]. Consequently, the kinetics of ketamine N-demethylation mediated by CYP3A4

and its inhibition by ketoconazole was characterized [20]. In this off-line enzyme kinetics assay, alkaline extracts of incubations were analyzed by CE using sulfated β-cyclodextrin or highly sulfated γ-cyclodextrin as chiral selectors. Relevant kinetic parameters were determined and the metabolic reaction was confirmed to be stereoselective. As a continuation of that project, the aim of this study was to develop a suitable EMMA method to characterize the N-demethylation of ketamine mediated by CYP3A4, to determine kinetic parameters V_{max} and K_m, to investigate the stereoselectivity of this pathway analogously to the off-line assay and to compare the results. To our knowledge, this is the first EMMA based assay comprising a cytochrome P450 enzyme combined with a stereoselective separation of the products formed during the enzymatic reaction.

2 Materials and Methods

2.1 Chemicals and reagents

Racemic ketamine hydrochloride was obtained from CU Chemie Uetikon (Lahr, Germany). Norketamine as hydrochloride solution in methanol (1 mg/mL of the free base) was from Cerilliant (Round Rock, TX, USA). Highly sulfated γ-cyclodextrin (20 % w/v solution) was purchased from Beckman Coulter (Fullerton, CA, USA). Tris was obtained from Merck (Darmstadt, Germany), H_3PO_4 (85%), potassium dihydrogen phosphate and di-potassium hydrogen phosphate from Fluka (Buchs, Switzerland). Calibrators and controls used for quantification were prepared in 100 mM phosphate buffer (pH 7.4). Baculovirus-insect-cell-expressed human CYP3A4+P450 reductase+cytochrome b5 SUPERSOMES™ as well as the nicotinamide adenine dinucleotide phosphate (NADPH) regenerating system were obtained from Gentest (Woburn, MA, USA, distributed through Anawa Trading, Wangen, Switzerland). The enzyme was stored as aliquots at –80°C, while the NADPH regenerating system was stored as aliquots at -20°C.

2.2 CE instrumentation and analytical conditions

A Proteome Lab PA 800 instrument (Beckman Coulter) equipped with a 50 μm id fused-silica capillary (Polymicro Technologies, Phoenix, AZ, USA) of 44 cm total length (effective length of 34 cm) was used. The temperature in the capillary cartridge was set to 37

°C for establishment of proper EMMA conditions and reduced to 25 °C for the electrophoretic separation, while the sample tray was kept at the lowest possible temperature (around 10 °C). The running buffer was composed of 50 mM Tris, phosphoric acid (pH 2.5) and 2 % w/v of highly sulfated γ-cyclodextrin as chiral selector. Fresh buffer was prepared daily. Before each EMMA experiment, the capillary was sequentially rinsed with 0.1 M NaOH (3 min, 20 psi (1 psi = 56894.8 Pa)), bidistilled water (2 min, 20 psi) and running buffer (2 min, 20 psi). After introduction of the plugs and incubation (see Section 2.3) the capillary was cooled down to 25°C during 3 min. For the electrophoretic separation, both inlet and outlet ends of the capillary were dipped into the running buffer containing the chiral selector (Fig. 1B) and a positive pressure of 0.1 psi was used to induce a buffer flow towards the anode. The applied voltage for the separation was -10 kV (current about -35 μA). An on-column UV variable wavelength detector set to 195 nm was employed for analyte detection. For quantitation, norketamine was incubated on-line as described for ketamine in Section 2.3. The calibration was based on corrected peak areas (areas divided by detection time). Aqueous calibrators containing 10.0, 20.0, 40.0, 80.0 and 160.0 μM of each enantiomer were employed.

2.3   EMMA procedure

After filling the capillary with running buffer, and if not stated otherwise, four plugs of equal length were introduced by applying a vacuum of 1.0 psi for 4 s (Fig. 1A). The order and composition of the four plugs was as follows: 1) Incubation buffer consisting of 100 mM potassium phosphate buffer (pH 7.4); 2) racemic ketamine ranging from 10 – 500 μM per enantiomer, 40 mM NaOH and NADPH regenerating system comprising of 16.12 mM $NADP^+$, 34.32 mM glucose-6-phosphate, 4.8 U/mL glucose-6-phosphate dehydrogenase, 34.32 mM $MgCl_2$ and 600 μM sodium citrate; 3) CYP3A4 (500 pmol/mL) in 100 mM potassium phosphate buffer (pH 7.4); 4) Incubation buffer. Between injections of plugs, the capillary was shortly dipped into water to avoid unwanted carryover of reactants and buffer components. The plugs were mixed by applying a voltage of -10 kV for 10 s, with the inlet end dipped into incubation buffer and the outlet end in running buffer (Fig. 1A). To determine the kinetic parameters in the kinetic study, the incubation time at 37 °C was 8 min.
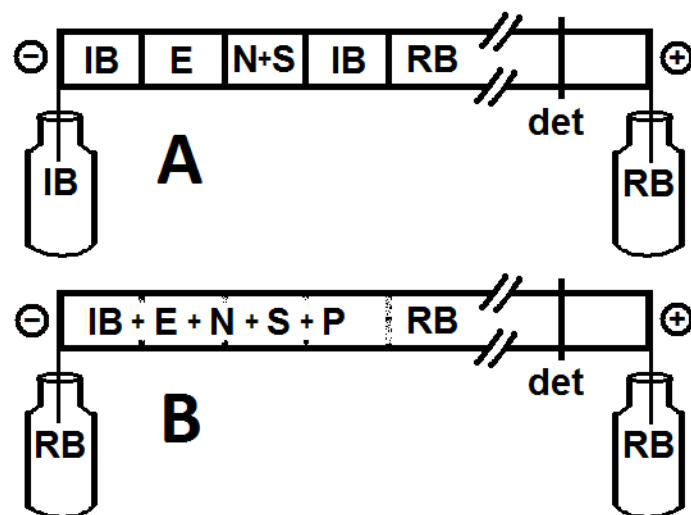
Figure 1. Schematic representation of EMMA with (A) initial arrangement of plugs and configuration used during mixing, incubation and temperature adjustment, and (B) configuration employed during CE separation and detection. In the configuration of panel A, voltage is applied only during mixing. Key: IB, incubation buffer; E, CYP3A4 as metabolizing enzyme; N, NADPH regenerating system; S, racemic ketamine as substrate; RB, running buffer with 2 % highly sulfated γ-cyclodextrin as chiral selector; P, norketamine as product of the metabolic reaction; det, detector. CE conditions are described in Section 2.2 and composition of plugs and details of EMMA procedure are given in Section 2.3.

2.4   Data analysis

Initial enantiomer substrate concentration was plotted against the norketamine formation rate (pmol norketamine/min/pmol CYP) and analyzed by two mathematical models (Michaelis–Menten and Hill) using nonlinear least square regression analysis on the Graph Pad Prism 4 software (Graph Pad Software, San Diego, USA) and SigmaPlot version 10.0 (SPSS, Chicago, IL, USA). Curves were compared between enantiomers with a paired student's t-test using Microsoft Excel software (Microsoft, Seattle, USA). A p-value <0.05 was considered significant.

3   Results and discussion

3.1   Optimization of EMMA conditions

The plug mode as shown in Fig. 1A was applied to perform the EMMA assay. When using an EMMA method, the enzymatic reaction must be ensured throughout the incubation time. Ketamine should not be complexed with the chiral selector before being metabolized by

CYP3A4. Therefore, a plug with incubation buffer is injected prior to the plug which comprises the substrate and the co-factors and the vial on the injection side contains incubation buffer during mixing and incubation (Fig. 1A). Furthermore, the plug with incubation buffer behind the enzyme plug prevents the exposure of the enzyme to the low pH of the running buffer.

Another aspect is the distribution of pH. While the metabolizing CYP3A4 enzyme is already provided in a 100 mM phosphate buffer at pH 7.4, the pH of the reaction plug with ketamine and NADPH regenerating system has to be adjusted to physiological pH. In the initial configuration employed, the pH in this plug was not adapted and no metabolic reaction was observed (Fig. 2A). After addition of 40 mM NaOH (pH between 7 – 7.5 as confirmed by a pH indicator paper), the anticipated reaction took place which was confirmed via detection of norketamine enantiomers during the electrophoretic separation (Figs. 2B, 2C, 2D). It is important to note that for electrophoretic separation and detection of the norketamine enantiomers the vial on the inlet side had to contain running buffer (Fig. 1B). The chiral selector bearing multiple negative charges thereby penetrates the reaction mixture and complexes the positively charged enantiomers of ketamine and norketamine. Ketamine and norketamine complexes are negatively charged and migrate towards the anode as reported previously [17,20].

The temperature for the incubation was kept at 37°C, the body temperature. Analysis by CE directly after incubation at the same temperature would ease the experiment and shorten the analysis time. However, complete operation at 37 °C caused frequent breakdowns due to high current and permitted the metabolic reaction to continue. Therefore, a cooling time of 3 min was applied before starting the electrophoretic separation at 25 °C which provided reliable results. Optimization of plug length was another aspect. Plugs established with an injection time interval > 4 s would allow for a higher metabolite production but were found to broaden the peaks of the products (data not shown). On the other hand, with shorter plugs (2 s injection) lower amounts of products were generated (Fig. 2C) and bubbles were often formed which caused a breakdown of the current flow. No better data were obtained with unequal plug lengths.
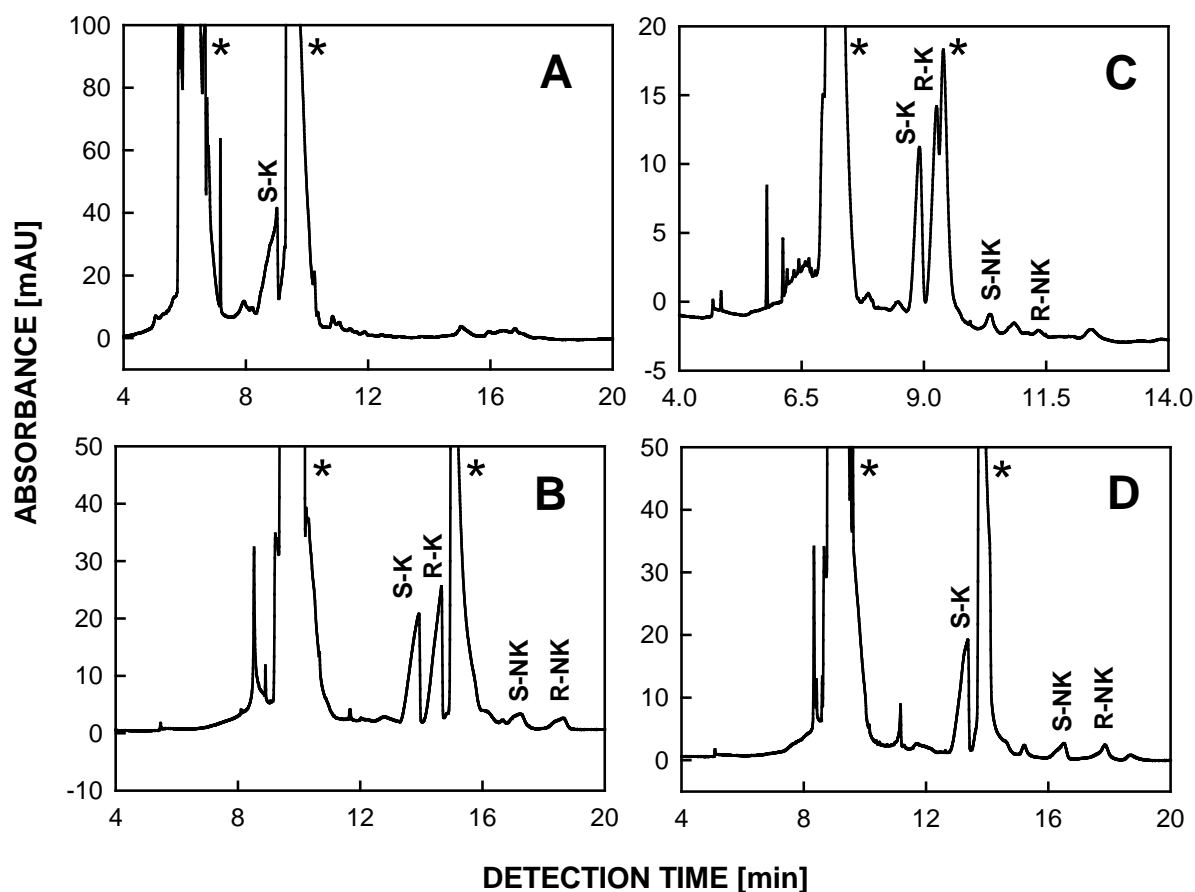
Figure 2. Electropherograms obtained after incubation of 1 mM racemic ketamine for 8 min at 37 °C. (A) Initial configuration without mixing of plugs by voltage application. Plugs were injected by applying 1 psi for 6 s, pH of the NADPH / ketamine plug was not adjusted with NaOH, and running buffer contained 3.3 % highly sulfated γ-cyclodextrin. All other conditions as described in Sections 2.2 and 2.3. (B) Conditions as described in (A) but pH of NADPH / ketamine plug was adjusted with 40 mM NaOH, plug lengths were reduced to 1 psi for 4 s and 2 % of chiral selector was used. (C) Conditions as in (B) but plug lengths were shortened to 0.5 psi for 4 s and plugs were mixed by applying -10 kV for 10 s. (D) Conditions as in (B) with plug mixing by applying a voltage of -10 kV for 10 s (method as described in Section 2.3). Peaks marked with asterisks stem from the NADPH regenerating system. Key: S-K, S-ketamine; R-K, R-ketamine; S-NK, S-norketamine; R-NK, R-norketamine.

Separation of the formed metabolites from the components of the matrix is necessary for quantitation. Fluid flow, differencies of conductivity and viscosity in the plugs, and migration of many components with unknown mobility have an impact on the final electropherogram. When the plugs were mixed by diffusion only, i.e. without application of voltage, norketamine enantiomers were detected showing that the metabolic reaction occurred (Fig. 2B). While peaks of both ketamine enantiomers were detected separately, S-norketamine was found to be close to the second large peak produced by components of the NADPH

regenerating system (Fig. 2B). After applying a mixing voltage of -10 kV for 10 s shortly after insertion of the plugs, the R-ketamine peak was found to comigrate with the second large peak from the NADPH regeneration system. Peaks for S- and R-norketamine, however, became better separated from the matrix (Fig. 2D). Furthermore, a higher metabolite production could be achieved. Using normal polarity, lower voltages or shorter time intervals for electrokinetic mixing, norketamine peaks were not fully resolved from other peaks. Electrophoretic separation in all cases was performed under the conditions described in Section 2.2 which are essentially those used previously for the off-line assay [20].

Compared to the off-line assay, a higher amount of enzymes (500 nM) was applied to obtain sufficient metabolite formation. With the incubation performed within the capillary, it is important to mention that the fluid volume in which the reaction occurs is not exactly defined. Due to the low pH of the running buffer (pH 2.5), the appropriate conditions for the metabolic reaction are only assured in the four plug arrangement at pH 7.4 (Fig. 1). Each plug was created by a 4 s injection at 1 psi (Fig. 2D). Using the CE Expert Lite calculater of Beckman Coulter, the physical length of each of the four plugs inserted at 37 °C was estimated as being about 7 mm (1.6 % of total column length). In such a configuration, mixing of reactants is assumed to occur by both longitudinal diffusion and transverse diffusion from the laminar flow profile generated during pressure injection as was described in detail by Krylova et al. [30]. As application of an electric field for a short time (10 s) was found to increase metabolite production, it can be assumed that electrophoretic transport contributed to the mixing of the reactants as well. Proper analysis of the impact of electrophoretic mixing is beyond the scope of this work and will be dealt with separately.

3.2 Assay characterization

As proof of concept of the on-line incubation, qualitative studies were performed by incubating racemic ketamine at a concentration of 1 mM and 37 °C for 0, 8, 30 and 60 min (Fig. 3). Using the configuration as described in Section 2.3, metabolite production was found to increase during an incubation time investigated up to 60 min. Even when the incubation time at 37 °C was 0 min, norketamine was detected which indicates that the metabolic reaction occurred during the 3 min cooling time interval (lowest graph in Fig. 3). The data presented in Fig. 3 revealed that an incubation time interval of 8 min at 37 °C provided a substantial amount of norketamine enantiomers. No norketamine was detected when blank

incubations were performed using the same plug configuration both in absence of CYP3A4 or ketamine. For that purpose, corresponding plugs were replaced with a plug of incubation buffer (Fig. 4).
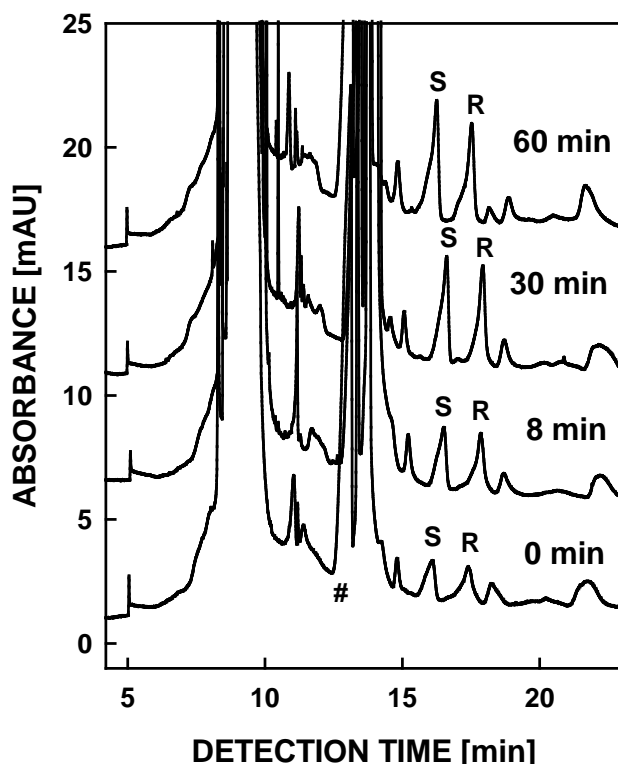

Figure 3. Electropherograms obtained for incubation of racemic ketamine (1 mM) with CYP3A4 for 0, 8, 30 and 60 min at 37 °C. On-line incubation and CE analysis were performed as described in Sections 2.3 and 2.2, respectively, and data are presented with a y-axis offset. Key: #, S-ketamine; S, S-norketamine; R, R-norketamine.

Figure 4. Electropherograms obtained after incubation for 30 min in absence of (A) CYP3A4 or (B) ketamine by replacing the corresponding plug with a plug of incubation buffer and (C) in presence of all components showing the occurrence of the metabolic reaction. On-line incubation and CE analysis were performed as described in Sections 2.3 and 2.2, respectively, and data are presented with a y-axis offset. Key: #, S-ketamine; S, S-norketamine; R, R-norketamine.
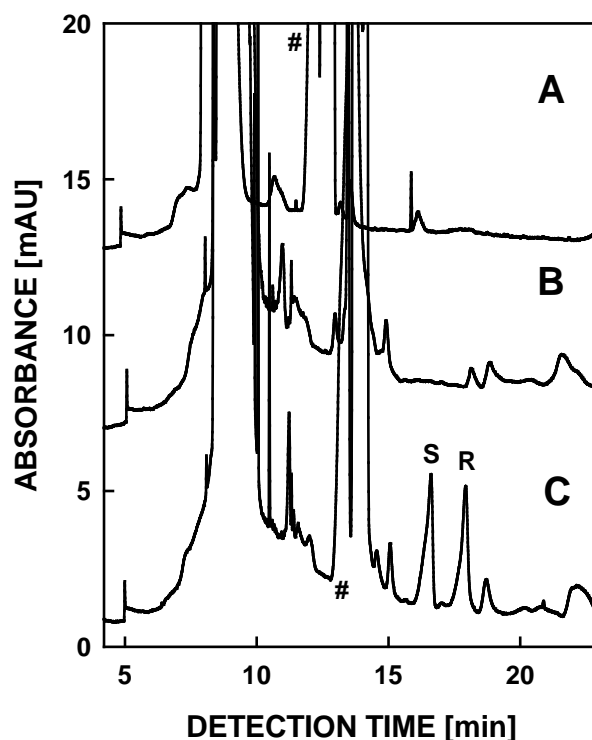
From a previous study it is known that norketamine is not metabolized by CYP3A4 [17]. Thus, calibration of norketamine formation was possible via incubation of norketamine (10-160 µM per enantiomer) instead of ketamine and otherwise identical conditions. Typical electropherograms of calibration samples are shown in Fig. 5. Over the tested concentration range, regression analysis revealed linear relationships. Mean (n= 6) values of the coefficients of determination R^2 for S-norketamine and R-norketamine were calculated to be 0.992 and 0.990, respectively. The RSD values were 0.64% and 0.46%, respectively. RSD values of the mean of the slopes were 5.34% and 7.11%, respectively, and the intercepts were smaller than the responses of the lowest calibrators. Two independent control samples containing 15 µM and 100 µM per norketamine enantiomer were analyzed on six different days. For the interday reproducibility of the higher control sample, the mean concentration values for S- and R-norketamine were 101.33 and 101.39 µM, respectively (RSD of 16.89% and 16.46 %, respectively). For the lower control sample, corresponding values were 16.24 and 15.58 µM, respectively (RSD was 25.5% and 12.43%, respectively). All quantitative data were evaluated by external calibration. The use of an internal standard should improve imprecision of the quantitative data. Thus, an internal standard which is not affected by the enzyme and can be detected after R-norketamine and without interferences should be included in future work.
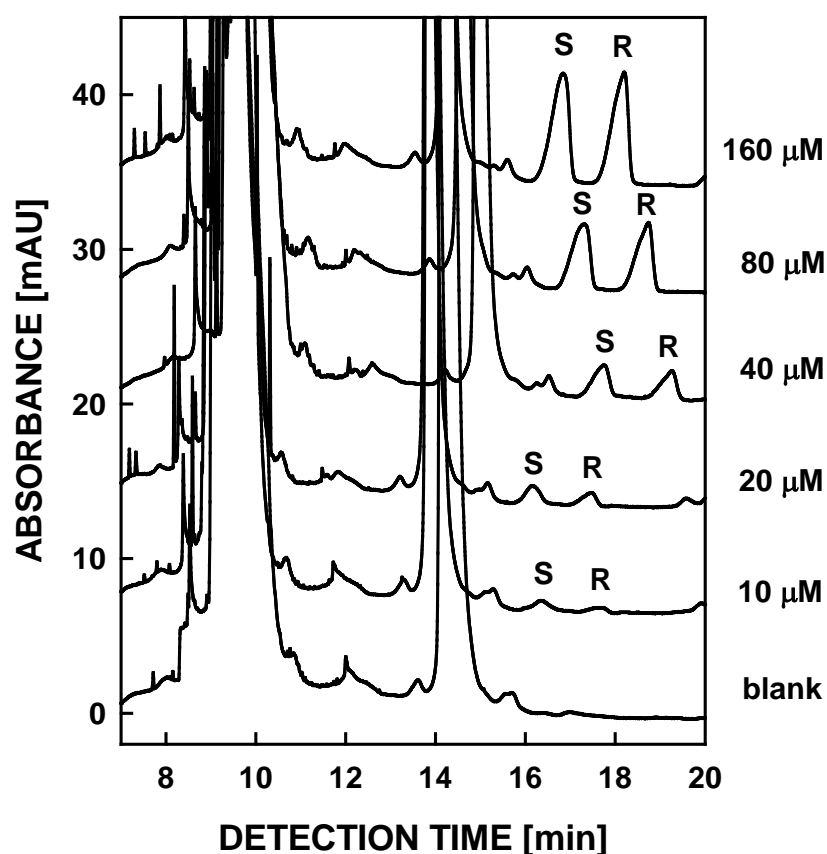

Figure 5. Electropherograms with 0 to 160 µM norketamine per enantiomer (from bottom to top, presented with a y-axis offset) used for calibration. Norketamine was incubated for 8 min at 37 °C and detected by CE as described in Sections 2.3 and 2.2, respectively. Key: S, S-norketamine; R, R-norketamine.

3.3 Determination of kinetic parameters

Based on the data of Figs. 3-5, the EMMA assay was used to determine the kinetic parameters of the CYP3A4 mediated N-demethylation of ketamine. For that purpose, racemic ketamine was incubated for 8 min at 37 °C. Formation rate was calculated in relation to the incubation time and to the estimated amount of enzymes involved. Initial enantiomer substrate concentration was plotted against the norketamine formation rate (pmol norketamine/min/pmol CYP). Data obtained were curve-fitted using nonlinear regression analysis according to the Michaelis-Menten and Hill models. While the single-site Michaelis-Menten model is expressed by $v = V_{max} [S] /(K_m+[S])$ and the Hill equation is based on $v = V_{max} [S]^n /(K'^n+[S]^n)$ where v is the product formation rate (velocity) of the metabolic reaction, $[S]$ is the substrate concentration, K_m is the Michaelis–Menten constant, which is the concentration at which the formation rate is 50% of V_{max}, V_{max} is the maximum formation rate, K' is a constant of the autoactivation model which is equivalent to K_m when n=1, and n is the Hill coefficient [31, 32]. Standard parameters such as the coefficient of determination (R^2) and F-test were used to determine the quality of a fit to a specific model. For model comparison with the F-test $p<0.05$ means that the alternative model (Hill model) fits the data significantly better. The determined parameters for the assumption of a two-fold dilution of the enzyme are summarized in Table 1.

Data obtained from on-line incubation of racemic ketamine with CYP3A4 resulted in a better fit to the Michaelis-Menten model (Fig. 6). The coefficients of determination (R^2) were similar and the Hill coefficients were smaller than unity. Nevertheless, model comparison using the F-test confirmed that the N-demethylation of ketamine via CYP3A4 can best be described with the Michaelis-Menten model ($p> 0.05$, Table 1). In the previous study with off-line incubation of racemic ketamine [20], the Michaelis-Menten model was also found to be superior for this pathway. Kinetic parameters V_{max} and K_m were determined in this study. Depending on the efficiency of plug-mixing by diffusion and electrokinetic transport during the short application of voltage, which is assumed to be associated with up to a four-fold dilution of the enzyme, the values for V_{max} vary between 13.33 to 53.34 pmol norketamine/min/pmol CYP for the formation of S-norketamine and 10.04 to 40.16 pmol norketamine/min/pmol CYP for the formation of R-norketamine (lowest value is for no dilution). These data compare well with those obtained in the off-line assay (38.95 and 31.79 pmol norketamine/min/pmol CYP for S- and R-norketamine, respectively, [20]). Furthermore, as observed in the off-line assay, kinetic parameters V_{max} and K_m obtained for the formation

Table 1. Kinetic parameters for N-demethylation of ketamine and model comparison [a]

Substrate	Product	Michaelis-Menten model				Hill model					F-test [f]
		R^2	K_m [μM]	V_{max} [pmol/min/ pmol CYP]	CL_{int} [b] [μL/min/ pmol CYP]	R^2	K' [c] [μM]	V_{max} [pmol/min/ pmol CYP]	CL_{max} [d] [μL/min/ pmol CYP]	n [e]	p-value
Rac. ketamine	S-NK	0.9825	122.3	26.67	0.218	0.9881	245.2	34.67	0.291	0.7616	0.1863
Rac. ketamine	R-NK	0.9705	107.5	20.08	0.187	0.9788	238.6	26.87	0.256	0.7203	0.2217

a) Data for all incubations derived from mean values of duplicate determinations and assuming that the enzyme was diluted two-fold.

b) $CL_{int} = V_{max} / K_m$

c) K' is equivalent to K_m when n=1

d) $CL_{max} = (V_{max} / K') [(|n\text{-}1|) / n(|n\text{-}1|)^{1/n}]$

e) n = Hill coefficient

f) model comparison

of S-norketamine were higher compared to R-norketamine. Using a paired Student's t-test, the formation rates of both enantiomers were shown to differ significantly (p = 0.006), suggesting a stereoselective N-demetyhlation of ketamine via CYP3A4. These results are in accordance with those from the off-line study [20]. While values of V_{max} were comparable to those obtained in the off-line study, the determined values for K_m were about two-fold larger. Interestingly, the ratio of K_m for S-norketamine formation to K_m for R-norketamine formation was the same in both, the on-line and the off-line study (1.138 and 1.147, respectively). Consequently, the calculated intrinsic clearances CL_{int} (Table 1) also differ from the values calculated in the off-line assay. However, such calculated values must be interpreted with caution. More studies and also *in vivo* results would be needed to emphasize the clinical relevance of the calculated kinetic parameters.
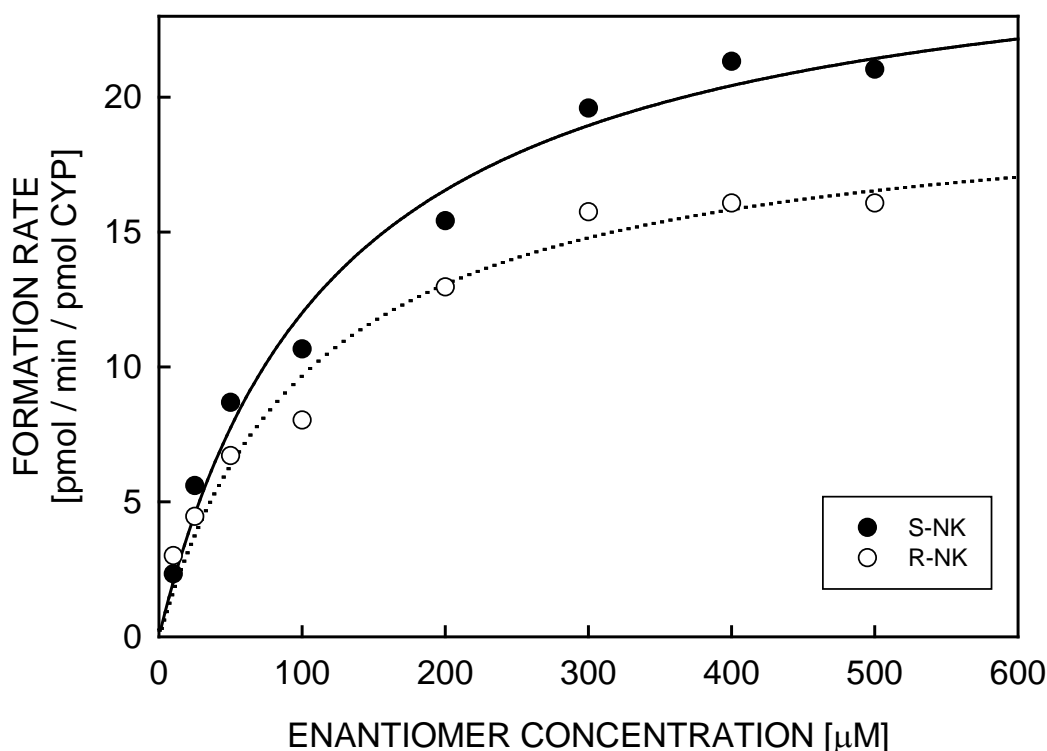
Figure 6. Kinetics of norketamine enantiomer formation by CYP3A4 after 8 min incubation with racemic ketamine at 37 °C. Symbols denote the mean of duplicates. Solid and dotted lines are predicted values based on nonlinear regression analysis using the Michaelis–Menten equation and assuming a two-fold dilution of the enzyme. Key: ● S-norketamine (S-NK) and ○ R-norketamine (R-NK).

It is known from the data presented in Fig. 3 that norketamine is also produced during the 3 min cooling period. Thus, the kinetic data were also evaluated considering a total

incubation time of 11 min (8 min incubation at 37 °C and 3 min cooling time). Analysis of the data revealed that only values for V_{max} and clearances are thereby affected. They become 27.28 % smaller compared to those obtained for the 8 min incubation time. With a reduction in temperature, the metabolite production rate is assumed to become lower such that the effective values should be between those obtained for incubation time intervals of 8 and 11 min. To avoid this uncertainty, conditions without a cooling phase prior to separation and analysis of the products should be worked out.

4   Concluding remarks

In the current study, the N-demethylation of racemic ketamine mediated by CYP3A4 *in vitro* was characterized using EMMA methodology. Injection of the reactants as multiple plugs enabled the enzymatic reaction and electrophoretic mixing enhanced product formation. By adding two incubation buffer plugs to bracket the plugs with the enzyme and substrates, these were well protected from the pH of the background electrolyte and the chiral selector in the running buffer. Additionally, optimization of other conditions, such as pH of the incubation medium, length of plugs, mixing voltage and temperature from rinsing to analysis were crucial for sufficient formation and detection of the metabolites. Although the running time of each analysis is higher compared with the off-line assay, the automated method with in-capillary incubation makes the off-line incubation followed by extraction of the products unnecessary. The amounts of reagents required and the overall workload are smaller for the on-line assay. Using highly sulfated γ-cylcodextrin as chiral selector, the kinetics of the stereoselective metabolism of ketamine via CYP3A4 was characterized and the relevant kinetic parameters were determined and found comparable to those of the off-line study [20]. The EMMA based study revealed that the metabolism of ketamine via CYP3A4 is stereoselective. To our knowledge, this is the first study using EMMA to assess the kinetics of enantioselective drug metabolism mediated by a CYP450 enzyme. Further work should be addressed to shorten the analysis time, e.g. by short-end injection as used in another EMMA assays [12, 33], to avoid the cooling phase after incubation, to understand the contribution of electrophoretic transport to plug mixing and to include an internal standard such that the EMMA method can be further improved and widely applied to assess enzymatic activity in a fast, low-cost and automated way.

Acknowledgments

References

[1]   Naylor, S., Benson, L.M., Tomlinson, A.J., J. Chromatogr. A. 1996, 735, 415-438.

[2]   Zaugg, S., Thormann, W., J. Chromatogr. A 2000, 875, 27-41.

[3]   Zhang, J., Konečný, J., Glatz, Z., Hoogmartens, J., Van Schepdael, A., Cur. Anal. Chem. 2007, 3, 197-217.

[4]   Scriba, G. K., J. Pharm. Biomed. Anal. 2011, 55, 688-701.

[5]   Caslavska, J., Thormann, W., J. Chromatogr. A 2011, 1218, 588-601.

[6]   Bao, J., Regnier, F. E., J. Chromatogr. 1992, 608, 217–224.

[7]   Fan, Y., Scriba, G. K., J. Pharm. Biomed. Anal. 2010, 53, 1076–1090.

[8]   Hai, X., Yang B.-F., Van Schepdael, A. Electrophoresis 2012, 33, 211-227.

[9]   Xue, Q. F., Yeung, E. S., Nature 1995, 373, 681–683.

[10] Martín-Biosca Y., Asensi-Bernardi L., Villanueva-Camañas R. M., Sagrado S., Medina-Hernández M. J., J Sep Sci. 2009, 32, 1748-1756.

[11] Zhang J., Hoogmartens J., Van Schepdael A., Electrophoresis 2008, 29(17), 3694-3700.

[12] Zeisbergerová, M., Řemínek, R., Mádr, A., Glatz, Z., Hoogmartens, J., Van Schepdael, A., Electrophoresis 2010, 31, 3256–3262.

[13] Hai, X., Adams, E., Hoogmartens, J., Van Schepdael, A., Electrophoresis 2009, 30, 1248–1257.

[14] Curcio R., Nicoli R., Rudaz S., Veuthey J. L., Anal Bioanal Chem. 2010, 398, 2163 – 2171.

[15] Schmitz, A., Theurillat, R., Lassahn, P.-G., Mevissen, M., Thormann, W., Electrophoresis 2009, 30, 2912–2921.

[16] Schmitz, A., Thormann, W., Moessner, L., Theurillat, R., Helmja, K., Mevissen, M., Electrophoresis 2010, 31, 1506–1516.

[17] Portmann, S., Kwan, H. Y., Theurillat, R., Schmitz, A., Mevissen, M., Thormann, W., J. Chromatogr. A. 2010, 1217, 7942–7948.

[18] Schmitz, A., Portier, C. J., Thormann, W., Theurillat, R., Mevissen, M., J. Vet. Pharmacol. Ther. 2008, 31, 446–455.

[19] Capponi, L., Schmitz, A., Thormann, W., Theurillat, R., Mevissen, M., Am. J. Vet. Res. 2009, 70, 777–786.

[20] Kwan, H. Y., Thormann, W., Electrophoresis 2011, 32, 2738-2745.

[21]   Baselt, R. C., Cravey, R. H., Disposition of Toxic Drugs and Chemicals in Man, 4th Edn, Chemical Toxicology Institute, Foster City, CA 1995, pp. 412–414.

[22]   Moffat, A. C., Osselton, M. D., Widdop, B., Galichet, L. Y. (Eds.), Clarke's Analysis of Drugs and Poisons in Pharmaceuticals, Body Fluids and Postmortem Material, 3rd Edn, Pharmaceutical Press, London, UK 2004, pp. 1152–1153.

[23]   Adams, H. A., Werner, C., Anaesthesist 1997, 46, 1026–1042.

[24]   Craven, R., Anaesthesia 2007, 62, 48–53.

[25]   Sinner, B., Graf, B. M., Handb. Exp. Pharmacol. 2008, 182, 313–333.

[26]   Aroni, F., Iacovidou, N., Dontas, I., Pourzitaki, C., Xanthos, T., J. Clin. Phramacol. 2009, 49, 957–964.

[27]   Machado-Vieira, R., Salvadore, G., DiazGranados, N., Zarate, C. A., Pharmacol. Ther. 2009, 123, 143–150.

[28]   Kharasch, E. D., Labroo, R., Anesthesiology 1992, 77, 1201–1207.

[29]   Turfus, S. C., Parkin, M. C., Cowan, D. A., Halket, J. M., Smith, N. W., Braithwaite, R. A., Elliot, S. P., Steventon, G. B., Kicman, A. T., Drug Metab. Dispos. 2009, 37, 1769–1778.

[30]   Krylova, S.M., Okhonin, V., Evenhuis, C.J., Krylov, S.N., Trends Anal. Chem. 2009, 28, 987-1010.

[31]   Houston, J. B., Kenworthy, K. E., Drug Metab. Dispos. 2000, 28, 246–254.

[32]   Tracy, T. S., Hummel, M. A., Drug Metab. Rev. 2004, 36, 231–242.

[33]   Stahl, J. W., Catherman, A. D., Sampath, R. K., Seneviratne,C. A., Strein, T. G., Electrophoresis 2011, 32, 1492–1499.

C. Conclusions

Enantioselective CE was confirmed to be an attractive, effective, low-cost and automatable methodology to assess drug metabolism. The principles of stereoselective separation using cyclodextrins were studied through computer simulation with GENTRANS. This valuable dynamic simulation tool provided better and improved comprehension of the complexation between analyte and chiral selector and insights into the buffer systems. Complexation constants and mobilities of analyte-chiral selector-complexes between charged weak bases and neutral cyclodextrins were determined experimentally at acidic pH. These data as well as other parameters describing the buffer systems were used as input data to perform the simulations. Simulated electropherograms were shown to be in good agreement with those obtained from the experiments. Furthermore, simulation with GENTRANS illustrated that the configuration with the sample dissolved in diluted buffer without complexing chiral selector resulted in a sample stacking effect and increased analytical sensitivity (Chapter B.1.; *Electrophoresis 2012, 33, in press*).

Using CE with sulfated cyclodextrins as chiral selectors, the kinetics of the CYP3A4 catalyzed N-demethylation of ketamine was characterized via analysis of extracts of incubations of racemic ketamine and single enantiomers together with CYP3A4 Supersomes. The Michaelis-Menten model was shown to fit best for the incubation of racemic ketamine, while the Hill equation provided the better fit for the formation of norketamine after incubations of single enantiomers. For both enantiomers, the elucidated kinetic parameters K_m and V_{max} were considerably higher after incubations of single enantiomers compared to those obtained from racemic ketamine. Furthermore, after incubations of ketamine as racemate and single enantiomers, formation rate of S-norketamine was higher compared to R-norketamine. Metabolisms of both enantiomers were shown to differ significantly confirming the stereoselective metabolism of ketamine (Chapters B.2./B.3.; [54,55]).

Due to batch-to-batch variations of sulfated β-cyclodextrins used thus far, highly sulfated γ-cyclodextrins were firstly used in this ketamine project and were shown to nicely separate the ketamine and norketamine enantiomers. Highly sulfated γ-cyclodextrins provided reliable CE data for the inhibition study in which racemic ketamine and single enantiomers were incubated with CYP3A4 in the presence of ketoconazole, an antimycotic known as a potent CYP3A4 inhibitor. When data were fitted to various inhibition models by nonlinear regression analysis, the one-site competitive model was found to fit best for the inhibition kinetics. Using the equation of Cheng and Prusoff [58], inhibition constants were determined

and found to be in the range of the literature values for ketoconazole in inhibition studies of CYP3A4 and different substrates [59,60]. No stereoselective difference could be shown in the inhibition kinetics. Incubation of racemic ketamine with ketoconazole resulted in higher K_i values for both enantiomers compared to incubations of single enantiomers. This corresponds to our expectation as higher inhibitor concentrations are required to reduce the enzyme activity, measured as norketamine formation rate, when both enantiomers as substrates with different affinities to the enzyme are present, compared to incubations of single enantiomers where only one enantiomer is competing with the inhibitor for the enzyme. However, such *in vitro* determined kinetic parameters must be interpreted with caution. To emphasize the clinical relevance, further studies including *in vivo* data are necessary. Nevertheless, drug-drug interactions must be considered when chiral drugs are administrated as racemic mixtures (Chapter B.3.; [55]).

Chiral CE was successfully used to investigate drug metabolism of ketamine qualitatively and also quantitatively. As a progress of the current study, a method based on the EMMA technique was designed to characterize the CYP3A4 catalyzed N-demethylation of ketamine in an on-line modus. Reactants were injected into the capillary as multiple plugs bracketed by two incubation buffer plugs, assuring proper reaction conditions and protecting enzymes and ketamine from the extreme pH and from the chiral selector of the running buffer. Optimization of other conditions such as pH of the incubation medium, length of plugs, mixing voltage and temperature from rinsing to analysis were necessary to enable the enzymatic reaction, which was additionally enhanced by short electrophoretic mixing. After 8 min incubation at 37°C, a cooling period of 3 min was introduced before the CE analysis was performed at 25°C. Norketamine formation rate was calculated by external calibration. Data obtained were fitted using nonlinear regression analysis and revealed a better fit for the Michaelis-Menten compared to the Hill equation. However, as a notable amount of norketamine was detected during the 3 min of cooling time, the enzymatic reaction must be assumed to continue during these 3 min at a reduced rate and thus, the total incubation time is between 8 – 11 min. Also, as no homogenous mixing of the reactants could be assured, the effective concentrations of enzymes could not be defined exactly. After consideration of these uncertainties, the value for V_{max} could vary in a range which is comparable with the results obtained in the off-line study. Furthermore, as observed in the off-line assay, the investigated metabolic pathway was found to occur stereoselectively (Chapter B.4.; *submitted for publication in Electrophoresis*).

Although the running time of each analysis is higher compared to the off-line assay, the amounts of reagents and overall workload could be reduced with this automated EMMA method. A further effort to continue this project would include additional optimization of the EMMA method such as shortening of the analysis time, e.g. by short-end injection as used in other EMMA studies [61, 62], avoidance of the cooling phase after incubation, inclusion of an appropriate internal standard, which must not interfere with the enzymatic reaction and can be well separated from other components. Furthermore, a comprehensive insight into the contribution of electrophoretic transport to plug mixing could be gained by computer simulation for which input data should be elucidated. After all these improvements, the EMMA method should be widely applicable to assess enzymatic activity in a fast, low-cost and automated way.

D.   References

[1]   Francotte, E., Lindner, W., Eds., Chirality in Drug Research, Wiley-VCH, Weinheim, Germany, 2006.

[2]   Unceta, N., Goicolea, M. A., Barrlo, R. J., Biomed. Chromatogr. 2011, 238-257.

[3]   Smith, S. W., Toxicol. Sci. 2009, 110, 4–30.

[4]   Lin, C-C., Li, Y-T., Chen, S-H., Electrophoresis 2003, 24, 4106 – 4115.

[5]   Naylor, S., Benson, L.M., Tomlinson, A.J., J. Chromatogr. A 1996, 735, 415-438.

[6]   Zaugg, S., Thormann, W., J. Chromatogr. A 2000, 875, 27-41.

[7]   Zhang, J., Konečný, J., Glatz, Z., Hoogmartens, J., Van Schepdael, A., Cur. Anal. Chem. 2007, 3, 197-217.

[8]   Scriba, G. K., J. Pharm. Biomed. Anal. 2011, 55, 688-701.

[9]   Caslavska, J., Thormann, W., J. Chromatogr. A 2011, 1218, 588-601.

[10]   Mikuš, P., Maráková, K., Electrophoresis, 2009, 30, 2773-2802.

[11]   Mandrioli, R., Mercolini L., Raggi M.A., Electrophoresis, 2011, 32, 2629-2639.

[12]   Bonato, P. S., Electrophoresis 2003, 24, 4078–4094.

[13]   Van Eeckhaut, A. V., Michotte, Y., Electrophoresis, 2006, 27, 2880-2895.

[14]   Mangelings, D., Heyden, Y. V., Electrophoresis, 2011, 32, 2583-2601.

[15]   Kamande, M. W., Zhu, X., Kapnissi-Christodoulou, C., Warner, I. M., Anal. Chem. 2004, 76, 6681–6692.

[16]   Mosher, R. A., Saville, D. A., Thormann, W., The Dynamics of Electrophoresis, VCH Publishers, Weinheim, 1992.

[17]   Thormann, W., Caslavska, J., Breadmore, M. C., Mosher, R. A., Electrophoresis 2009, 30, S16-S26.

[18]   Thormann, W., Breadmore, M. C., Caslavska, J., Mosher, R. A., Electrophoresis 2010, 31, 726-754.

[19]   Thormann, W., Zhang, C.-X., Caslavska, J., Gebauer, P., Mosher, R. A., Anal. Chem. 1998, 70, 549-562.

[20]   Hruška, V., Jaroš, M., Gaš, B., Electrophoresis 2006, 27, 984-991.

[21]   Bercovici, M., Lele, S. K., Santiago, J.G., J. Chromatogr. A 2009, 1216, 1008-1018.

[22]   Mosher, R. A., Breadmore, M. C., Thormann, W., Electrophoresis 2011, 32, 532-541.

[23]   Breadmore, M. C., Kwan, H. Y., Caslavska, J., Thormann, W., Electrophoresis 2012, 33, in press.

[24] Hruška, V., Beneš, M., Svobodová, J., Zusková, I., Gaš, B., Electrophoresis 2012, 33, in press.

[25] Degenhardt, L., Copeland, J., Dillon, P., Subst. Use Misuse 2005, 40, 1241-1256.

[26] Domino, E. F., Anesthesiology 2010, 113, 678-686.

[27] Aroni, F., Iacovidou, N., Dontas, I., Pourzitaki, C., Xanthos, T., J. Clin. Phramacol. 2009, 49, 957–964.

[28] Kochs, E., Adams, H. A., Spies, C. Anästhesiologie, 2009, 2nd Edition, Georg Thieme Verlag KG, Stuttgart, Deutschland.

[29] Rang, H. P., Dale, M. M., Ritter, J. M., Flower, R. J., Rang and Dale's Pharmacology 2007, 6th Edition, Churchill Livingstone Elsevier, Philadelphia, US.

[30] Visser, E., Schug, S. A., Biomed. Pharmacother. 2006, 60, 341–348.

[31] Weinbroum, A. A., Pharmacol. Res. 2012, in press.

[32] Machado-Vieira, R., Salvadore, G., DiazGranados, N., Zarate, C. A., Pharmacol. Ther. 2009, 123, 143–150.

[33] Adams, H. A., Werner, C., Anaesthesist 1997, 46, 1026–1042.

[34] Sinner, B., Graf, B. M., Handb. Exp. Pharmacol. 2008, 182, 313–333.

[35] Craven, R., Anaesthesia 2007, 62, 48–53.

[36] Adams, J. D., Baillie, T. A., Trevor, A. J., Castagnoli, N., Biomed. Mass Spectrom. 1981, 8, 527–538.

[37] Woolf, T. F., Adams, J. D., Xenobiotica 1987, 17, 839–847.

[38] Kharasch, E. D., Labroo, R., Anesthesiology 1992, 77, 1201–1207.

[39] Savchuk, S. A., Brodskii, E. S., Rudenko, B. A., Formanovskii, A. A., Mikhura, I. V., Davydova, N. A., J. Anal. Chem. 1997, 52, 1175–1186.

[40] Yanagihara, Y., Kariya, S., Ohtani, M., Uchino, K., Aoyama, T., Yamamura, Y., Iga, T., Drug Metab. Dispos. 2001, 29, 887–890.

[41] Hijazi, Y., Boulieu, R., Drug Metab. Dispos. 2002, 30, 853–858.

[42] Turfus, S. C., Parkin, M. C., Cowan, D. A., Halket, J. M., Smith, N. W., Braithwaite, R. A., Elliot, S. P., Steventon, G. B., Kicman, A. T., Drug Metab. Dispos. 2009, 37, 1769–1778.

[43] Schmitz, A., Theurillat, R., Lassahn, P.-G., Mevissen, M., Thormann, W., Electrophoresis 2009, 30, 2912–2921.

[44] Schmitz, A., Thormann, W., Moessner, L., Theurillat, R., Helmja, K., Mevissen, M., Electrophoresis 2010, 31, 1506–1516.

[45] Rentsch, K. M., J. Biochem. Biophys. Methods 2002, 54, 1 –9.

[46]   Sahajwalla, C., Regulatory Considerations in Drug Development of Stereoisomers, in Reddy, I. K., Mehvar, R., Chirality in Drug Design and Development 2004, 1st Edition, Mercel Dekker Inc., New York, US.

[47]   Theurillat, R., Knobloch, M., Schmitz, A., Lassahn, P. G., Mevissen, M., Thormann, W., Electrophoresis 2007, 28, 2748–2757.

[48]   Schmitz, A., Portier, C. J., Thormann, W., Theurillat, R. Mevissen, M., J. Vet. Pharmacol. Ther. 2008, 31, 446–455.

[49]   Capponi, L., Schmitz, A., Thormann, W., Theurillat, R., Mevissen, M., Am. J. Vet. Res. 2009, 70, 777–786.

[50]   Knobloch, M., Portier, C. J., Levionnois, O. L., Theurillat, R., Thormann, W., Spadavecchia, C., Mevissen, M., Toxicol. Appl. Pharmacol. 2006, 216, 373–386.

[51]   Larenza, M. P., Landoni, M. F., Levionnois, O. L., Knobloch, M., Kronen, P. W., Theurillat, R., Schatzmann, U., Thormann, W., Br. J. Anaesth. 2007, 98, 204–212.

[52]   Theurillat, R., Knobloch, M., Levionnois, O., Larenza, P., Mevissen, M., Thormann, W., Electrophoresis 2005, 26, 3942–3951.

[53]   Theurillat, R., Knobloch, M., Schmitz, A., Lassahn, P. G., Mevissen, M., Thormann, W., Electrophoresis 2007, 28, 2748–2757.

[54]   Portmann, S., Kwan, H. Y., Theurillat, R., Schmitz, A., Mevissen, M., Thormann, W., J. Chromatogr. A. 2010, 1217, 7942–7948.

[55]   Kwan, H. Y., Thormann, W., Electrophoresis 2011, 32, 2738-2745.

[56]   Fan, Y., Scriba, G. K., J. Pharm. Biomed. Anal. 2010, 53, 1076–1090.

[57]   Hai, X., Yang B.-F., Van Schepdael, A. Electrophoresis 2012, 33, 211-227.

[58]   Cheng, Y., Prusoff , W. H., Biochem. Pharmacol. 1973, 22, 3099–3108.

[59]   U.S. Department of Health and Human Services, Guidance for Industry: Drug Interactions Studies – Study Design, Data Analysis and Implications for Dosing and Labeling, Center for Drug Evaluation and Research and Center for Biologics Evaluation and Research, Rockville, MD, USA 2006, pp. 1–52.

[60]   Thummel, K. E., Wilkinson, G. R., Annu. Rev. Pharmacol. Toxicol. 1998, 38, 389–430.

[61]   Zeisbergerová, M., Řemínek, R., Mádr, A., Glatz, Z., Hoogmartens, J., Van Schepdael, A., Electrophoresis 2010, 31, 3256–3262.

[62]   Stahl, J. W., Catherman, A. D., Sampath, R. K., Seneviratne, C. A., Strein, T. G., Electrophoresis 2011, 32, 1492–1499.

E. Publications

E.1. Publications related to the dissertation

Portmann, S., Kwan, H. Y., Theurillat, R., Schmitz, A., Mevissen, M., Thormann, W. Enantioselective capillary electrophoresis for identification and characterization of human cytochrome P450 enzymes which metabolize ketamine and norketamine *in vitro*. J. Chromatogr. A 2010, 1217, 7942–7948.

Kwan, H. Y., Thormann, W. Enantioselective capillary electrophoresis for the assessment of CYP3A4-mediated ketamine demethylation and inhibition *in vitro*. Electrophoresis 2011, 32, 2738–2745.

Breadmore, M. C., Kwan, H. Y., Caslavska, J., Thormann, W. Dynamic high-resolution computer simulation of electrophoretic enantiomer separations with neutral cyclodextrins as chiral selectors. Electrophoresis 2012, 33, in press.

Kwan, H. Y., Thormann, W. Electrophoretically mediated microanalysis for characterization of the enantioselective CYP3A4 catalyzed N-demethylation of ketamine. Accepted for publication in Electrophoresis.

E.2. Publications unrelated to the dissertation

Knoblauch, A., Kwan, H. Y., Pavelic-Ferretti, D., Stoller, R. Lungenembolie: der verflixte Weg zur Diagnose. Schweiz. Ärztezeitung 2010, 91(47), 1859-1861.

De Geyter, C., Meyer, C.R., Pavelic-Ferretti, D., Kwan H. Y., Stoller R. Venöse Thromboembolien unter kombinierten oralen Kontrazeptiva. PharmaJournal 2009, 21, 4-6 und Schweiz. Ärztezeitung 2009, 90(43), 1654-1657

Kwan, H. Y., Reinke C., Mühlebach, S. Veranstaltung zur Klinischen Pharmazie: Standortbestimmung in Theorie und Praxis. PharmaJournal 2009, 5, 21-22.

F. Congress participations and poster presentations

F.1. Congress participations and poster presentations related to the dissertation

3rd Swiss Pharma Science Day, Swiss Society of Pharmaceutical Sciences (SSPhS). Bern, 8 September 2010. „Characterization of ketamine N-demthylation by CYP3A4 and CYP2B6 using enantioselective capillary electrophoresis".

4th Swiss Pharma Science Day, Swiss Society of Pharmaceutical Sciences (SSPhS). Bern, 31 August 2011. „CYP3A4 mediated ketamine N-demethylation and its inhibition *in vitro* assessed by enantioselective capillary electrophoresis".

27th International Symposium in MicroScale Bioseparations and Analysis (MSB). Geneva, 12-15 February 2012. „CYP3A4 mediated ketamine N-demethylation and its inhibition *in vitro* assessed by enantioselective capillary electrophoresis".

27th International Symposium in MicroScale Bioseparations and Analysis (MSB). Geneva, 12-15 February 2012. „Electrophoretically mediated microanalysis for characterization of the enantioselective CYP3A4 catalyzed N-demethylation of ketamine".

27th International Symposium in MicroScale Bioseparations and Analysis (MSB). Geneva, 12-15 February 2012. "Dynamic high-resolution computer simulation of electrophoretic enantiomer separations with neutral cyclodextrins as chiral selectors".

F.2. Congress participations and poster presentations unrelated to the dissertation

2nd Swiss Pharma Science Day, Swiss Society of Pharmaceutical Sciences (SSPhS). Bern, 7 September 2009. „Stereoselective Serum and Plasma Methadone analysis for Patients using the Ph. Helv. Oral Solution".

14èmes JFSPH (Journées Franco-Suisses de Pharmacie Hospitalière), Lausanne, 14-16 November 2007. „Stereoselective Serum and Plasma Methadone analysis for Patients using the Ph. Helv. Oral Solution".

G. Oral presentation

22. Doktorandenseminar Hohenroda. Hohenroda (D), 8-10 February 2012. „CYP3A4 mediated ketamine N-demethylation and its inhibition *in vitro* assessed by enantioselective capillary electrophoresis"

H.   Curriculum Vitae

Name: Kwan, Hiu Ying
Date of Birth: 5 July 1984
Place of Birth: Hong Kong
Nationality: Switzerland
Citizen: Bern (BE)

Education

1990 – 1995	Primary School, Hong Kong
1995 – 1997	Primary School, Bern
1997 – 1999	Secondary School, Bern
1999 – 2003	High school, Mathematisch-Naturwissenschaftliches Gymasium Bern-Neufeld, Schwerpunkt Biologie / Chemie, leading to Matura
2003 – 2005	Study of Pharmacy, University of Bern
2005 – 2006	Study of Pharmacy, University of Basel, leading to Bachelor of Science in Pharmaceutical Sciences
2006 – 2008	Study of Pharmacy, University of Basel, leading to Master of Science in Pharmacy, University of Basel
Mar. – Aug. 2007	Master thesis „Methadonhydrochlorid Trinklösung 10mg/ml Ph. Helv.: Stereoselektive Wirkstoff-bestimmung im Plasma" (Grade 6). Institute of Clinical Pharmacy, University of Basel / Swissmedic, Bern
Sep. 2007 – Jun. 2008	Assisstant Pharmacist, Zähringer Apotheke Ballinari
25 Aug 2008	Swiss Federal Diploma in Pharmacy
Feb. 2009 – Mar. 2012	Dissertation, Institute of Clinical Pharmacology / Clinical Pharmacology Laboratory, Institute for Infectious Diseases, University of Bern

As a student and PhD student I have attended lectures and courses given by

Albrecht, C.; Altermatt, R.; Altmann, M.; Altwegg, K.; Ammann, K.; Anderegg-Wirth, E.; André, C.; Benz, W.; Betz, G.; Bigler, P.; Bütikofer, P.; Burkart, T.; Calzaferri, G.; Drewe,J.; Eberle, A.; Ernst, B.; Folkers, G.; Gertsch, J.; Guentert, T.W.; Häner, R.; Hamburger, M.; Haschke, M.; Hauser, P.; Hersberger, K.; Honegger, U.; Hüsler, J.; Hulliger, J.; Huwyler, J.; Imanidis, G.; Imboden, H.; Kessler, M.; Kohli, J.; Krähenbühl, S.; Krähenbühl, U.; Kropf, A.; Kuhlemeier,

C.; Lampert, M.; Lauterburg, B.; Leuenberger, H.; Leutwyler, S.; Meier, C.; Meier, C.; Mühlebach, S.; Potterat, O.; Pretzl, K.; Rätz-Bravo, A.; Rehmann-Sutter, C.; Renaud, P.; Rentsch D.; Reymond, J-L.; Rothen, C.; Schacher, J.; Schittny, J.; Schlienger, R.; Schmidt, R.; Scholer, A.; Schümperli, D.; Schürch S.; Seebeck, T.; Stadler, B.; Stocker, T.; Streit, J.; Stroka, D.; Studer, T.; Suter, B.; Tschan, M.; Vedani, A.; Zimmer, Y.; Zimmermann H.